SYNOPTIC SCALE FEATURES ASSOCIATED WITH VERTICAL DISTRIBUTION OF IR AEROSOL EXTINCTION

James Norman Heil

NAVAL POSTGRADUATE SCHOOL
Monterey, California

THESIS

SYNOPTIC SCALE FEATURES ASSOCIATED WITH
VERTICAL DISTRIBUTIONS OF
IR AEROSOL EXTINCTION

by

James Norman Heil

March 1981

Thesis Advisor: K.L. Davidson

Approved for public release; distribution unlimited

REPORT DOCUMENTATION PAGE

READ INSTRUCTIONS BEFORE COMPLETING FORM

1. REPORT NUMBER	2. GOVT ACCESSION NO. / 3. RECIPIENT'S CATALOG NUMBER
4. TITLE (and Subtitle): Synoptic Scale Features Associated With Vertical Distributions of IR Aerosol Extinction	5. TYPE OF REPORT & PERIOD COVERED: Master's Thesis, March 1981
	6. PERFORMING ORG. REPORT NUMBER
7. AUTHOR(s): James Norman Heil	8. CONTRACT OR GRANT NUMBER(s)
9. PERFORMING ORGANIZATION NAME AND ADDRESS: Naval Postgraduate School, Monterey, California 93940	10. PROGRAM ELEMENT, PROJECT, TASK AREA & WORK UNIT NUMBERS
11. CONTROLLING OFFICE NAME AND ADDRESS: Naval Postgraduate School, Monterey, California 93940	12. REPORT DATE: March 1981
	13. NUMBER OF PAGES: 115
14. MONITORING AGENCY NAME & ADDRESS (if different from Controlling Office)	15. SECURITY CLASS. (of this report): Unclassified
	15a. DECLASSIFICATION/DOWNGRADING SCHEDULE

16. DISTRIBUTION STATEMENT (of this Report)

Approved for public release; distribution unlimited.

17. DISTRIBUTION STATEMENT (of the abstract entered in Block 20, if different from Report)

18. SUPPLEMENTARY NOTES

19. KEY WORDS (Continue on reverse side if necessary and identify by block number)

aerosol extinction
observational results
synoptic features
atmospheric mixed layer
extinction model
LOWTRAN 3B
Wells-Katz model

20. ABSTRACT (Continue on reverse side if necessary and identify by block number)

Observed vertical profiles of optical extinction due to aerosol scattering were examined relative to prevailing synoptic scale features. This examination was on the suitability of an existing wind speed and humidity dependent extinction model during different synoptic conditions. The primary synoptic features in question are the depth of the atmospheric well mixed layer and the nature of the capping inversion. Aerosol extinction profiles

were calculated from aerosol size distributions measured from an aircraft in the vicinity of Monterey Bay. Mixed layer descriptions were obtained from temperature and humidity profiles obtained from aircraft spiral ascents and shipboard and shoreline radiosonde launches. The presence of the inversion reduced the accuracies of the current Navy (Wells-Katz) and Air Force (LOWTRAN 3B) models in estimating the extinction profile. The inversion represents a cap to the vertical transport of surface generated aerosols. This is not accounted for in the models. LOWTRAN 3B was found to be inadequate in most respects whereas the Wells-Katz model could be modified to obtain reasonable predictions. Model specification of the continental component was also found to be a significant factor in the comparisons.

Approved for public release; distribution unlimited

Synoptic Scale Features Associated with Vertical Distributions of IR Aerosol Extinction

by

James Norman Heil
Captain, United States Air Force
B.S., University of Texas at El Paso, 1972
M.A., Pepperdine University, 1978

Submitted in partial fulfillment of the
requirements for the degree of

MASTER OF SCIENCE IN METEOROLOGY

from the

NAVAL POSTGRADUATE SCHOOL
March 1981

ABSTRACT

Observed vertical profiles of optical extinction due to aerosol scattering were examined relative to prevailing synoptic scale features. This examination was on the suitability of an existing wind speed and humidity dependent extinction model during different synoptic conditions. The primary synoptic features in question are the depth of the atmospheric well mixed layer and the nature of the capping inversion. Aerosol extinction profiles were calculated from aerosol size distributions measured from an aircraft in the vicinity of Monterey Bay. Mixed layer descriptions were obtained from temperature and humidity profiles obtained from aircraft spiral ascents and shipboard and shoreline radiosonde launches. The presence of the inversion reduced the accuracies of the current Navy (Wells-Katz) and Air Force (LOWTRAN 3B) models in estimating the extinction profile. The inversion represents a cap to the vertical transport of surface generated aerosols. This is not accounted for in the models. LOWTRAN 3B was found to be inadequate in most respects whereas the Wells-Katz model could be modified to obtain reasonable predictions. Model specification of the continental component was also found to be a significant factor in the comparisons.

TABLE OF CONTENTS

LIST OF TABLES

LIST OF FIGURES

I. INTRODUCTION

The Department of Defense (DOD) and its agencies are interested in optical properties because of optically guided weapon systems. The Air Force is particularly interested in aerosol extinction for its precision guided munitions (PGM) [Cottrell et al, 1979]. DOD has PGM's that operate at differing wavelengths which range from the visible to the microwave regions. The PGM has a greater ability to hit a target than conventional munitions, but an important controlling factor is the ability of the guidence system to "see" the target. The ability for the PGM to "see" the target is dependent on the wavelength for which sensors are designed and the properties of the intervening atmosphere. The degrading properties of the atmosphere are principally molecular absorption and aerosol scattering. The wavelengths for the different sensors are primarily selected so that molecular absorption is minimized. Therefore, scattering by aerosols becomes the main concern, once a relatively molecular absorption free window has been found.

Relatively absorption free windows exists in the visible, infrared (IR), millimeterwave, and microwave wavelengths. While both absorption and scattering by aerosols are affected by weather elements, scattering appears to be more affected than absorption in most cases [Cottrell et al, 1979].

The ability to assess aerosol extinction from synoptic scale descriptions would help in decisions of which type of system to use against a target. Because some systems are launched from the air, it is important that descriptions include vertical distributions of aerosol extinction. Models exist for estimating vertical extinction profiles but they have not been validated sufficiently. To do this, profiles of actual extinction must be compared to the extinction predicted by existing models. If the models do not work and if modifications cannot be made, new models must be developed. The purpose of the study is to describe the synoptic conditions occurring with a unique set of mixed layer and aerosol data to evaluate an existing model.

An experiment entitled Marine Aerosol Generation and Transport (MAGAT) was conducted in the vicinity of the Monterey Bay, California, during the period of April 28 to May 9, 1980. The purpose of this experiment is to examine the compatibility of optical and micrometerorological propagation theory, and to extend dynamic models of the evolving marine atmospheric boundary layer to include aerosol and turbulence profiles [Fairall, 1980 and Fairall et al, 1980]. Two platforms, the R/V ACANIA and an aircraft, were used.

In this study, overwater radiosonde profiles from the R/V ACANIA, profiles from the spiral flights of the aircraft, and overland radiosonde profiles at the Naval Postgraduate School (NPS) are compared to aerosol measurements and model

prediction made from ladder flights of the aircraft. The approach was to describe the prevailing synoptic conditions at the time of the soundings and to show how these conditions affected the vertical aerosol extinction at 3.75 microns. The results are compared to those presented by Hughes (1980), where both the height and the strength of the inversion were considered.

II. BACKGROUND

Background discussion will consist of a summary of the investigations by Hughes (1980) and Hughes and Richter (1980), and brief descriptions of the evaluated models.

The aerosol extinction coefficient, the parameter of interest, is a function of the wavelength of the radiation (λ), particle size (r), and particle index of refraction (n). Since aerosol absorption is negligible, aerosol extinction can be almost entirely attributed to scattering processes. There are three types of scattering (Rayleigh, Mie, and Non-selective) which depends on the ratio of the size of the particle to the wavelength. Rayleigh scattering applies to particles which are much smaller than the wavelength, Mie scattering to particles which are near the same size as the wavelength, and Non-selective scattering to particles which are much larger than the wavelength [Raby, 1981].

The scattering area coefficient, K, is the determining parameter in Mie scattering. K is the ratio of the incident wave front to the effective cross-sectional area of the particle. The extinction coefficient, b, is related to K as follows:

$$b = \int_{r_1}^{r_2} (DN/Dr)\ K(n, r/\lambda)\ A(r)\ dr \quad , \qquad (1)$$

where DN/Dr is the number of particles per size range Dr in a size interval centered at radius r. $K(n,r/\lambda)$ is the Mie scattering area coefficient, and $A(r)$ is the particle area, πr^2, for spherical particles. Extinction coefficients based on observed aerosol distributions can be computed, for either discrete wavelengths or a wavelength band, using exact Mie coefficients [Raby, 1981].

A. NAVAL OCEAN SYSTEM CENTER (NOSC) EXPERIMENT

H. G. Hughes (1980) evaluated extinction profiles determined from measurements of aerosol size distributions obtained by NOSC investigators in the vicinity of San Nicolas Island, California, during April-May 1978. He compared observed extinction coefficient variations with height to those predicted from the Wells-Gal-Munn (WGM) model [Wells et al, 1977] and to the LOWTRAN 3B model. Relative humidity, which is an input parameter of the WGM model, was calculated from the air and dew-point temperatures, which was measured coincident with the aerosol measurements.

Three days were chosen for evaluations because of the depth of the mixed layer and the strength of inversion. Conditions for one day (28 April) were a shallow mixed layer and weak inversion, conditions for the second day (5 May) were a deep mixed layer and a strong inversion, and conditions for the third day (11 May) were a shallow mixed layer and strong inversion. The surface wind speeds for these days were 3-5, 5-7, and 10-12 m/s, and visibilities were 16, 11, and 23 km, respectively.

Aircraft mounted instrumentation used in the measurements were (Hughes, 1980):

(1) An airborne Knollenberg ASSP-100 spectrometer probe for aerosol size distributions. The measurements gave a radius coverage from 0.225 to 14.7 microns. Data were summed for four second time spans.

(2) An HP200A quartz thermometer for air temperature.

(3) An EG&G TM 73-244 for dew-point temperature.

(4) A pressure sensor for measurements of elevation.

B. WELLS-GAL-MUNN MODEL

The WGM maritime aerosol model is a two component analytic expression for the aerosol size distribution. Continental and maritime aerosols are represented by two components of the analytic expression.

The maritime component was adopted from the Diermendjian's [Wells et al, 1977] haze model where the number distribution is described by

$$[dN(r)/d\ \log(r)] = ar^2 \exp(-br^{\gamma}). \qquad (2)$$

N(r) is the total number of particles per cubic centimeter, r is radius of the particle and dependent on relative humidity (RH), a and γ are dependent on the velocity of the wind (u) in m/s, and b is a constant. The values for a and were determined by empirical methods and have the form

$$a = 250 + 750\ u^{1.16} \qquad \text{for } u < 7 \text{ m/s} \qquad (3)$$
$$a = 6900\ u^{0.29} \qquad \text{for } u \geq 7 \text{ m/s}$$

and

$$\gamma = 0.384 - 0.00293\ u^{1.25} \quad . \qquad (4)$$

The reason for the change in the behavior of a at 7 m/s is that a rapid increase in the number of large particles occurs when white caps form. White caps form at approximately 7 m/s. Below 7 m/s, the aerosol size distribution takes on the characteristics of continental aerosols.

The model allows for aerosol particle size change in response to relative humidity changes. The equation for this is given by

$$r_{RH} = r_o F \qquad (5)$$

where r_o is the radius of the particle at zero percent relative humidity and F is the growth factor. F is

$$F = 1 - 0.9 \ln[1-(RH/100)] . \qquad (6)$$

(RH/100) is the decimal equivalent of percentage. It is noted that the expression for F is for sea salt aerosols with sodium iodide as the nucleus.

Including relative humidity, the altitude dependence, and the continental component in the equation yielded the final form of the equation used by Wells et al (1977):

$$[dN/dr] = \frac{\beta}{F'} \left\{ 0.47 \left(\frac{r}{F'}\right)^{-4} \exp\left(\frac{-h}{h_c}\right) + 2.3\,\alpha\, (C_1 + C_2\, u^{\delta}) \left(\frac{r}{F'}\right) \exp[-8.5 \left(\frac{r}{F'}\right)^{\gamma} - \frac{h}{h_m}] \right\} . \qquad (7)$$

$C_1 + C_2 u^{\delta}$ is defined as a in Equation 3. h is the altitude and h_c and h_m are scale heights for the continental and maritime components; values for these scale heights can be found in Table I of the published paper [Wells et al, 1977]. Hughes (1980) showed that the constant coefficient in the maritime component should be the inverse, 0.434 instead of 2.3.

C. WELLS - KATZ MODEL

A version (Wells-Katz) of the previously described model is that used to compare actual versus calculated extinction coefficients in this study. Modified through empirical methods, the Wells-Katz Model is as follows

$$[dN/dr] = 1.7 \left(\frac{r}{\alpha}\right)^{-4} + 1.62 \left(C_1 + C_2 v^{\delta}\right) \left(\exp\left[-\frac{Z}{h_o F} - 8.5\left(\frac{r}{\alpha}\right)\right]\right) F^{-1} \left(\frac{r}{\alpha}\right). \quad (8)$$

The first term is independent of elevation whereas it was not in the original model. The third term is still elevation dependent. r is the droplet radius in microns, Z is the elevation above sea surface in meters, and h_o is the scale height (800 m) for altitudes less than one km. α is given by

$$\alpha = 0.81 \exp[0.066\ RH / (1.058 - RH)] \quad (9)$$

where RH is the fracational relative humidity for relative humidity between 40% and 96.6%. v is the wind factor scaled from surface speed u, in this case the wind speed

was taken from ship height, and defined as 0.5 m/s for speeds less than or equal to 4 m/s and as (u - 3.5) m/s at speeds greater than 4 m/s. The growth factor, F, is defined as one plus the quantity v/60 cubed. Γ is the same as γ in the original equation. $C_1 + C_2 v^{\delta}$ is defined as a for velocities greater than 7 m/s, whereas the value becomes $350 - 1000 v^{1.15}$ for velocities less than or equal to 7 m/s [Moonkester, 1980].

D. SUMMARY OF HUGHES RESULTS

Results of comparisons between observed and predicted aerosol extinction by Hughes (1980) and Hughes and Richter (1980) appear in Figures 1 and 2. Those from Hughes are based on the NGM model and the LOWTRAN 3B maritime model. In general, the comparisons for both are not good, particularly below the inversion. Further, discussion on this is withheld until an examination of results from this study.

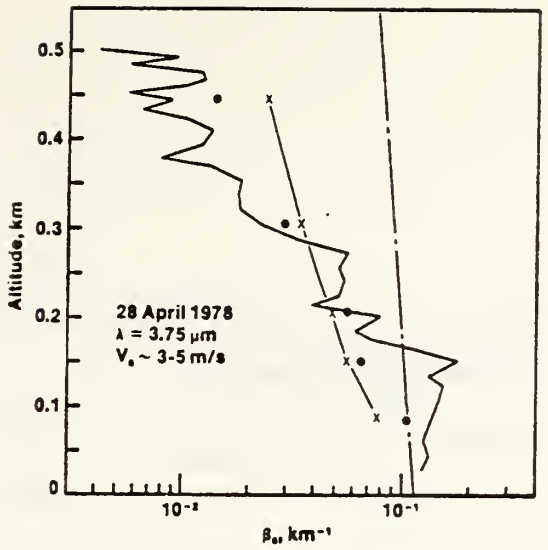

(a) Aerosol extinction coefficient variation with altitude calculated using aerosol size distributions measured during constant altitude (●) and spiral (——) aircraft flights; the NCK model (X——X); and the LOWTRAN 3B maritime model (— - —).

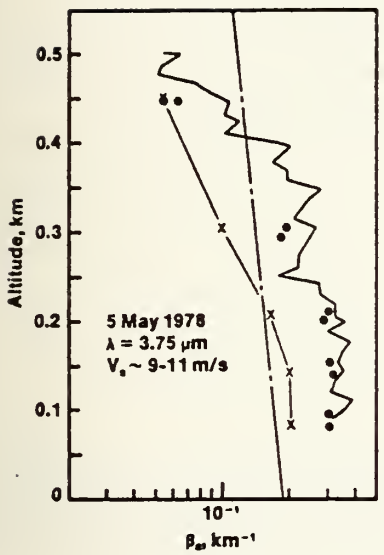

(b) As in (a)

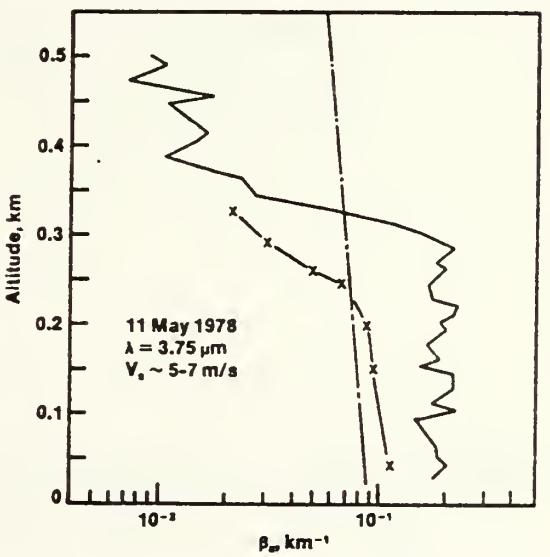

(c) As in (a) except no constant altitude aircraft flight.

Figure 1. Hughes' aerosol extinction coefficient variations with altitude. (Hughes, 1980)

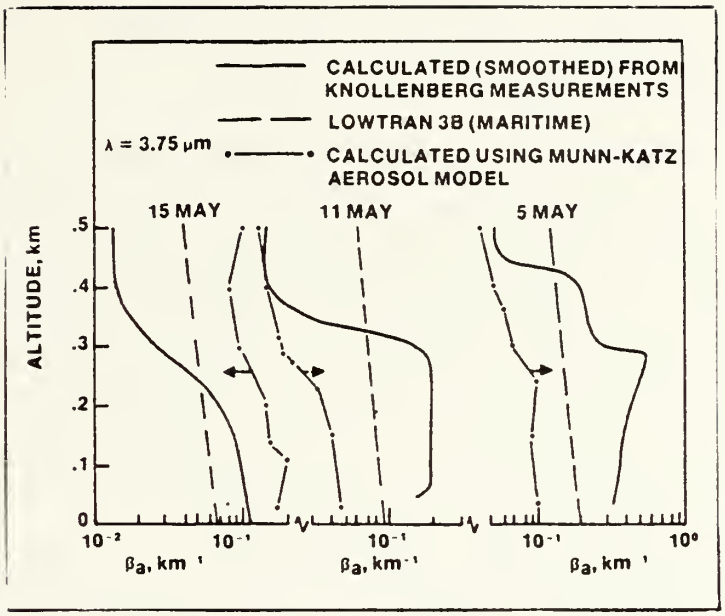

Figure 2. Comparison of extinction coefficient variations (smoothed) with altitude calculated using aircraft Knollenberg measurements and those calculated using the Munn-Katz and LOWTRAN 3B maritime model. (Hughes and Richter, 1980)

III. MAGAT DATA ACQUISITION

A. SHIP AND AIRCRAFT DATA

The data for aerosol extinction were measured from the Airborne Research Associates' turbo charged Bellanca, using the NOSC aerosol measurement system consisting of a Particle Measurements System (PMS) model ASSAP (Figure 3). All measured data were sampled every 2.5 seconds with a two-scan average every five seconds. The aircraft flew at a constant altitude for two minutes during measurements then went to a different altitude (ladder) and repeated the process. The data were stored on magnetic tape. The aircraft also measured air and dewpoint temperatures, which were used to compute relative humidity. The primary vertical profiles for this study are of aerosol extinction (actual and predicted) and relative humidity.

During flybys with the R/V ACANIA, aircraft aerosol distributions were compared with those obtained with two probes on the ship. The two probes on the R/V ACANIA were the PMS models CSAS (classical scattering) and ASAS (active scattering), Figures 4 and 5, controlled by a PMS data acquisition system (DAS-32) with a computer interface. The shipboard systems measured aerosols in 90 different size channels from 0.09 to 14.0 micron radius. Because the shipboard aerosol system had a wider size range, aircraft aerosol

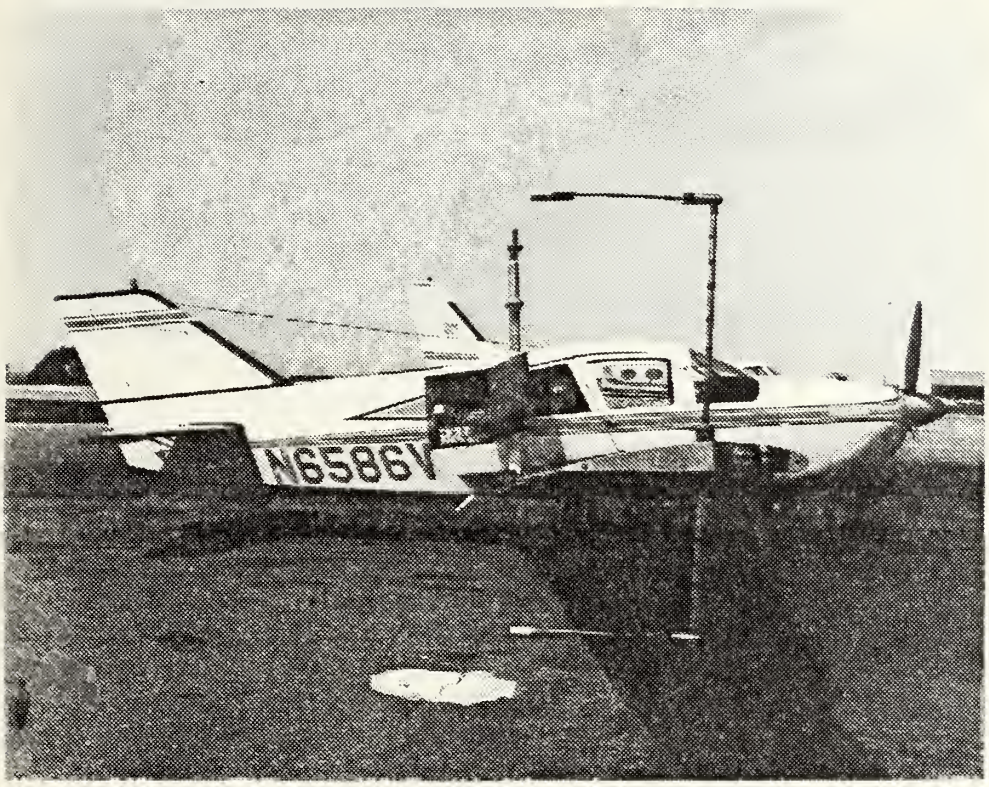

Figure 3. Spectrometer probe mounted on the aircraft.

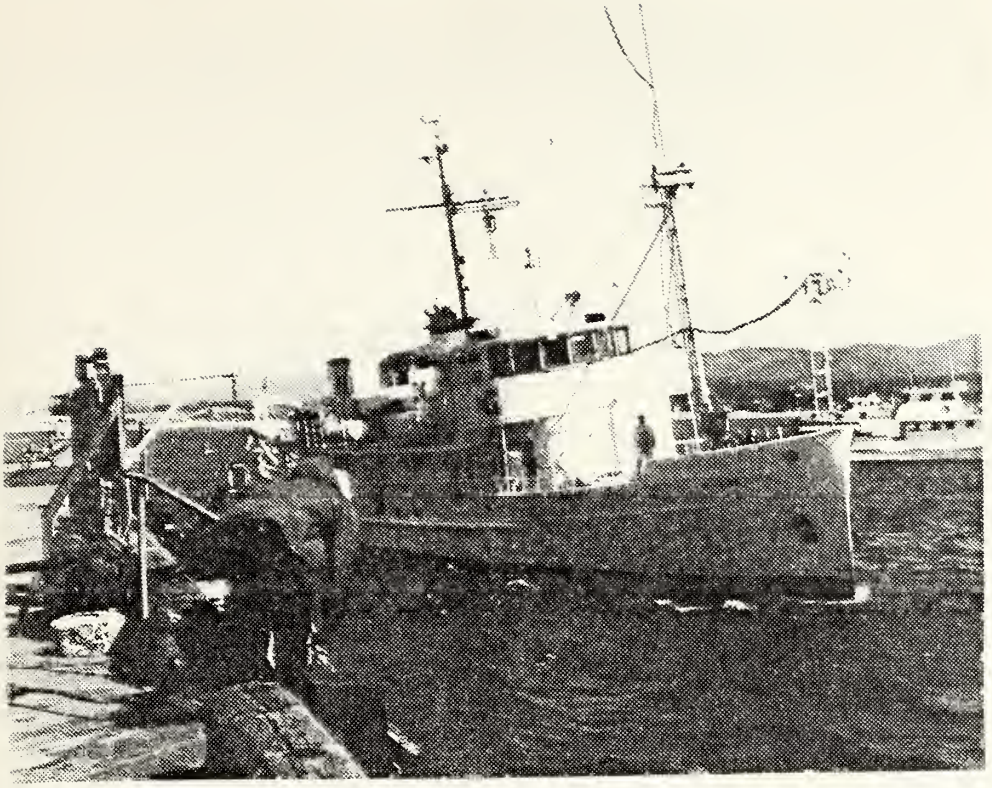

Figure 4. Spectrometer probes and lower level wind instruments mounted on the bow of the R/V ACANIA.

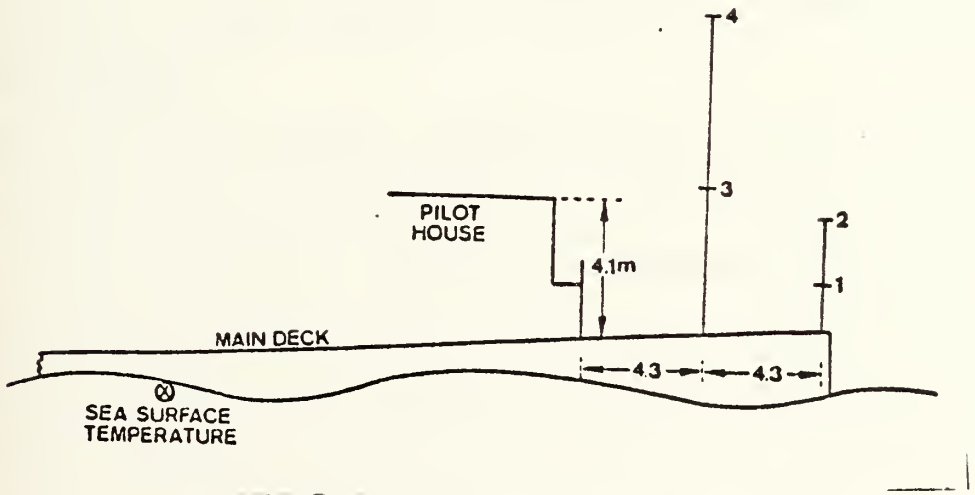

Figure 5. Sensor locations on board the R/V ACANIA: wind sensors at 2 and 4, spectrometer probes at 3.

data were corrected to agree with the ship aerosol data [Fairall, 1980 and Fairall et al, 1980]. The correction factors were used when computing the vertical extinction profiles.

Profiles of virtual potential temperature and mixing ratio were obtained from three different sources. The reason for using these two parameters, instead of temperature and dew point, is that the mixed layer and inversion are more easily identified with the former. The sources were spiral flights by the aircraft and radiosondes launched from NPS, and from the R/V ACANIA. The tracks of the ship and aircraft during the days of interest are shown in Figures 6-9 and Figures 10-16. The location of NPS is included in the ship tracks. When the R/V ACANIA was not on these tracks it was positioned between Point Pinos and Marina, (Figure 17). The locations of the ladder (L) and spiral (S) flights are given for the aircraft tracks.

Wind speed is an input variable for the Wells-Katz model, and is based on 30-minute averages observed aboard the R/V ACANIA. Some winds are averaged over shorter time periods because of maneuvering of the ship. These winds are measured at the 20.5 meter level and corrected for ship's speed and direction. In some cases the wind had to be calculated from the friction velocities calculated from aircraft measured values of the rate of dissipation of turbulent kinetic energy (ϵ). ϵ was the variable of interest in other analyses of the experiment and will not be discussed further

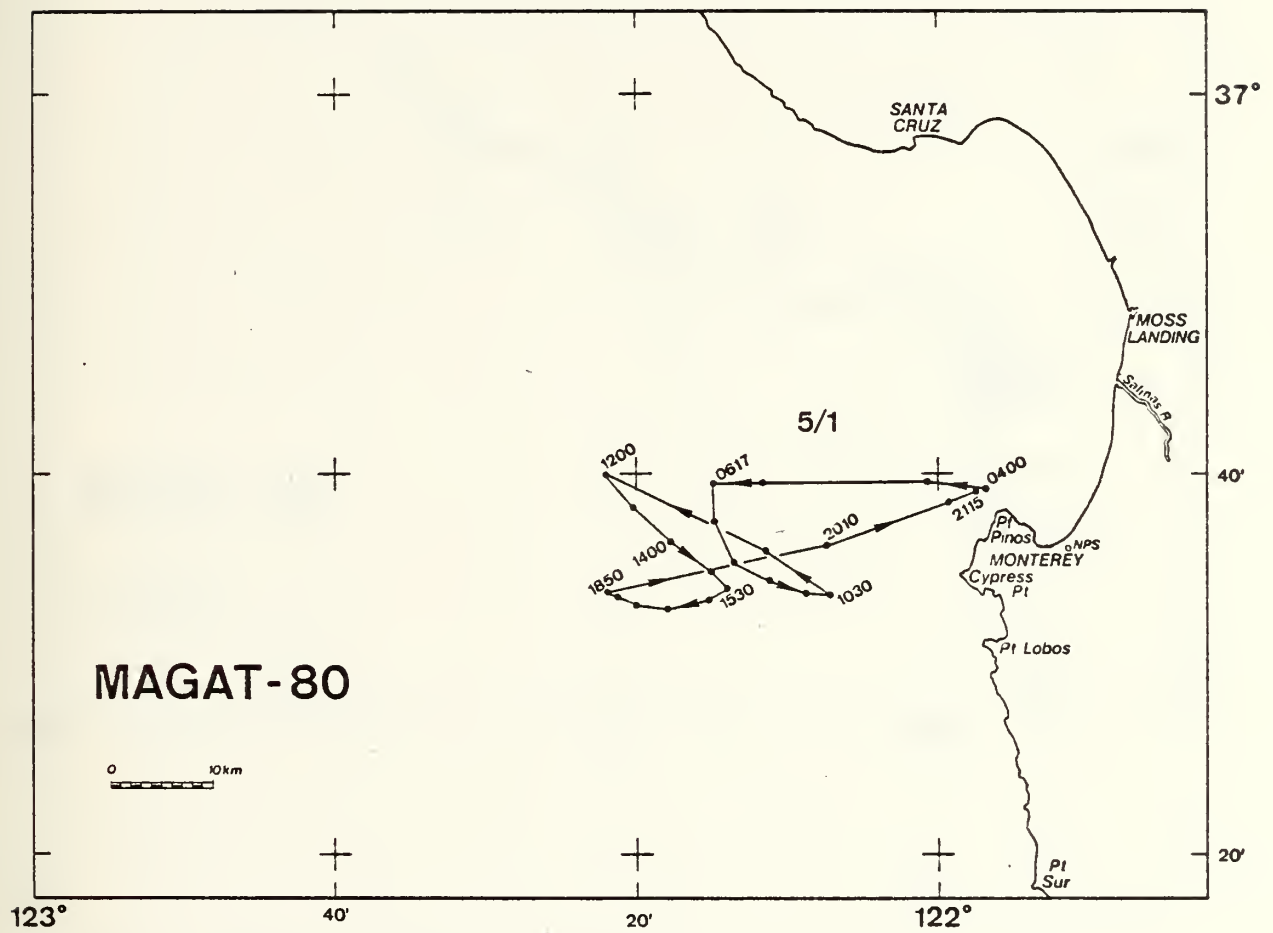

Figure 6. Cruise track of the R/V ACANIA on 1 May 1980.

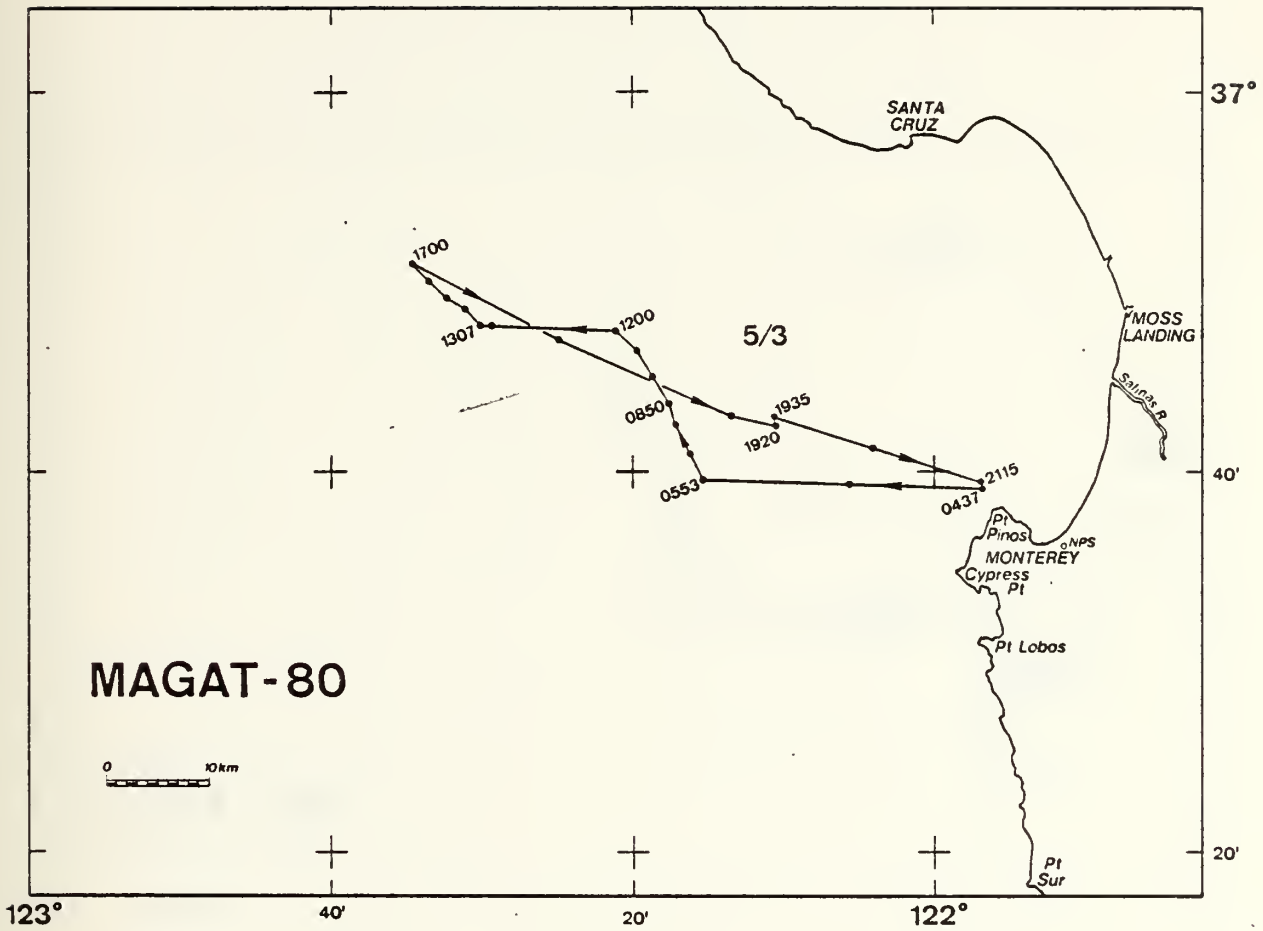

Figure 7. Same as Figure 6 except 3 May 1980.

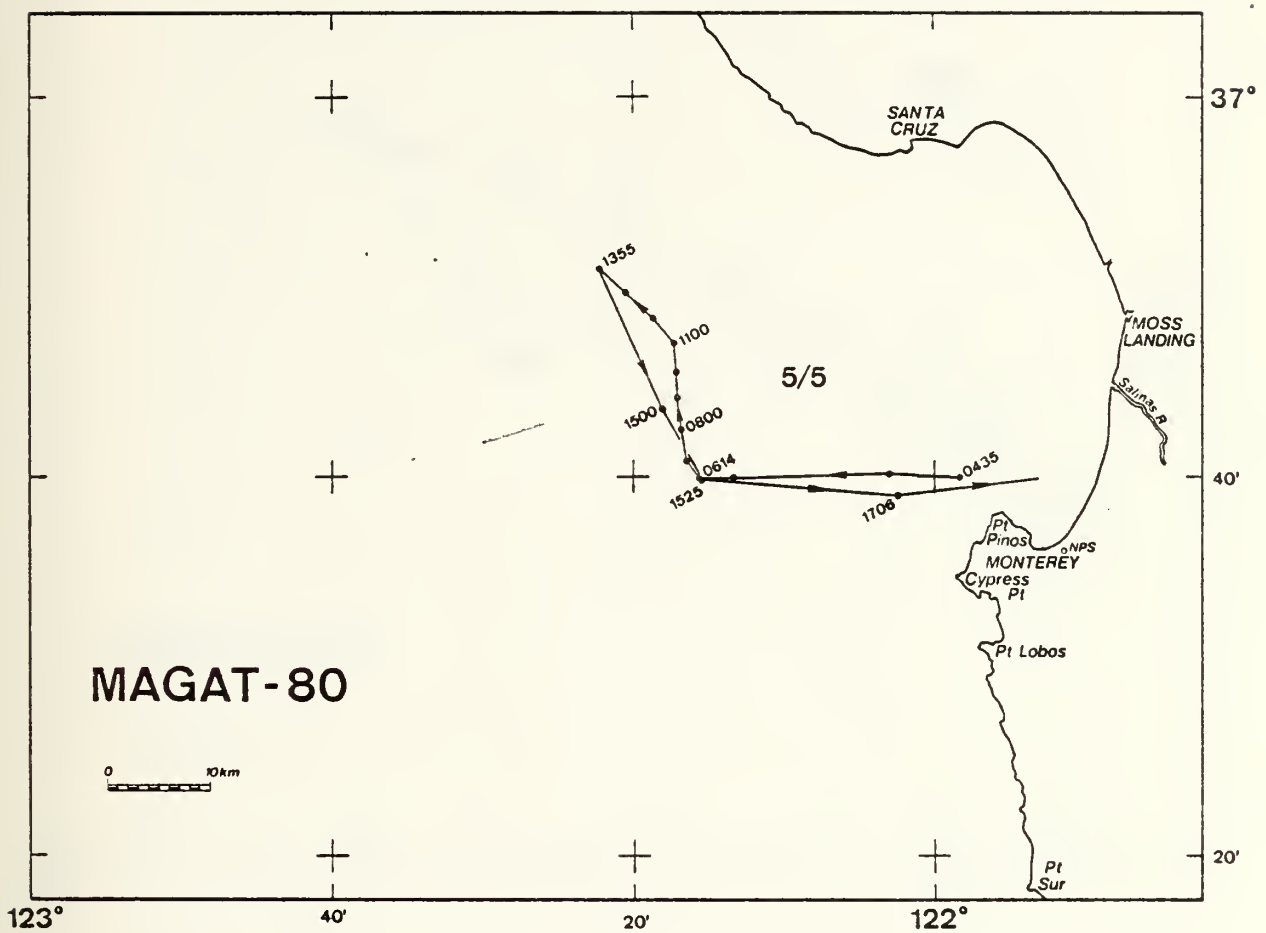

Figure 8. Same as Figure 6 except 5 May 1980.

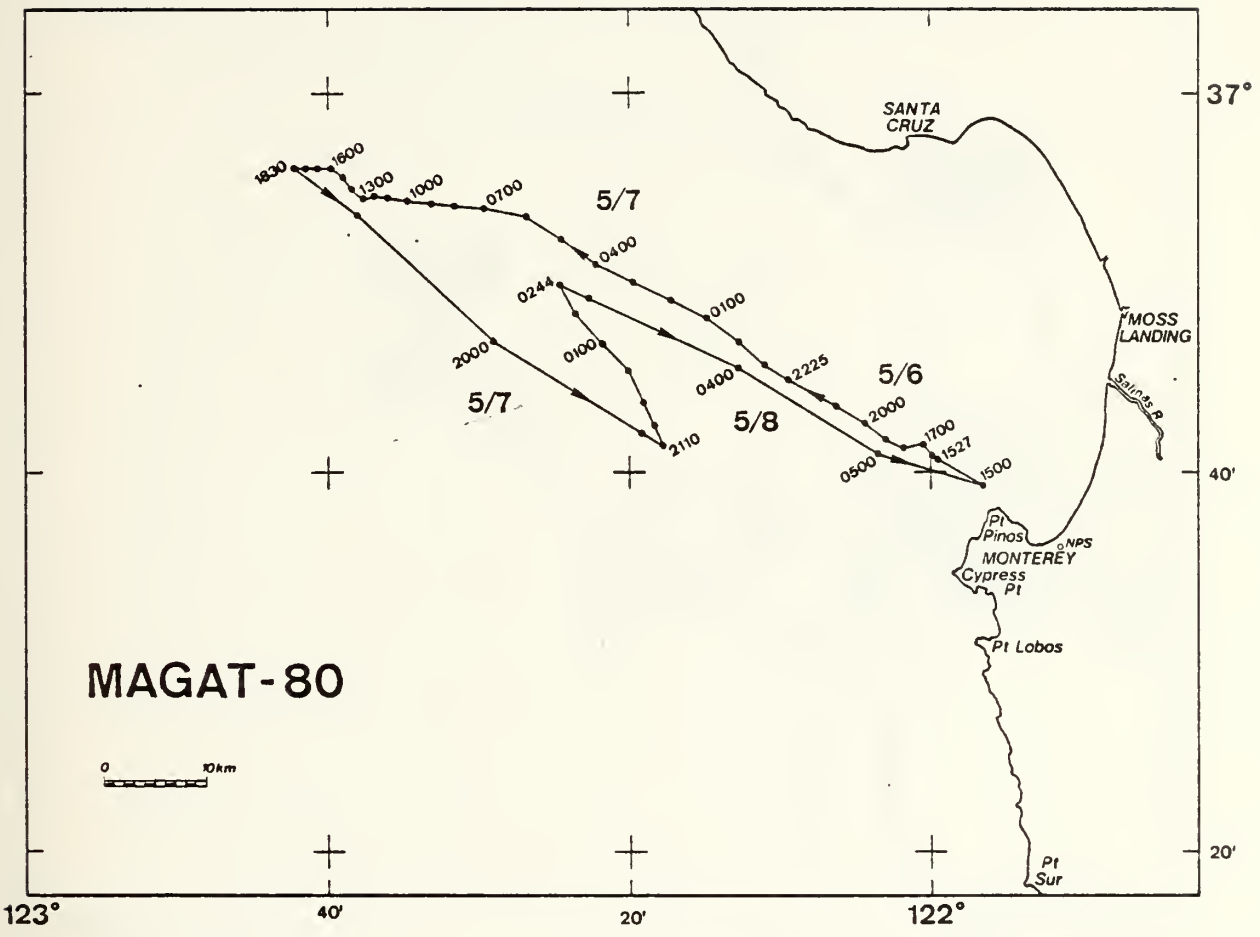

Figure 9. Same as Figure 6 except 6-8 May 1980.

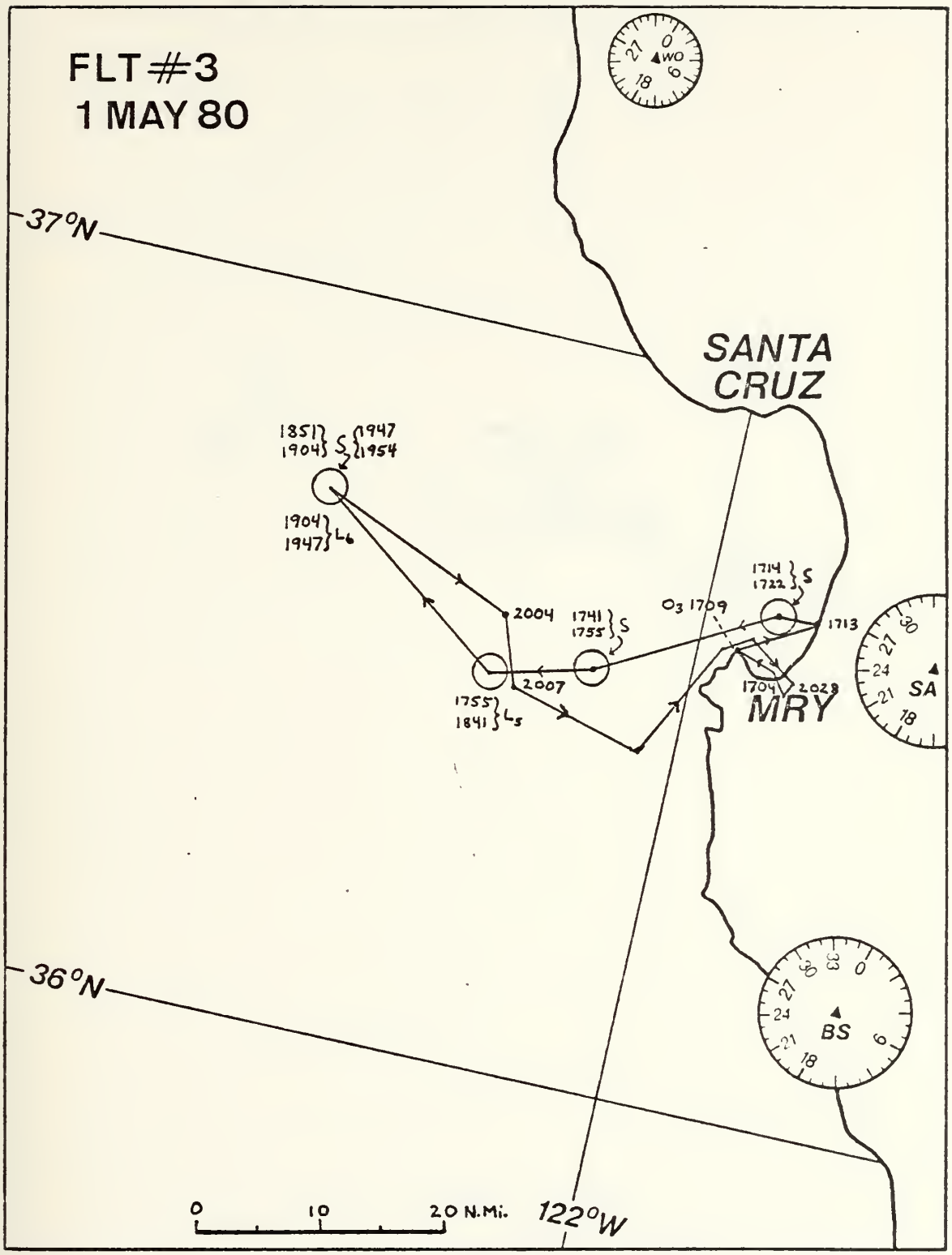

Figure 10. Flight path of the aircraft on the afternoon of 1 May 1980.

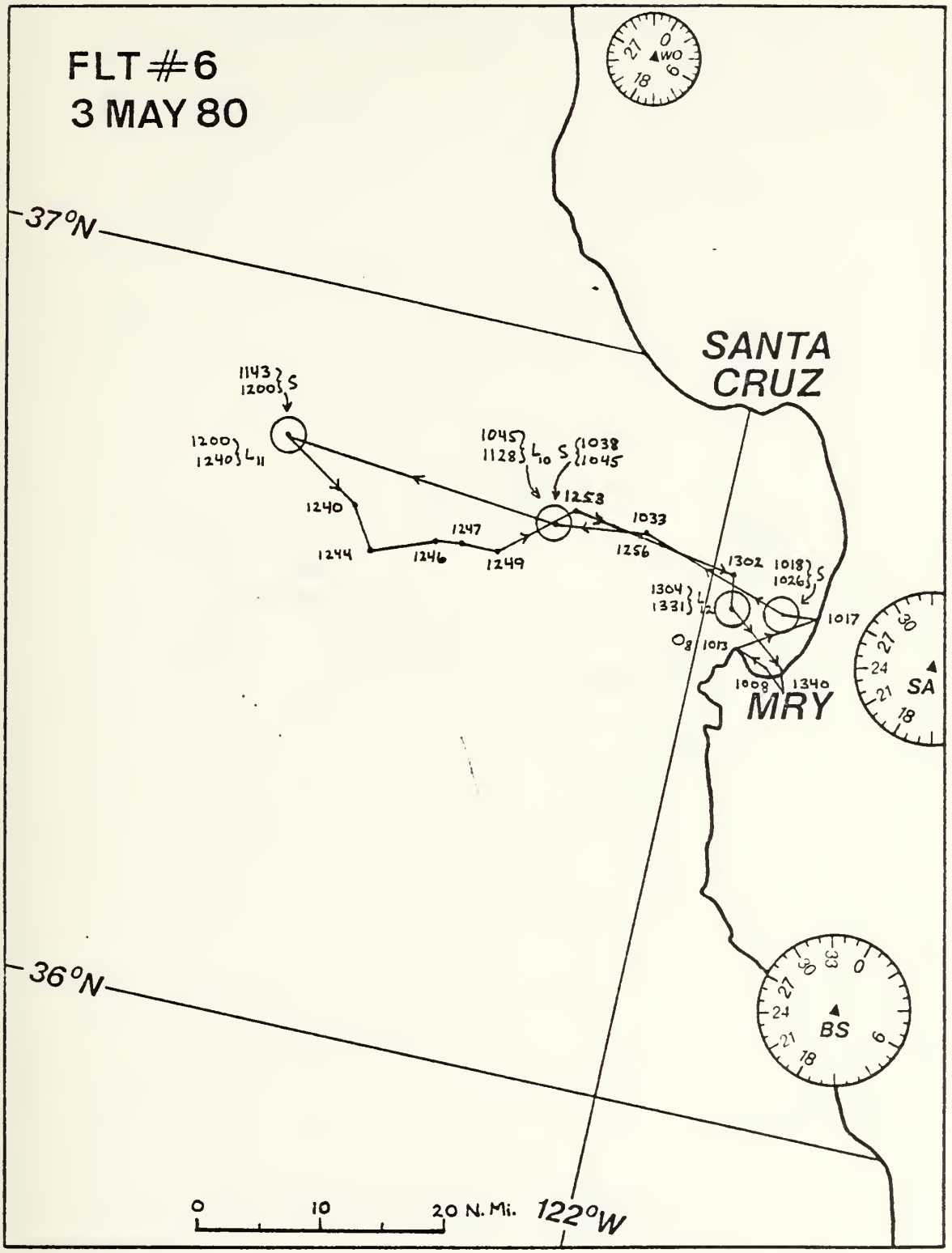

Figure 11. Same as Figure 10 except morning of 3 May 1980.

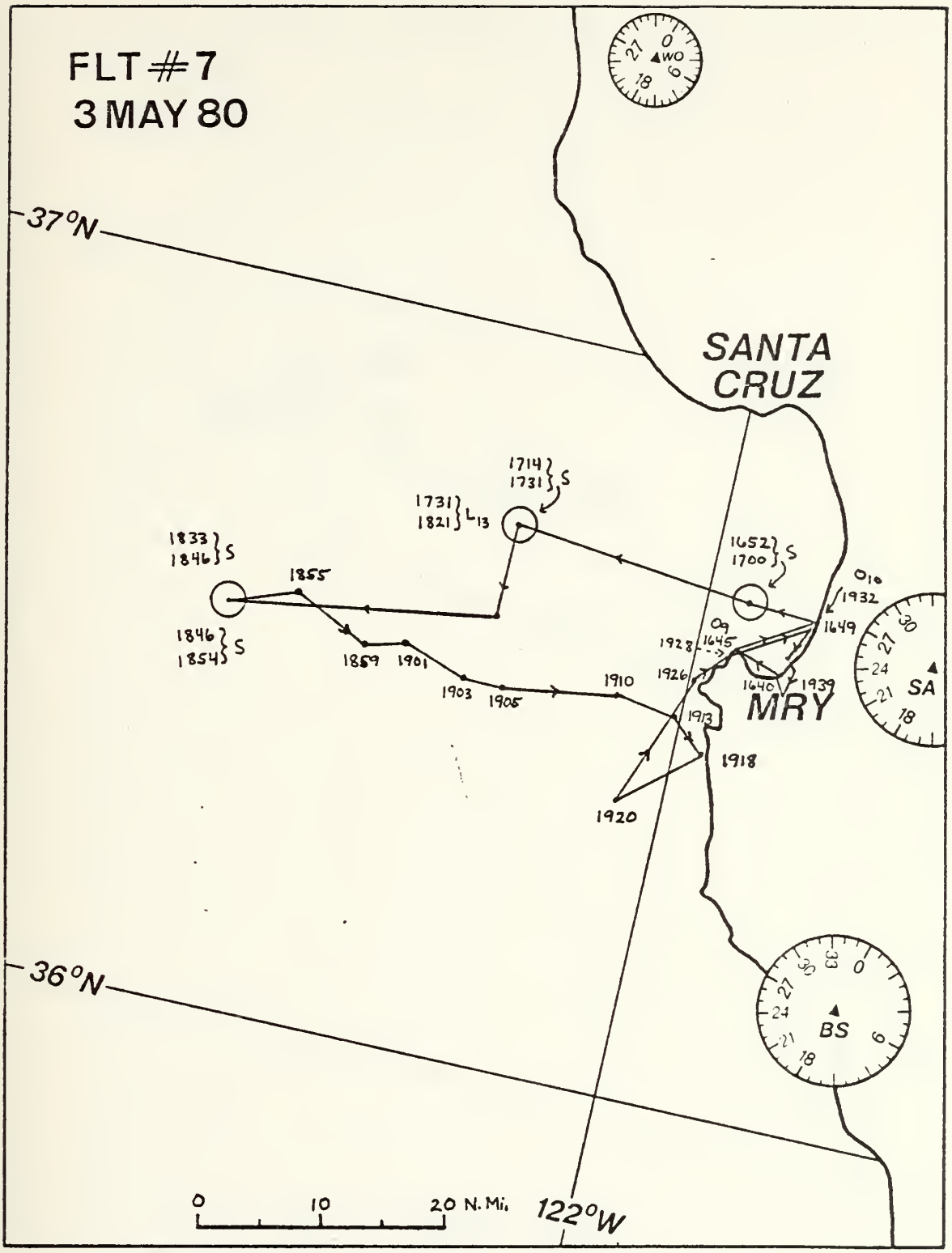

Figure 12. Same as Figure 10 except afternoon of 3 May 1980.

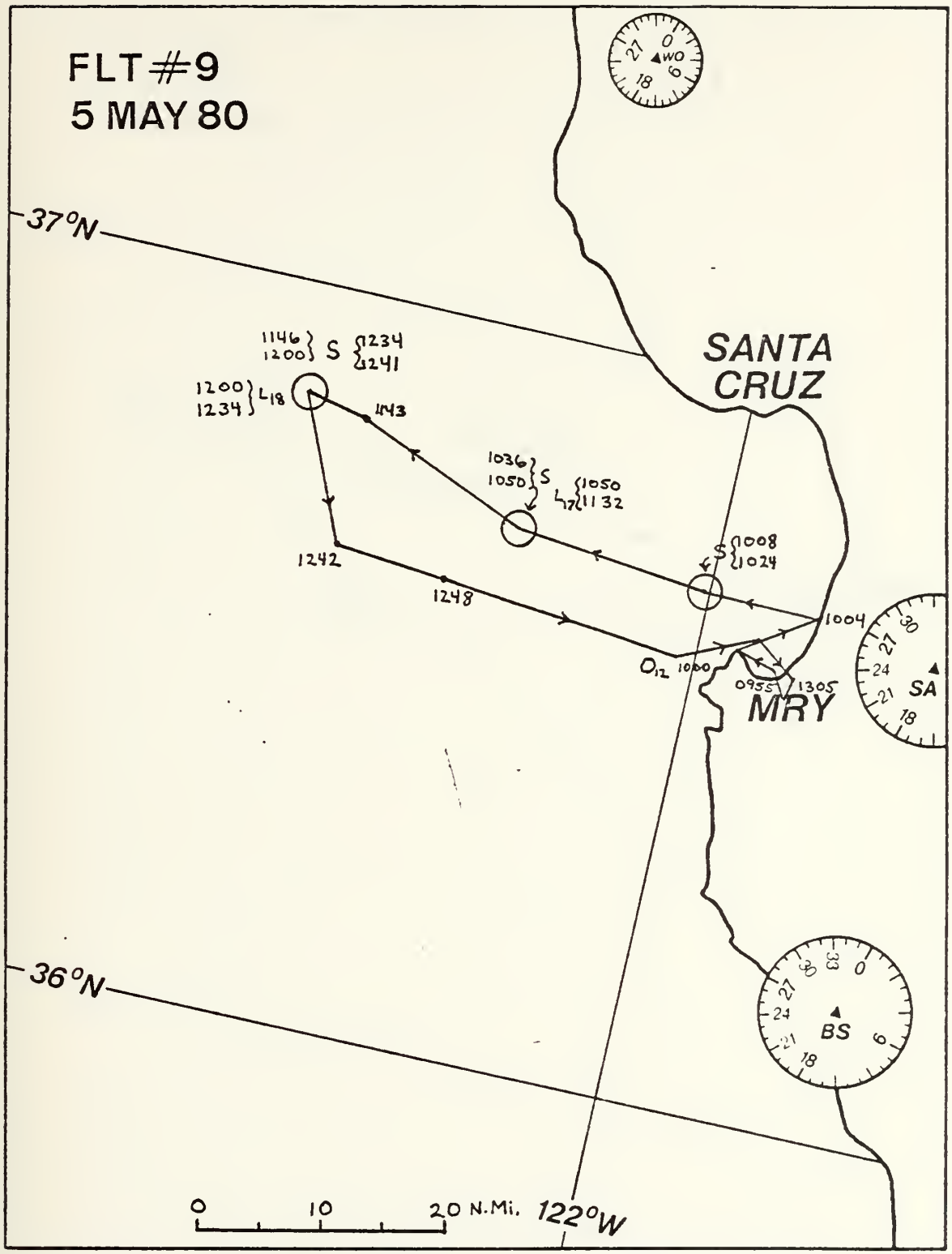

Figure 13. Same as Figure 10 except morning of 5 May 1980.

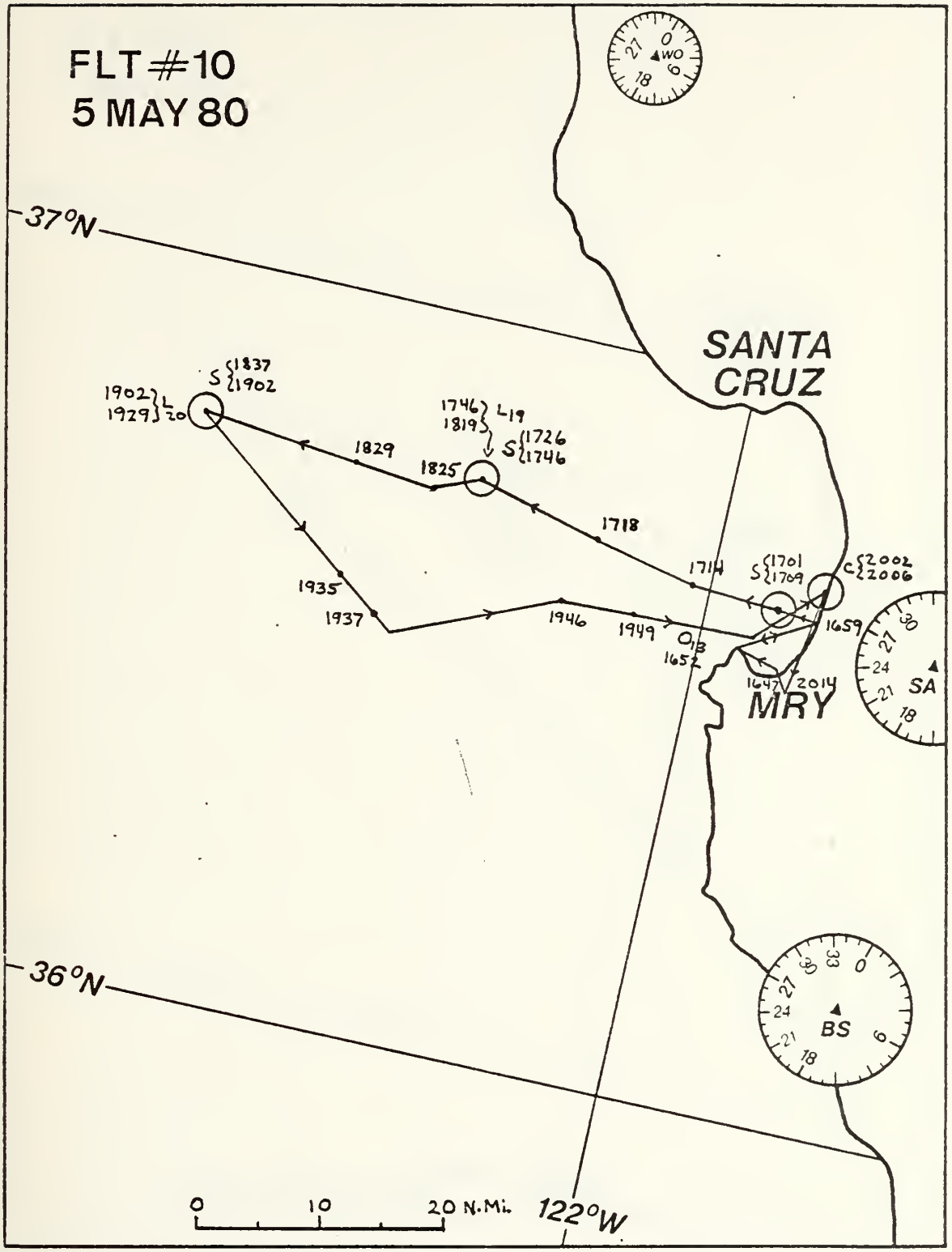

Figure 14. Same as Figure 10 except afternoon of 5 May 1980.

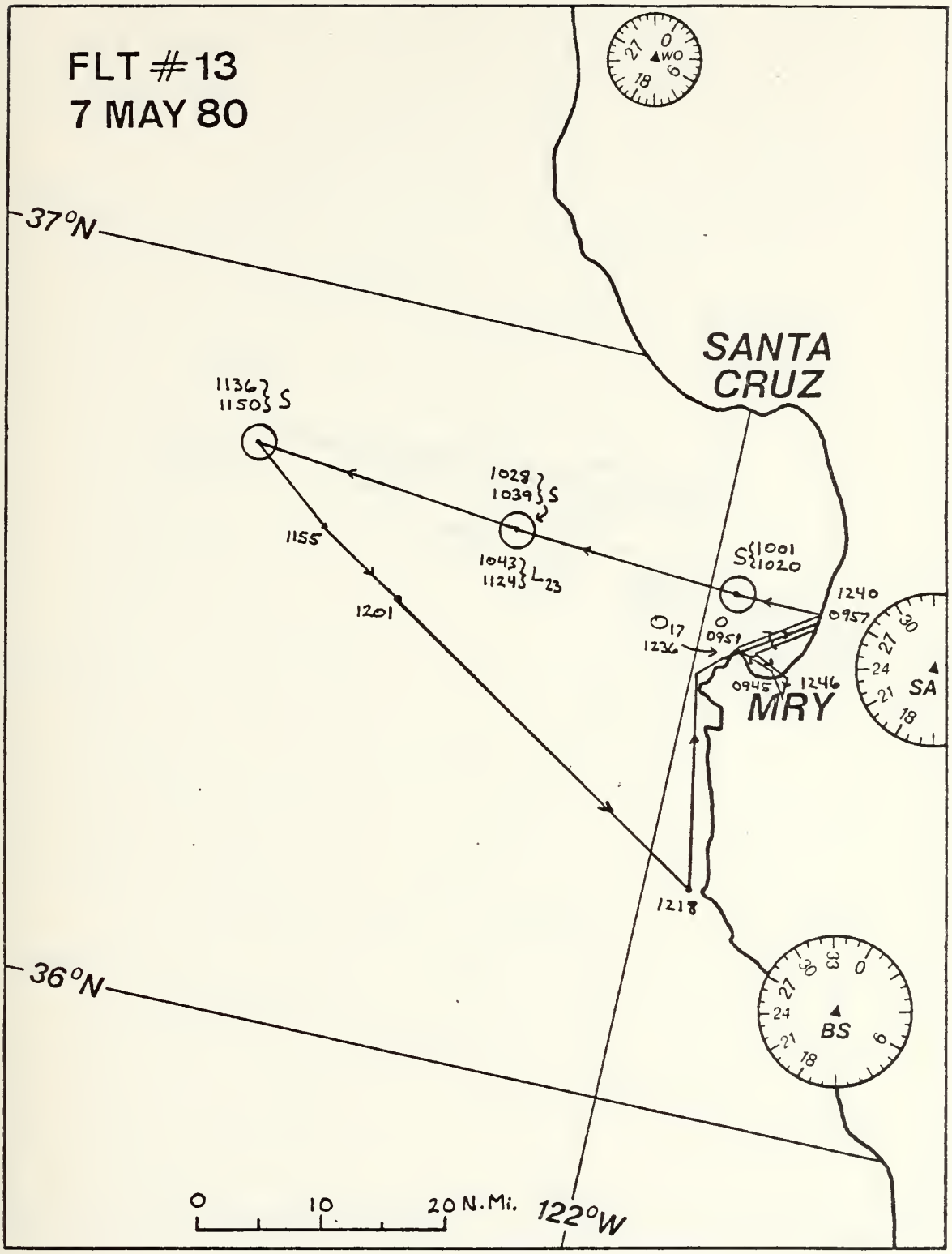

Figure 15. Same as Figure 10 except morning of 7 May 1980.

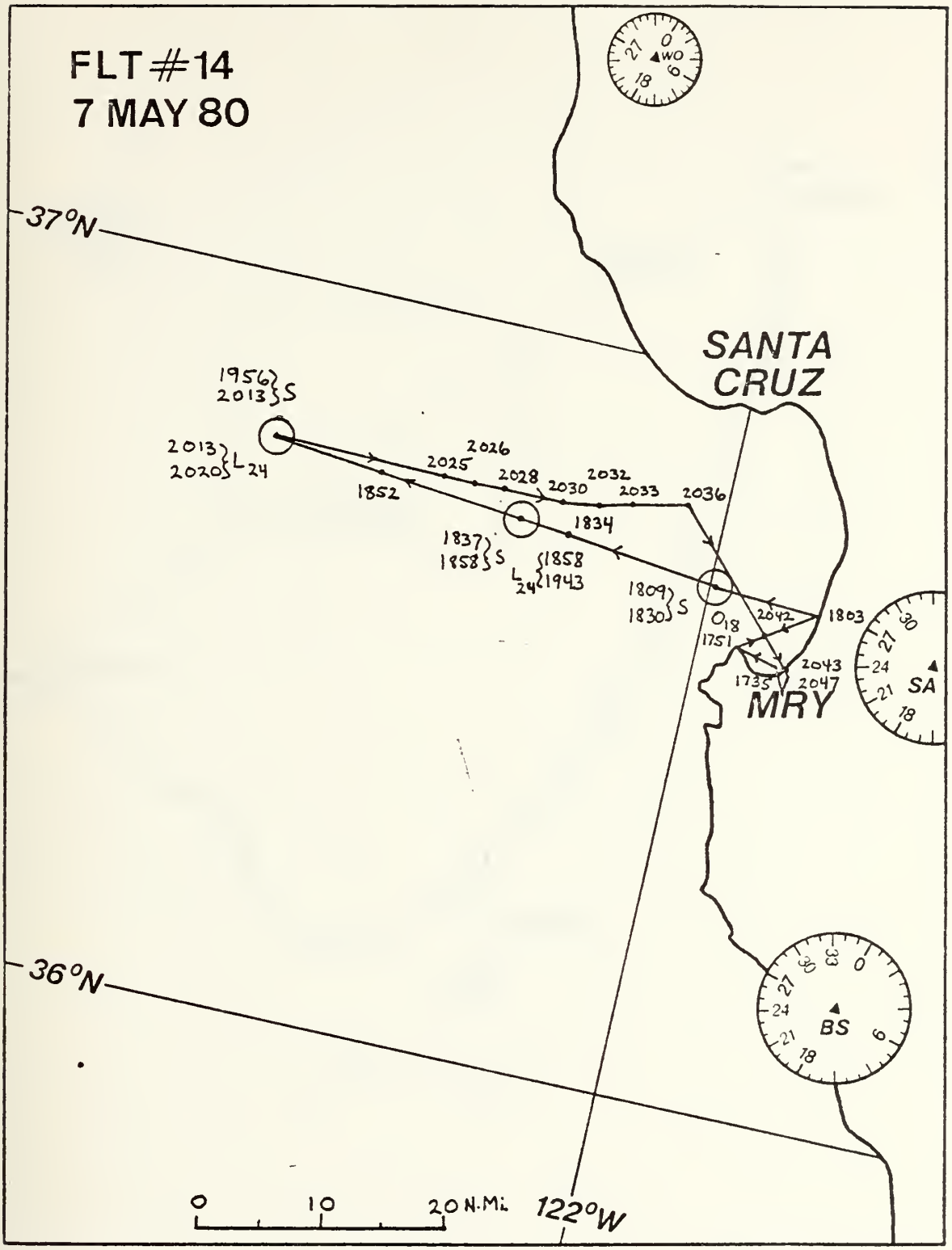

Figure 16. Same as Figure 10 except afternoon of 7 May 1980.

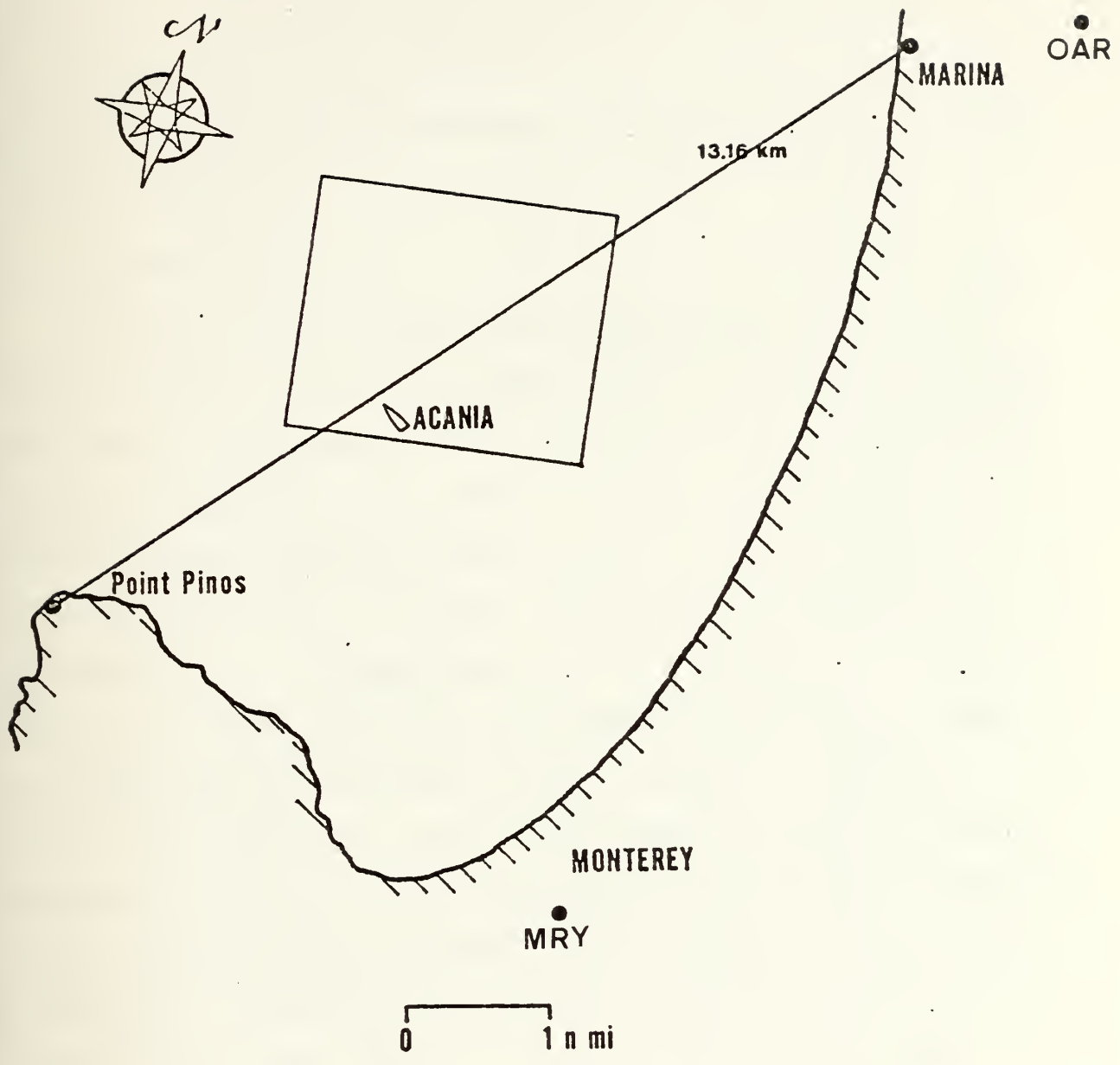

Figure 17. Map of Monterey Bay, location of the R/V ACANIA when not on track and locations of Fritzsche Field (OAR) and Monterey Airport (MRY).

here. The reason winds were estimated from aircraft measured ϵ values is that the shipboard measured winds to be representative. Wind speed is not measured by the aircraft.

Other non-aerosol instrumentation used on both the aircraft and ship are described by Fairall (1979) and Schacher et al (1980a).

D. SYNOPTIC DATA

The surface and 500 millibar synoptic charts and GOES West satellite imageries, Figures 18-25, are used to evaluate the synoptic situations. The charts used for this presentation are from NOAA weekly series of daily weather maps. Local weather conditions occurring are obtained from the U.S. Army, Fort Ord, Fritzsche Field weather observations when possible. Fritzche Field is not a 24-hour reporting station so observations from the Monterey airport are used at times when observations are not available. Fritzsche Field observations are chosen over those of Monterey airport because they are more representative of the weather conditions occurring out in the Bay where the ship and plane are operating. As shown in Figure 17, Monterey airport is protected by a land mass to the west which prevents fog from arriving at the airport until after its arrival at Fritzsche Field. Fritzsche Field is located 5 km from the Bay and 14 km to the north-northeast of NPS. Because of the land mass west of Monterey Bay and its orographic effect, fog forms west of Point Pinos and then back fills into Monterey.

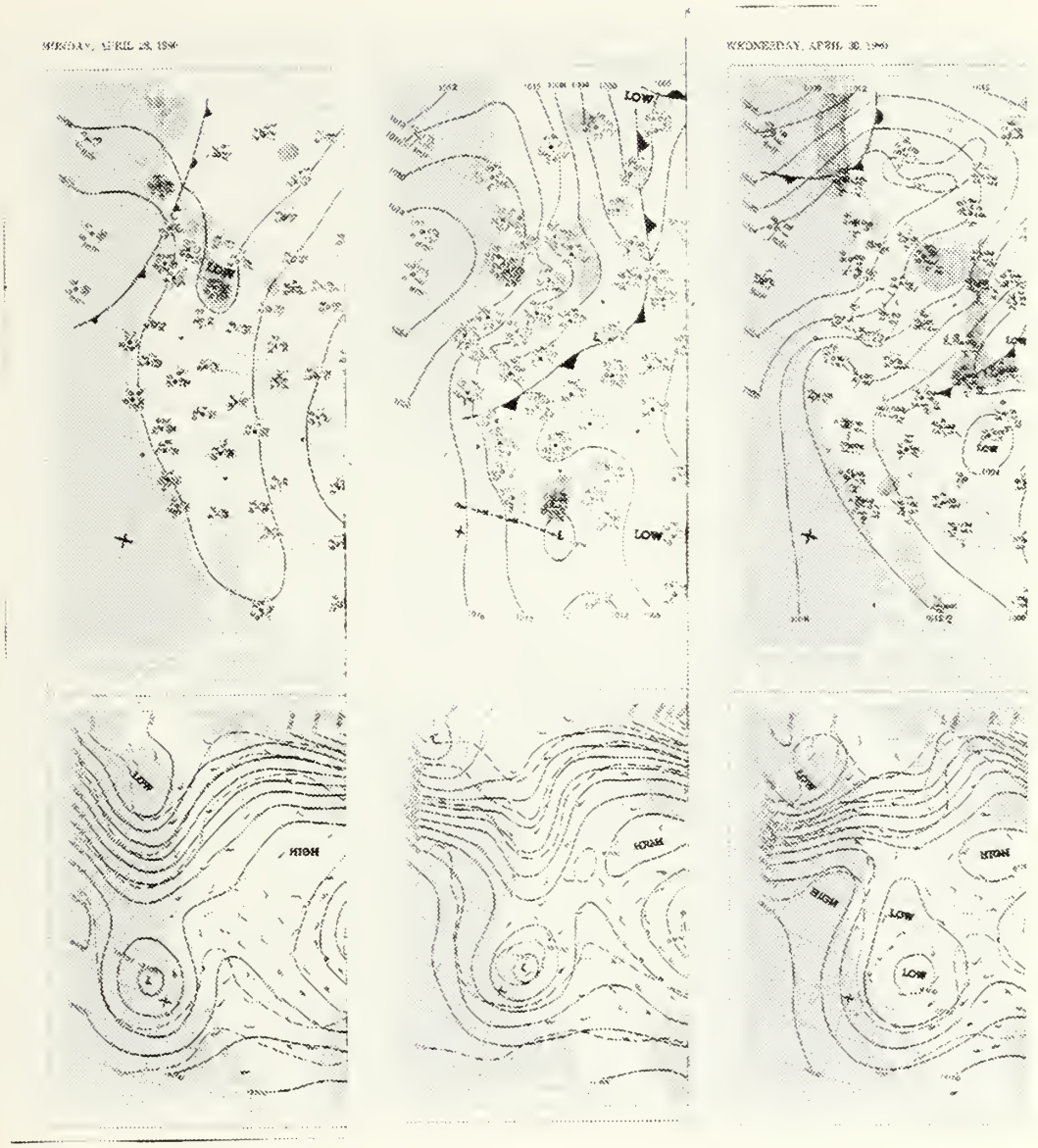

Figure 18. Surface and 500 millibar analyses for the western U.S. at 0500 PDT on 28, 29, and 30 April 1980. (NOAA)

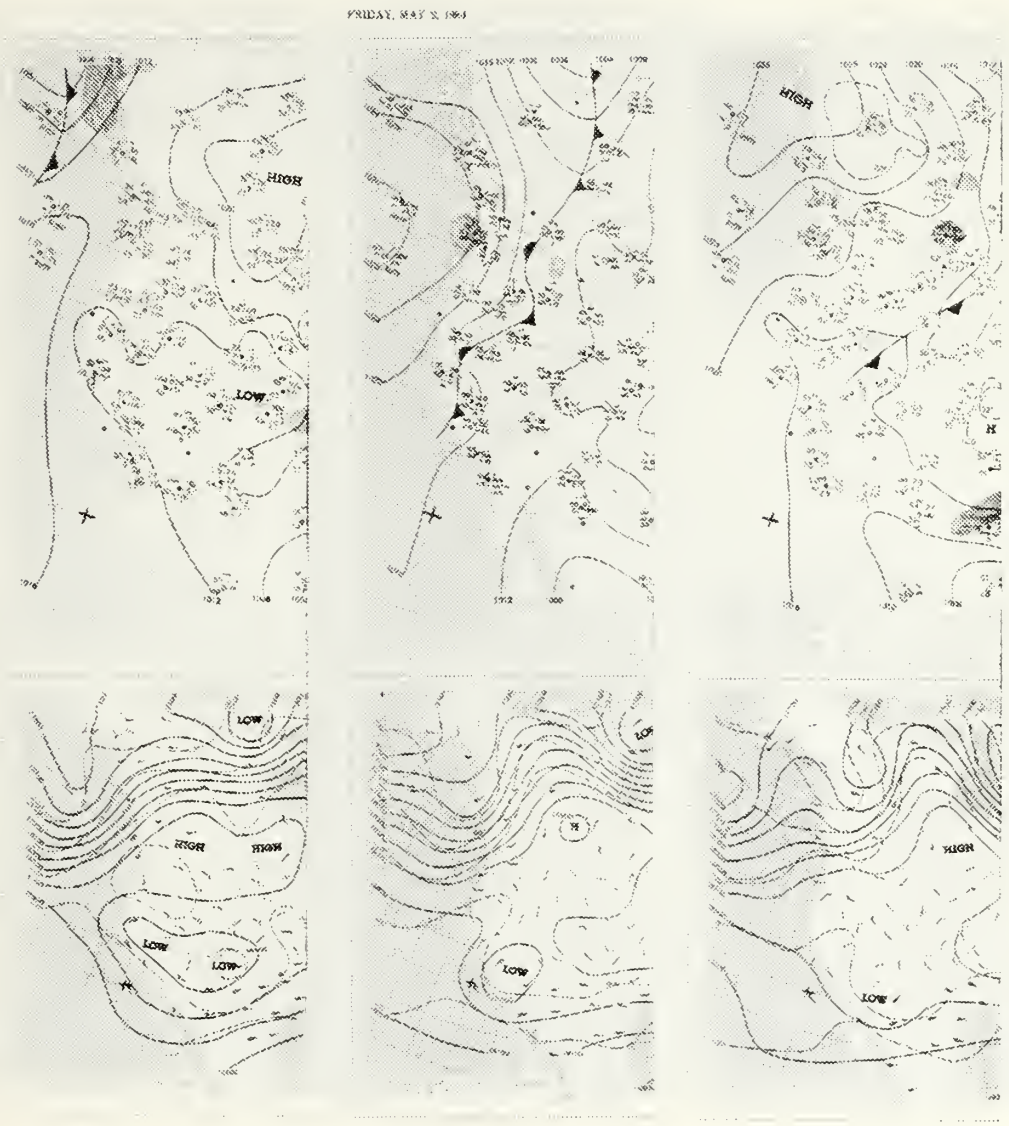

Figure 19. Same as Figure 18 except 1, 2, and 3 May 1980.

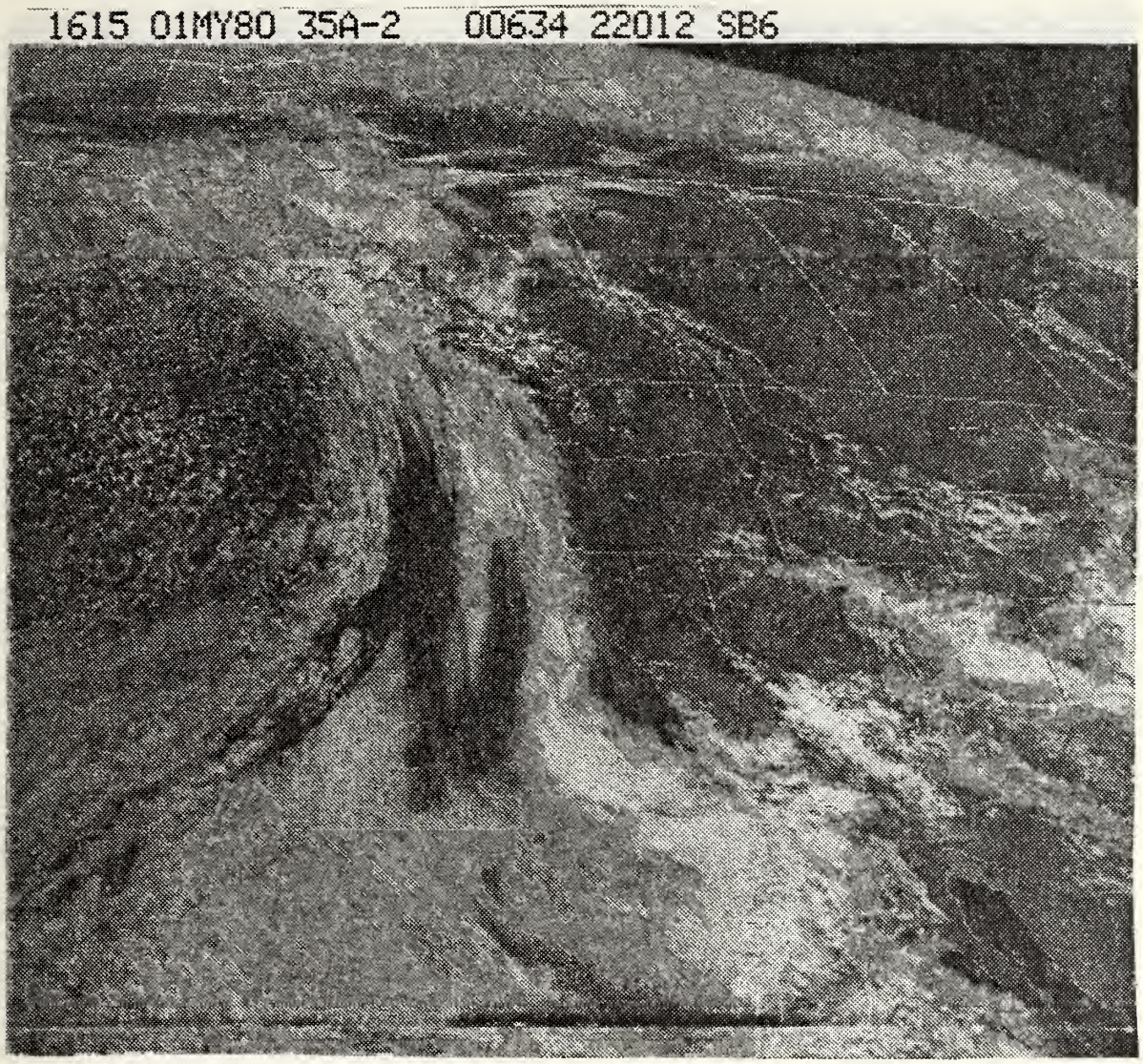

Figure 20. 1 May 1980 GOES West Satellite imagery at 0915 PDT.

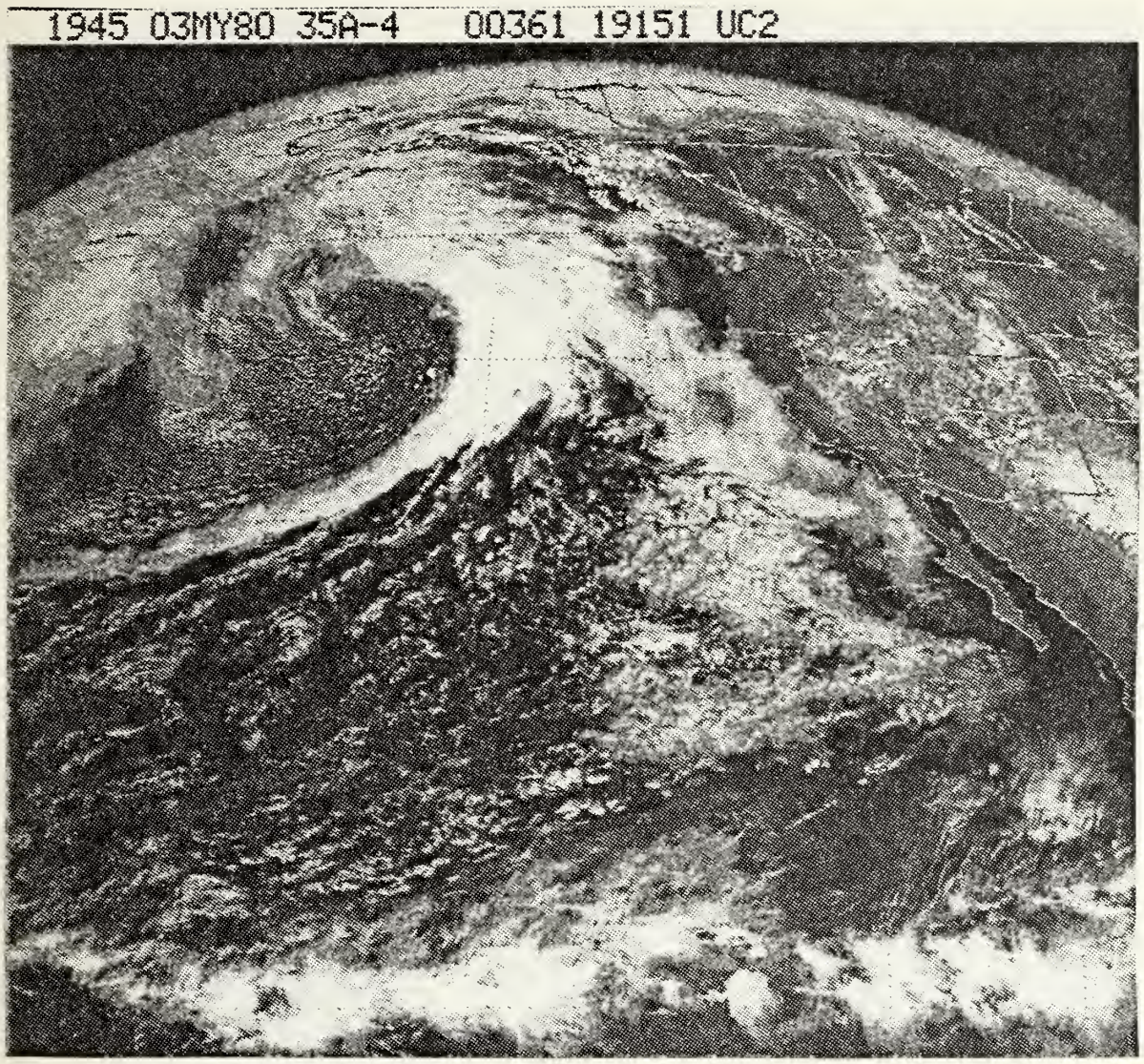

Figure 21. 3 May 1980 GOES West Satellite imagery at 1245 PDT.

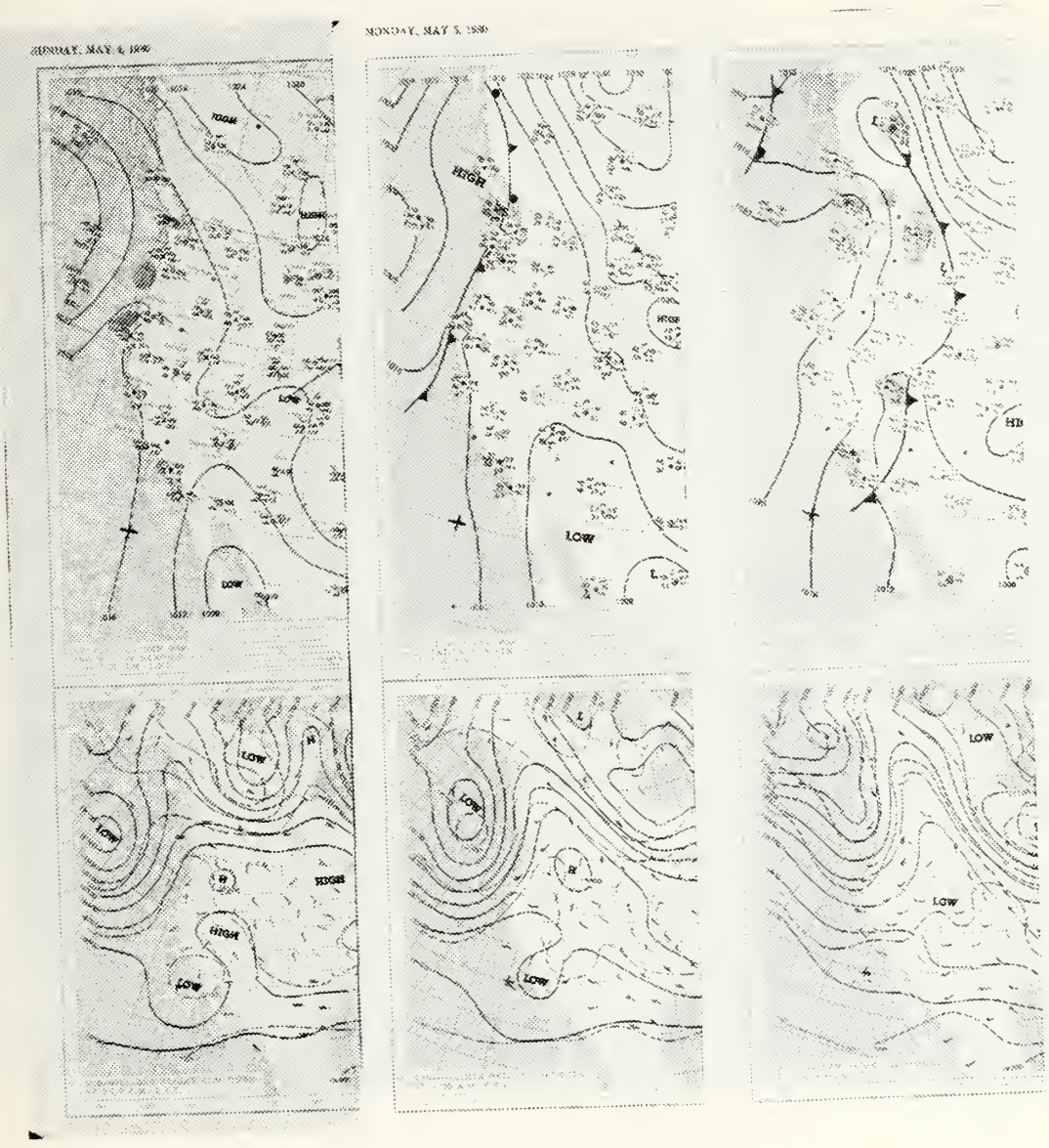

Figure 22. Same as Figure 18 except 4, 5, and 6 May 1980.

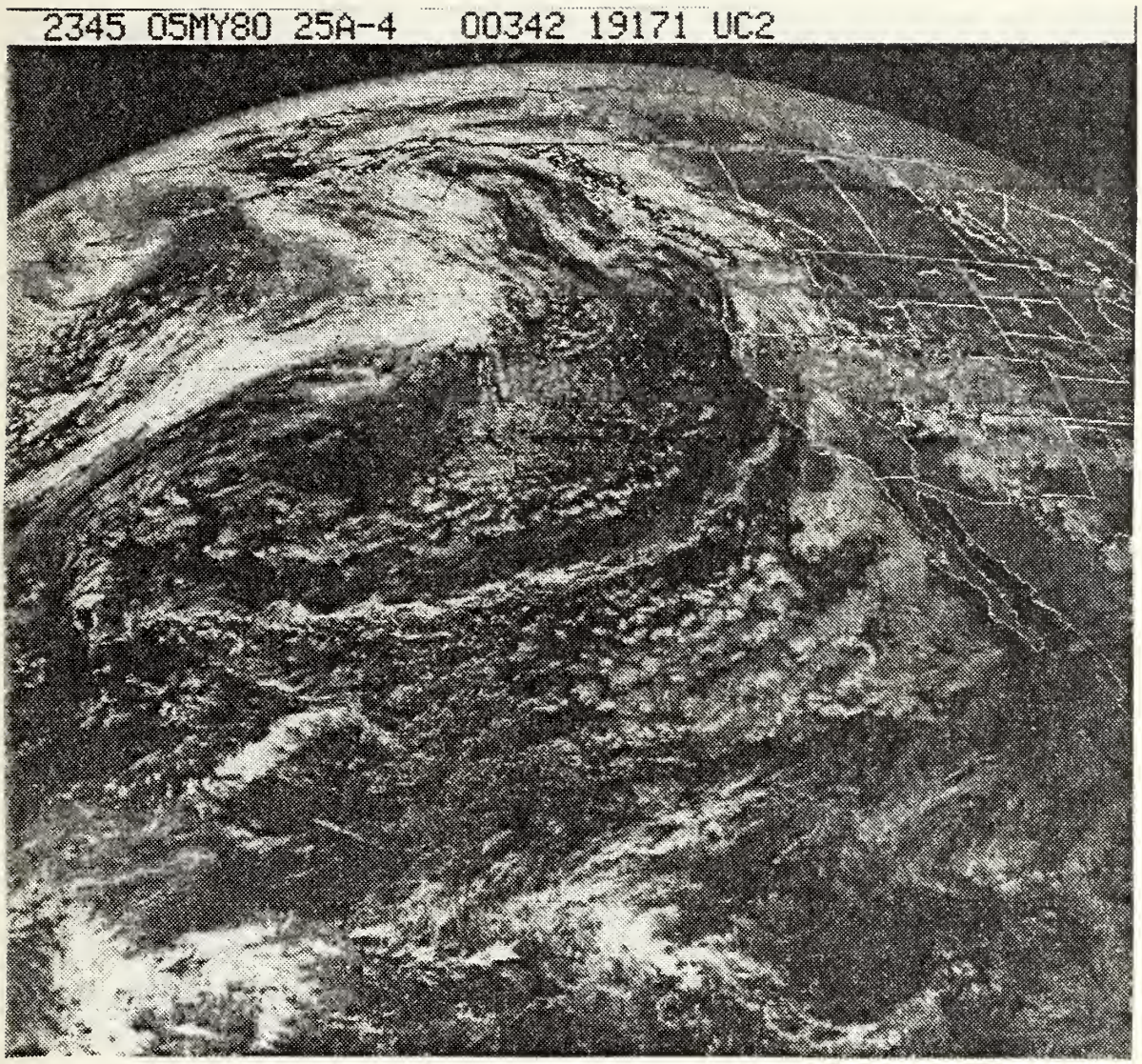

Figure 23. 5 May 1980 GOES West Satellite imagery at 1645 PDT.

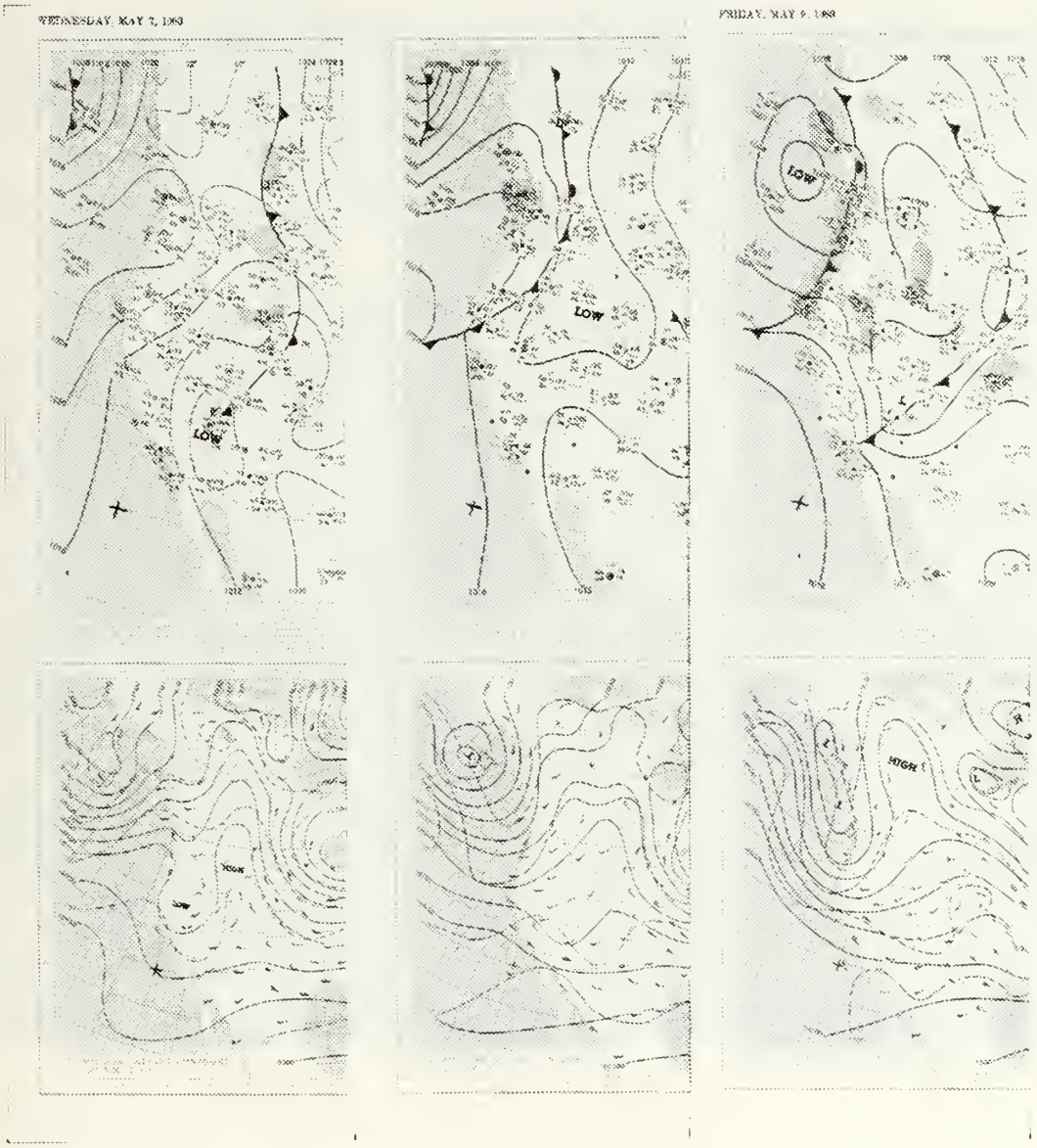

Figure 24. Same as Figure 18 except 7, 8, and 9 May 1980.

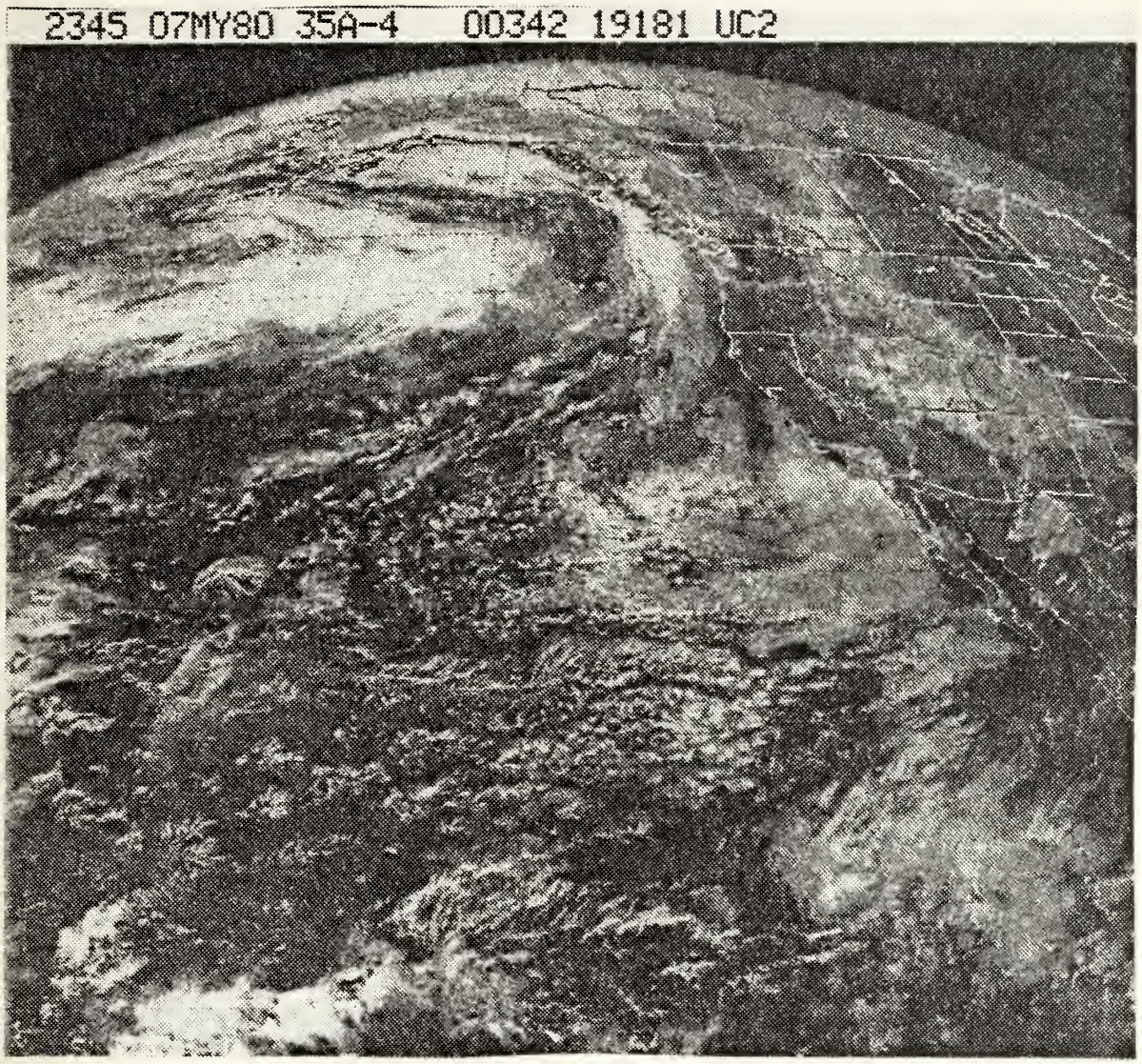

Figure 25. 7 May 1980 GOES West Satellite imagery at 1645 PDT.

IV. SYNOPTIC CONDITIONS

A. GENERAL CONDITIONS

The weather conditions were generally neutral with occasional moderately stable and moderately unstable conditions. Several weak frontal systems passed through the area during the experimental period. Showers occurred during the first and last days of the experiment in conjunction with frontal passages. Low cloudiness and fog occurred during the morning from 29 April to 5 May, with fog returning again on the 9th, the final day of the experiment.

At the beginning of the period, the area is dominated by a slowly eastward migration of a cut-off low at the 500 mb level, Figure 18 and 19. By early morning on 2 May, the area is under the influence of a weak ridge, Figure 19. On 3 May, the area is under divergent flow at the upper level, Figure 19. An upper level low has formed off of Baja, California on 4 May leaving the area under an influence of a Col, Figure 22. On 5 May, the area is between a trough and a ridge (Figure 22), and by 6 May, the area is on the backside of the trough (Figure 22). Because of deepening of the trough, the area is still on the backside of the trough on 7 May, Figure 24. A new upper level trough formed and is approaching the area on the final two days (8-9 May) of the experiment, Figure 24.

Surface winds are relatively light, 0 to 10 kt, during the period and increase toward the end of the period to 16 kt, with gusts to 22 kt.

An important feature in these interpretations is the nature of the mixed layer, often topped by an inversion, with regard to stability and hence mixing intensitites. It is assumed that mixing becomes greater as conditions become more unstable.

At the start of the experiment, the mixed layer exhibits stable to slightly stable conditions until around 1800 PDT 28 April when conditions become more neutral. The neutral condition remains until 1 May when conditions once again become stable. A weak frontal passage before 0500 PDT on 29 April does not appear to affect conditions of the mixed layer feature. The mixed layer remains stable until a frontal passage on 2 May when conditions become neutral and remains as such until 5 May. In the morning of 5 May, conditions are slightly stable, returning to neutral on 6 May, despite a frontal passage at 1300 PDT on the fifth. They remain neutral from 5 May to the end of the experiment on 9 May.

B. MIXED LAYER AND AEROSOL EXTINCTION RESULTS

Days chosen for further analysis are 1, 3, 5, and 7 May. Reasons for these choices are presented with the description of these days. On the first, the area is under the influence of a surface low in Colorado, with a frontal system approaching from the northwest, Figure 19. On the third,

the area is on the backside of a rather weak frontal system, which passed through early on the second, Figure 19. On the fifth, a frontal system passes through the area at approximately 1300 PDT (Figure 22), at this time the visibility improved to 25 miles and later to 45 miles. On the seventh, the area is behind the frontal system which passed through on the fifth while another system is approaching from the northwest, Figure 24.

The results are shown in the vertical profiles of specific humidity, virtual potential temperature, relative humidity, and comparisons of observed and predicted aerosol extinction at the 3.75 micron wavelength. The 3.75 micron wavelength is chosen because it is the wavelength used by Hughes (1980) and Hughes and Richter (1980). The locations of the ladder flights, from which the profiles were obtained, are designated L in the aircraft flight paths given in Figures 10-16. The ladder profiles have corresponding spiral profiles which appear in Figures 10-16.

The profiles of virtual potential temperature and specific humidity obtained by spiral and radiosonde ascents are shown in the following description of the chosen days. An aspect of these profiles will be the difference occurring between the locations and the types of measurement (spiral or radiosonde). These differences are described but there is no attempt to interpret the reason unless the difference represents an obvious horizontal change in the mixed layer depth. The objective in presenting the various profiles

is to provide a general picture of the mixed layer conditions. The general mixed layer depth and structure is viewed as a synoptic scale aspect of the observed extinction profiles.

1. 1 May 1980

The first of May is chosen because of a parallel research study pertaining to the use of satellite anomalous gray shades to predict extinction [Schultz, 1981].

The surface winds are light and the surface layer is unstable throughout most of 1 May becoming stable at the end of the day (Table I). The area is under the influence of a surface low in Colorado, with a frontal system approaching from the northwest, Figure 19. The early morning hours are dominated by low cloudiness and fog until 1000 PDT. The skies become scattered and visibilities improve after 1000 PDT, with the greatest visibility being 25 miles.

The airborne (spiral) profiles, Figures 26-28, show near-neutral to stable conditions within the mixed layer and stable conditions above. From 1710 to 1852 PDT, the mixed layer depth decreases from 450 to 300 m along a line extending from 13 to 76 km west of NPS, Figure 10. The soundings from the R/V ACANIA (Figure 29) and NPS (Figure 30) show very unstable conditions near the surface. The R/V ACANIA was 43 km west of NPS, Figure 6. The NPS sounding could be influenced by heat rising from the land. The ACANIA sounding, 1225 PDT (Figure 29), has lower virtual potential temperatures than the spiral profiles which also causes the mixing ratio to have lower values because it is computed from relative humidity and temperature measurements.

TABLE I

Surface Layer Values 1 May 1980

U is wind/speed (m/s), T(^{o}c) is temperature in degrees celsius, T_s(^{o}c) is sea surface temperature in degrees celsius, RH(%) is relative humidity in percent, and Z/L is the stability index.

Time	U	T(^{o}C)	Ts(^{o}c)	RH(%)	Z/L
05:00	3.5	12.02	12.61	92	-2.13E-01
05:30	4.8	11.89	12.99	91	-2.04E-01
06:00	3.3	11.87	13.04	93	-4.97E-01
06:30	2.8	11.90	13.41	93	-9.17E-01
07:00	1.7	12.10	13.41	92	-2.02E-00
07:42	3.1	12.17	13.47	93	-6.51E-01
08:30	4.4	12.19	13.35	95	-2.55E-01
09:00	4.8	12.44	13.07	92	-1.23E-01
09:30	4.3	12.53	13.02	92	-1.23E-01
10:00	4.6	12.44	13.09	93	-1.33E-01
10:30	4.2	12.49	13.27	93	-2.04E-01
11:00	1.5	12.64	13.36	92	-1.50E-00
11:30	1.0	12.96	13.84	90	-4.09E-00
12:00	0.9	12.96	14.46	89	-7.62E-00
12:09	1.9	13.00	14.43	89	-2.03E-00
12:30	2.5	13.08	14.53	88	-1.20E-00
13:00	2.0	13.25	15.01	87	-2.18E-00
13:30	1.7	13.46	15.60	86	-3.46E-00
14:00	1.6	13.68	16.03	86	-4.50E-00
14:30	1.2	13.95	15.89	85	-5.96E-00
15:00	0.8	14.14	15.63	84	-8.95E-00
15:30	1.8	14.34	15.36	84	-1.67E-00
16:00	2.2	14.37	15.75	83	-1.58E-00
16:30	3.1	14.59	15.66	81	-6.56E-01
17:00	4.5	14.69	15.07	79	-1.36E-01
17:30	5.4	14.62	14.83	80	-6.19E-02
18:00	4.9	14.66	14.66	81	-3.57E-02
18:30	4.5	14.62	14.70	83	-5.94E-02
18:51	4.9	14.57	14.51	83	-2.14E-02
21:00	5.7	13.91	13.64	87	8.51E-03
21:30	6.6	14.36	13.40	81	4.52E-02
23:37	2.3	13.64	13.15	84	3.18E-01

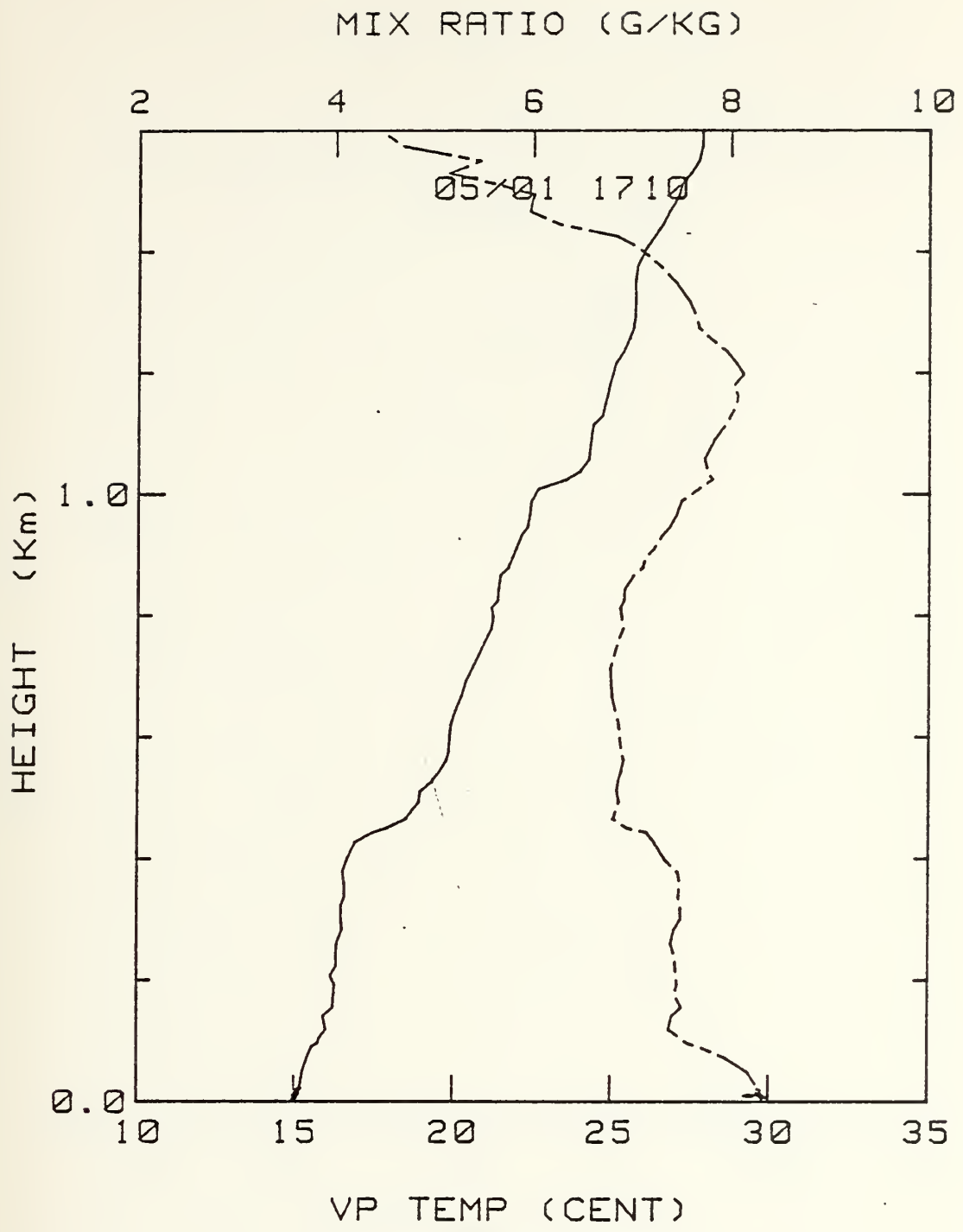

Figure 26. 1 May 1980 at 1710 PDT. Aircraft profile of virtual potential temperature (bottom scale, in degrees Celsius), solid line, and mixing ratio (top scale, in grams per kilogram), broken line, versus height.

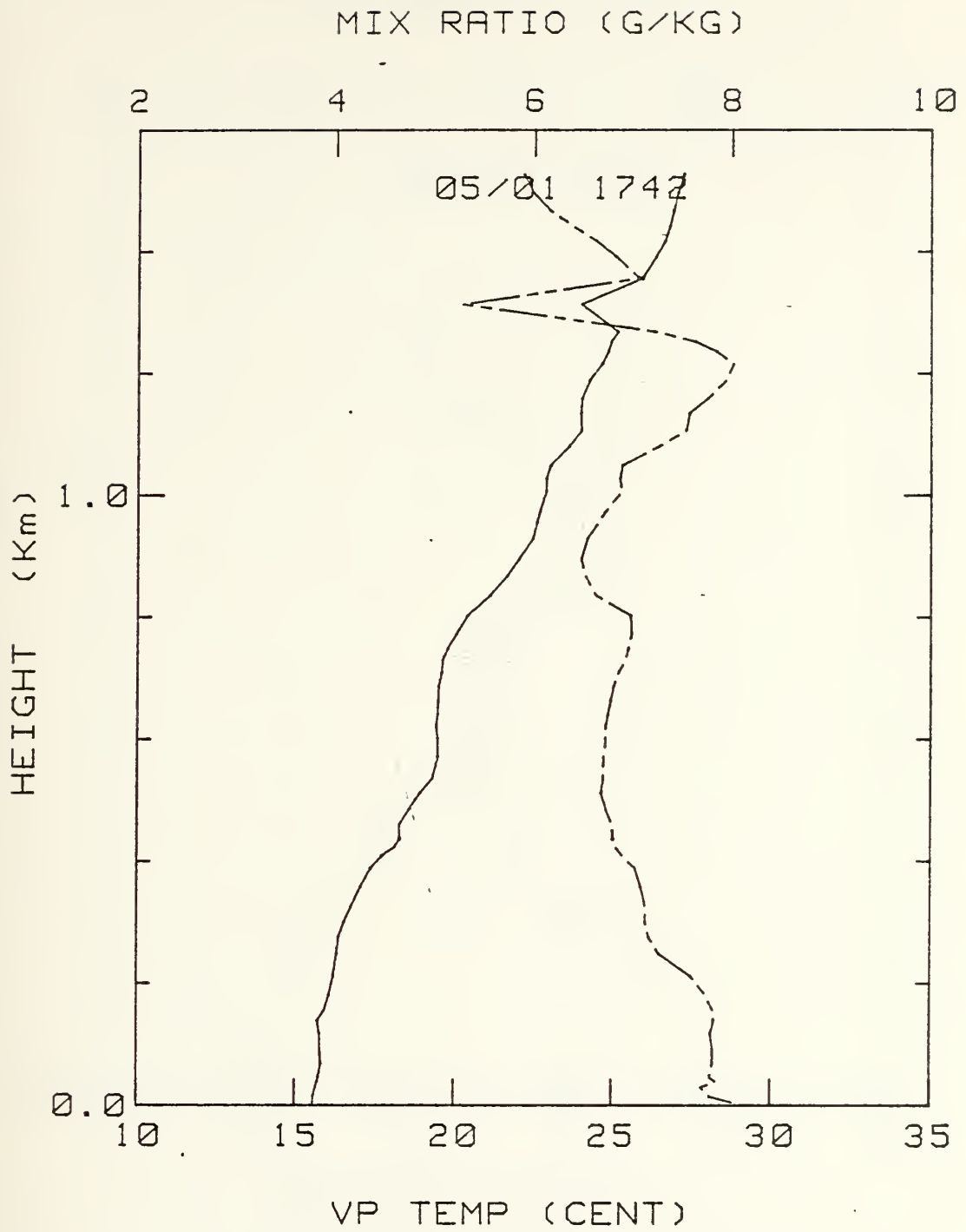

Figure 27. 1 May 1980 at 1742 PDT. Aircraft profile of virtual potential temperature (bottom scale, in degrees Celsius), solid line, and mixing ratio (top scale, in grams per kilogram), broken line, versus height.

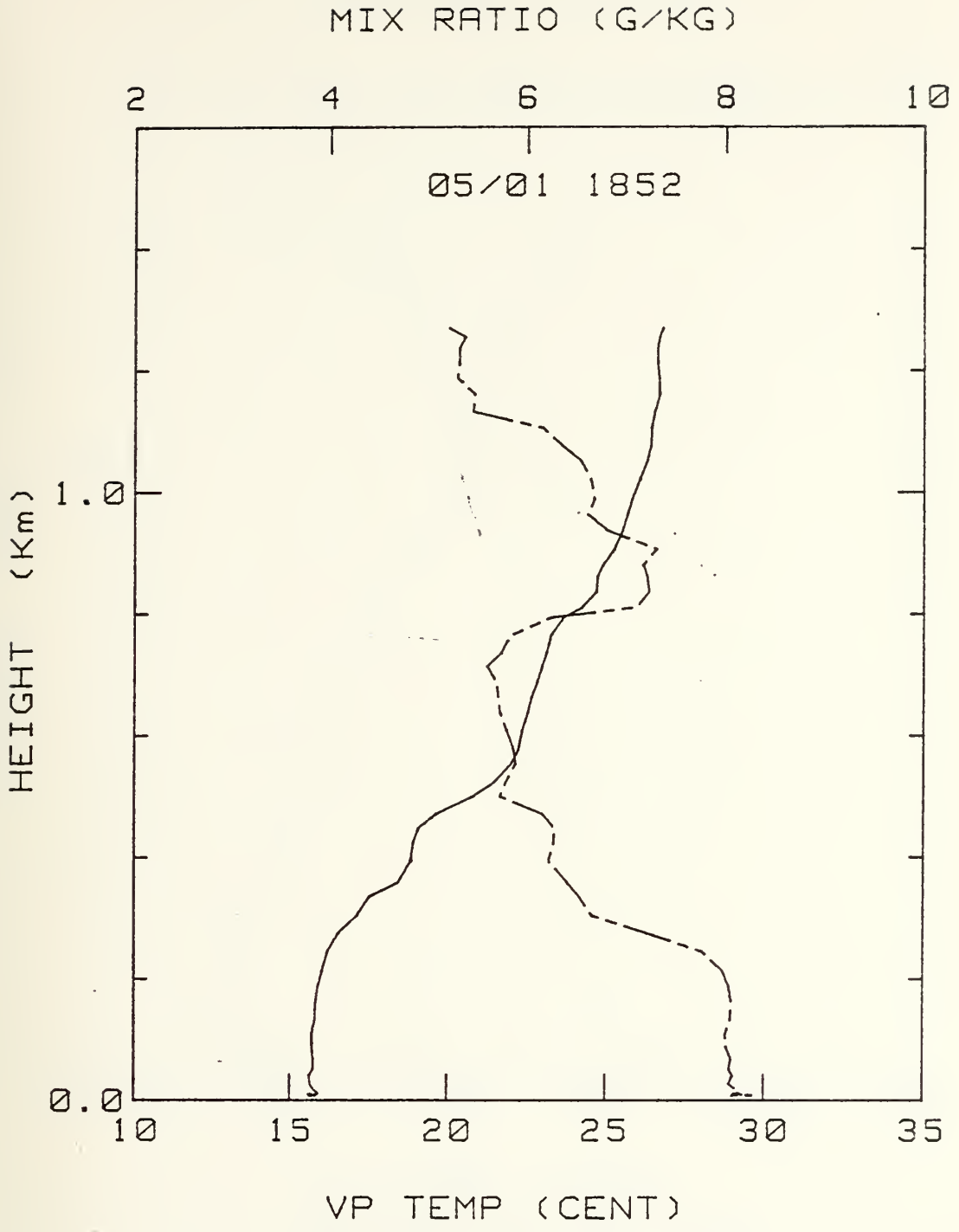

Figure 28. 1 May 1980 at 1852 PDT. Aircraft profile of virtual potential temperature (bottom scale, in degrees Celsius), solid line, and mixing ratio (top scale, in grams per kilogram), broken line, versus height.

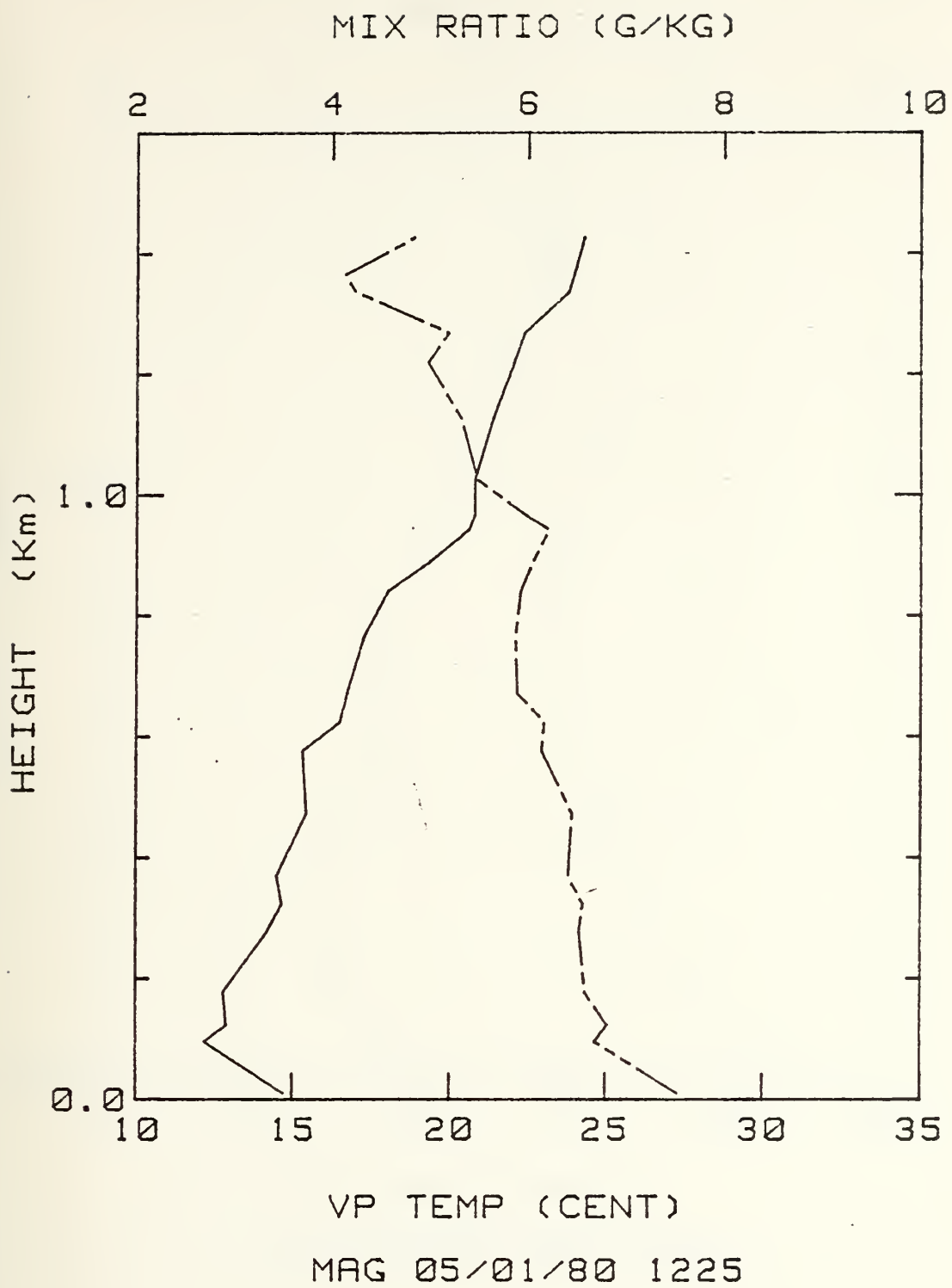

Figure 29. 1 May 1980 at 122 PDT. ACANIA profile of virtual potential temperature (bottom scale, in degrees Celsius), solid line, and mixing ratio (top scale, in grams per kilogram), broken line, versus height.

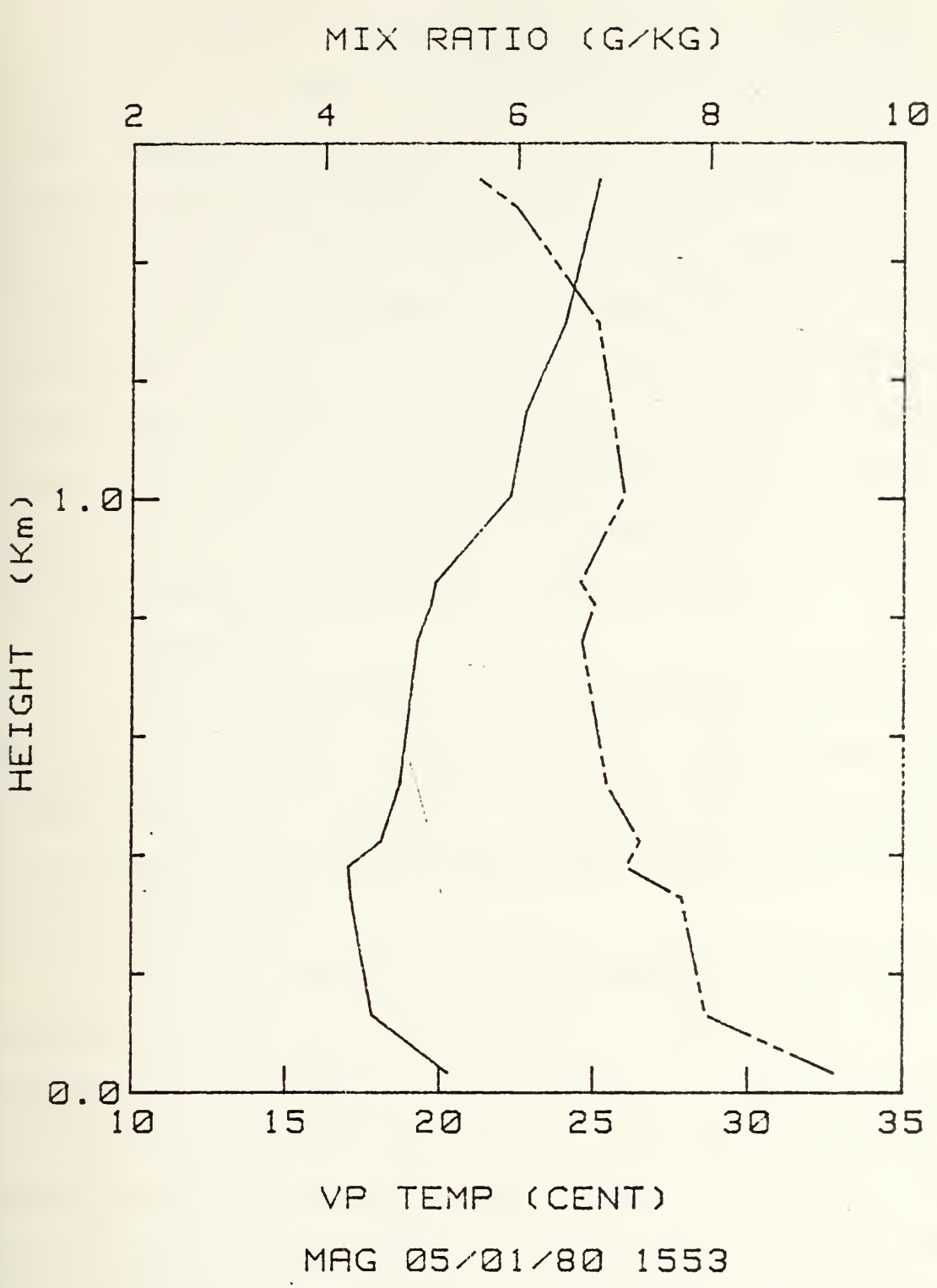

Figure 30. 1 May 1980 at 1553 PDT. NPS profile of virtual potential temperature (bottom scale, in degrees Celsius), solid line, and mixing ratio (top scale, in grams per kilogram), broken line, versus height.

The 1742 PDT spiral profile, Figure 27, does not show a definite mixed layer. The predicted extinction profile has a near exponential shape at 1754 PDT, Figure 31, which is not correlated with the observed aerosol extinctions. It is believed that the low wind speeds, 4.9 m/s, causes the predicted values to be primarily continental and to be determined by relative humidity. In contrast, the 1903 PDT (Figure 32) profile shows a definite inversion and the predicted extinction values are better correlated with observed values within the mixed layer. Predicted extinction values are definitely less than the observed values above the mixed layer.

2. 3 May 1980

The third of May is chosen because all spiral profiles show classic examples, Figures 33-37, of a well mixed boundary layer capped by an inversion. This assessment is based on both the virtual potential temperature and mixing ratio distributions with height.

The winds are 7 to 10 kt; therefore, production is occurring during the afternoon and the surface layer is unstable through the whole day (Table II). Therefore, production is with quite good mixing. The area is behind a weak frontal system, which passed through the area in the early hours of the day before. Again, early morning hours are dominated by low clouds and fog, with a lowest visibility of two miles. The skies become scattered and the fog dissipates by 1000 PDT. Low clouds occurring again in the area at 1700 PDT, but the visibility remains unrestricted.

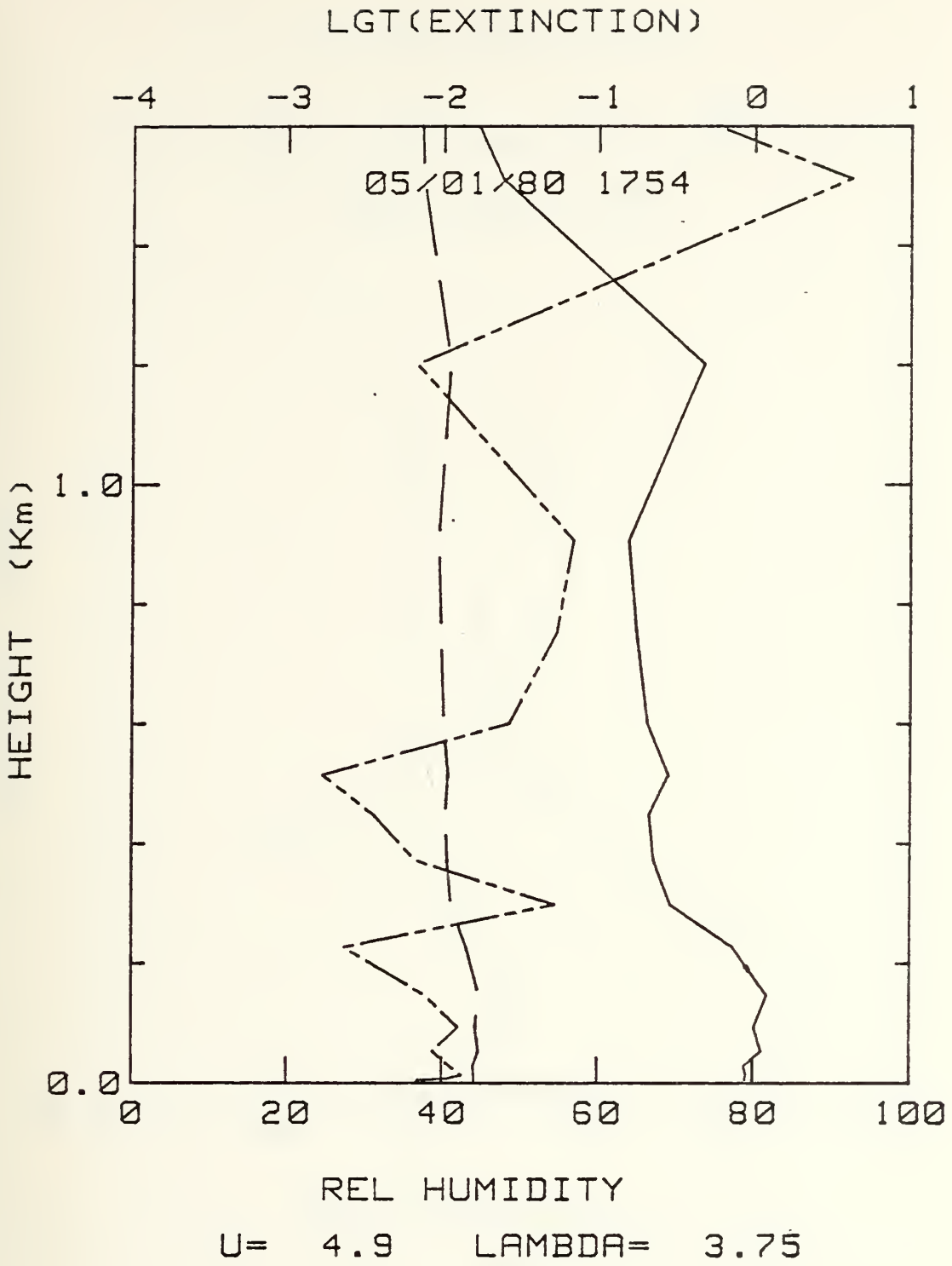

Figure 31. 1 May 1980 at 1754 PDT profile of relative humidity (bottom scale) solid line, observed extinction coefficients (top scale), series of short solid and dashed lines, and predicted extinction coefficients, series of short solid lines versus height. Top scale is logarithmic, where 1 is 10. Wind speed (U) at 4.6 m/s and wavelength (LAMBDA) at 3.75 microns.

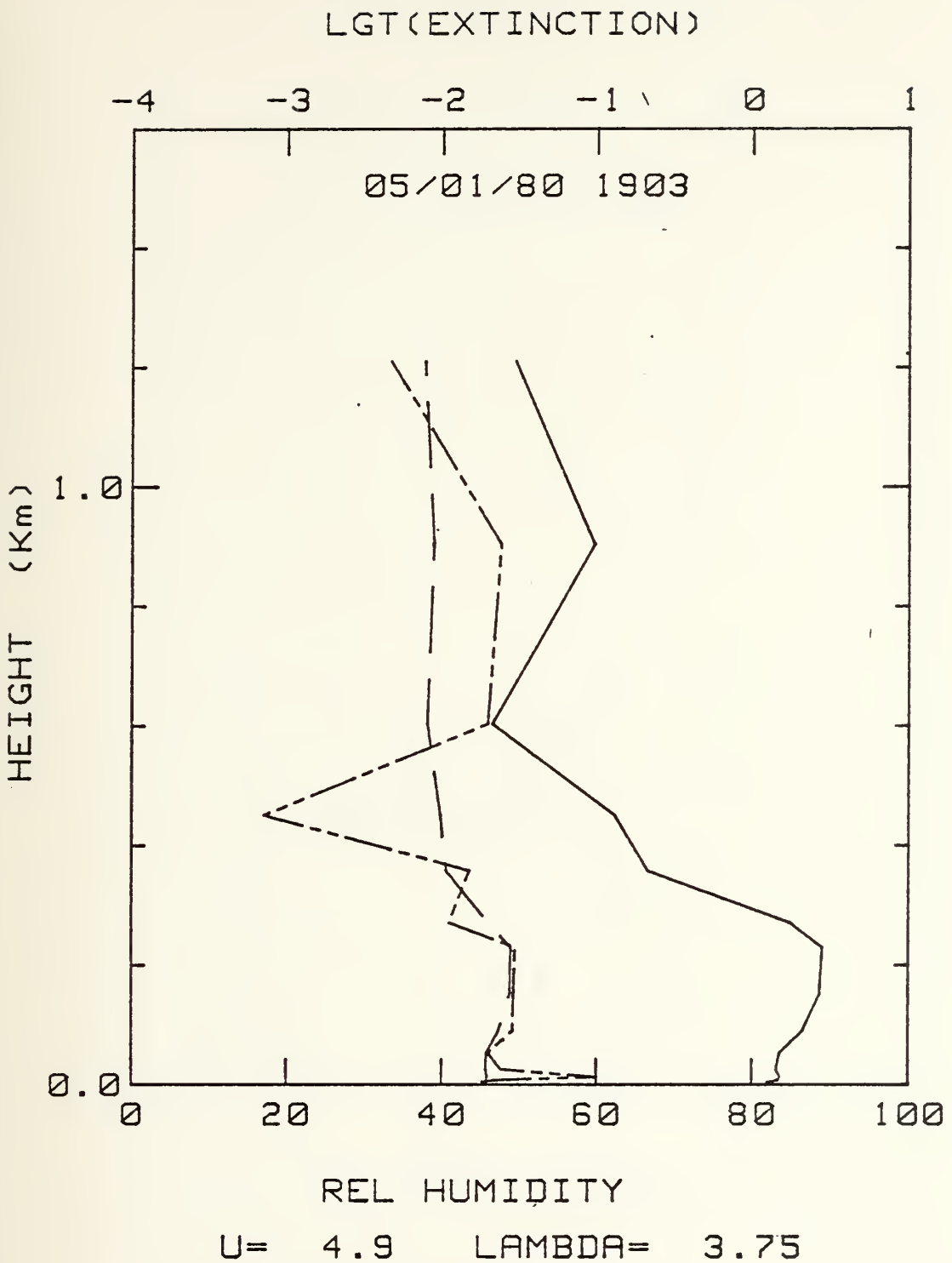

Figure 32. 1 May 1980 at 1903 profile of relative humidity (bottom scale) solid line, observed extinction coefficients (top scale), series of short solid and dashed lines, and predicted extinction coefficients, series of short solid lines versus height. Top scale is logarithmic, where 1 is 10. Wind speed (U) at 4.6 m/s and wavelength (LAMBDA) at 3.75 microns.

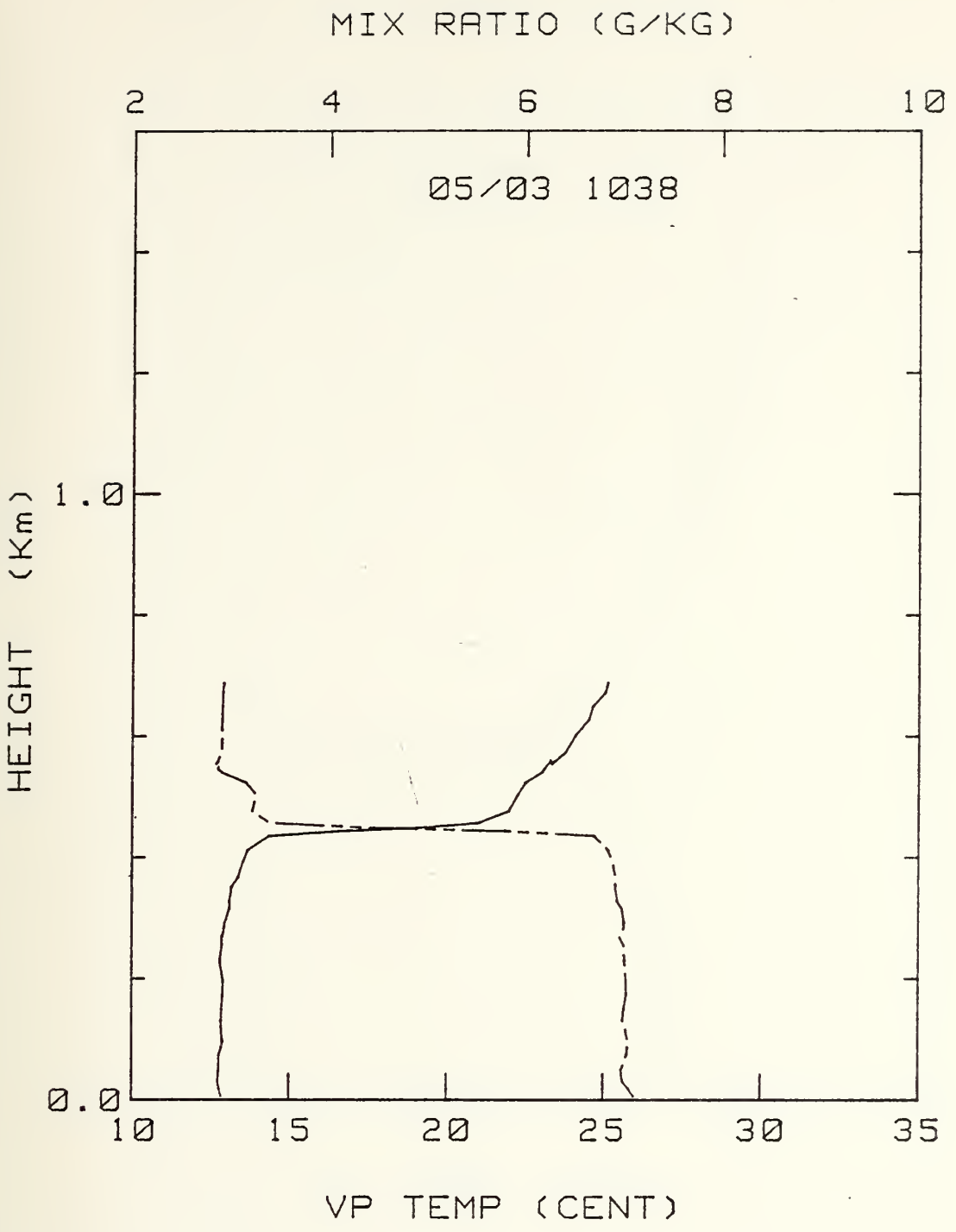

Figure 33. 3 May 1980 at 1038 PDT. Aircraft profile of virtual potential temperature (bottom scale, in degrees Celsius), solid line, and mixing ratio (top scale, in grams per kilogram), broken line, versus height.

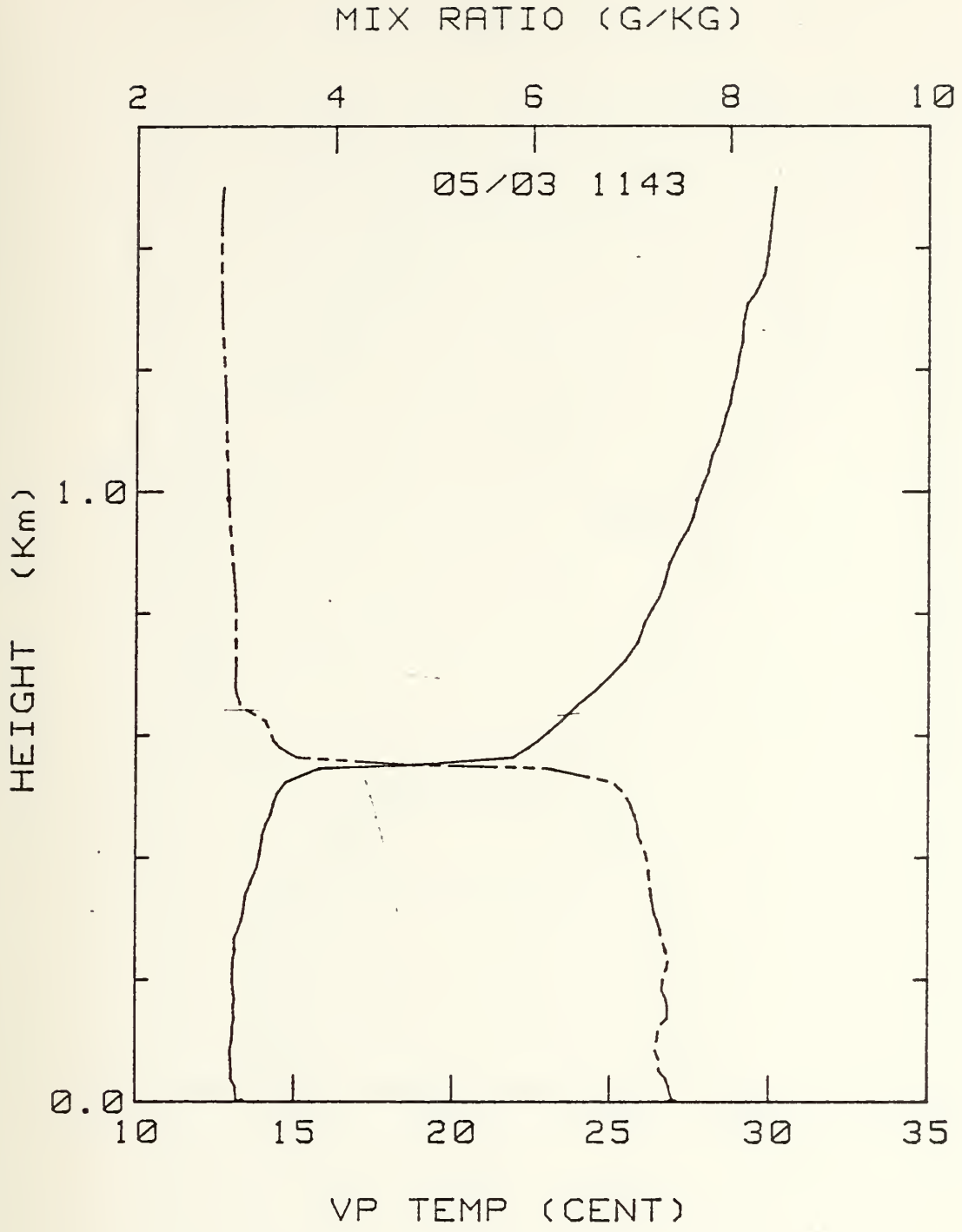

Figure 34. 3 May 1980 at 1143 PDT. Aircraft profile of virtual potential temperature (bottom scale, in degrees Celsius), solid line, and mixing ratio (top scale, in grams per kilgram), broken line, versus height.

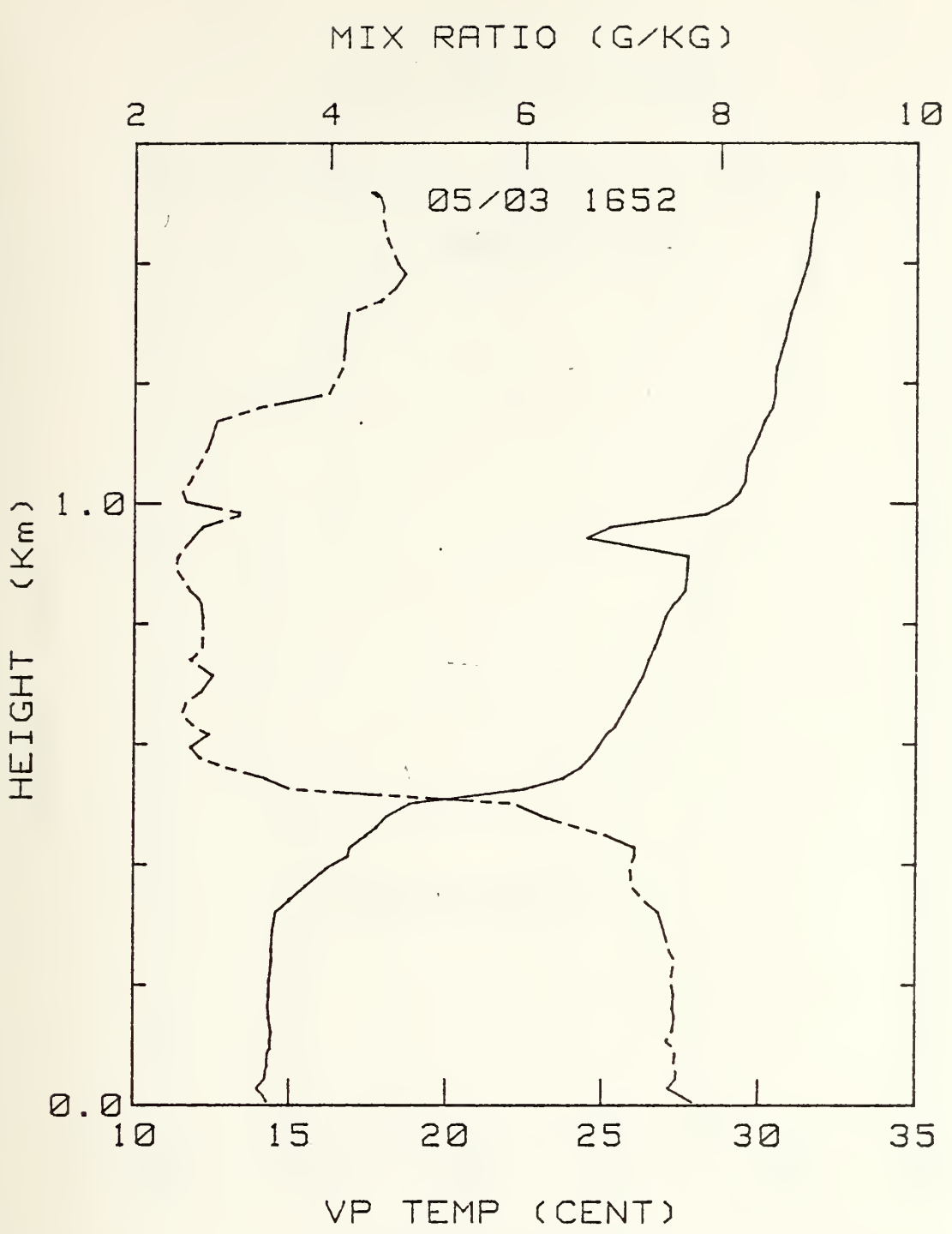

Figure 35. 3 May 1980 at 1652 PDT. Aircraft profile of virtual potential temperature (bottom scale, in degrees Celsius), solid line, and mixing ratio (top scale, in grams per kilogram), broken line, versus height.

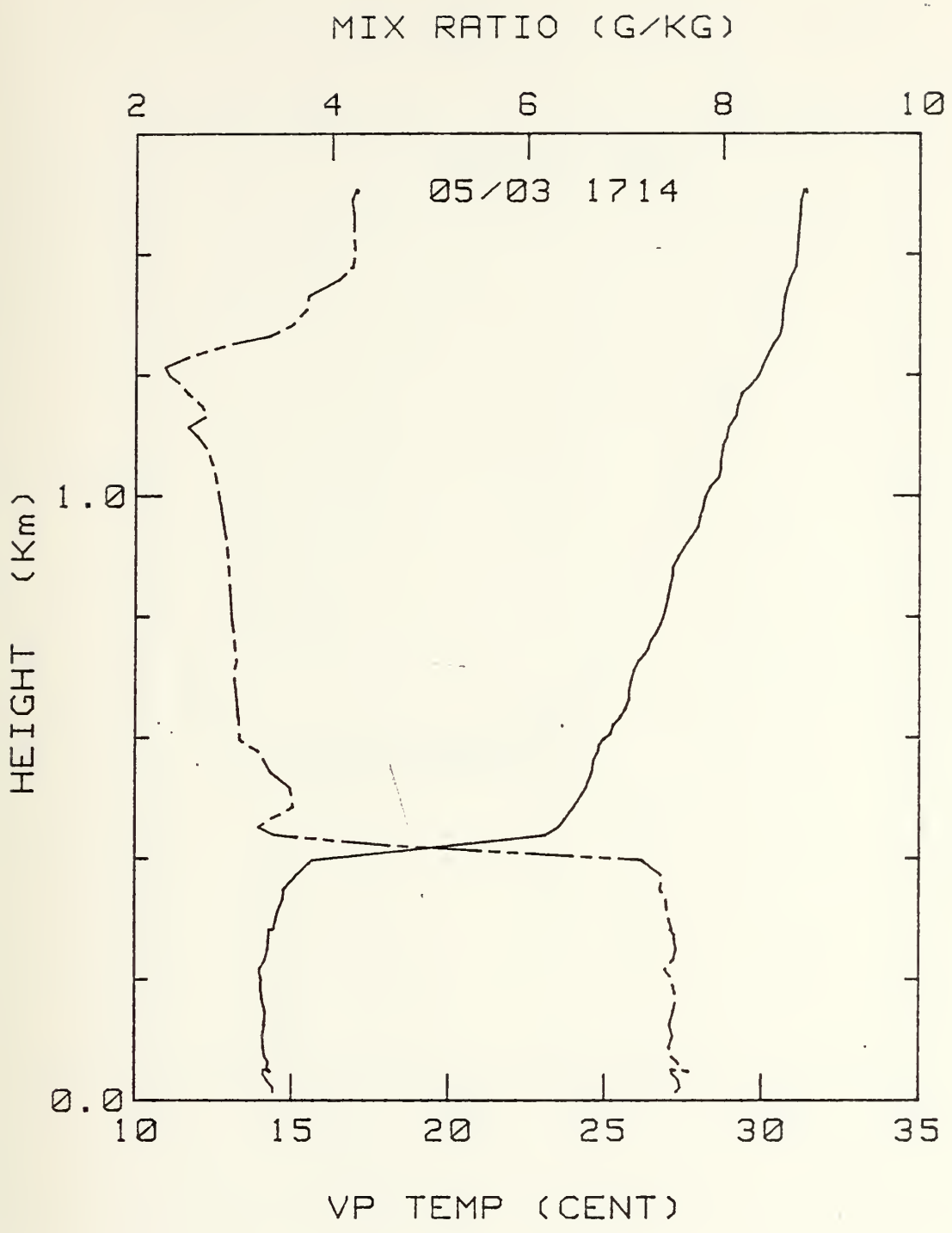

Figure 36. 3 May 1980 at 1714 PDT. Aircraft profile of virtual potential temperature (bottom scale, in degrees Celsius), solid line, andmixing ratio (top scale, in grams per kilogram), broken line, versus height.

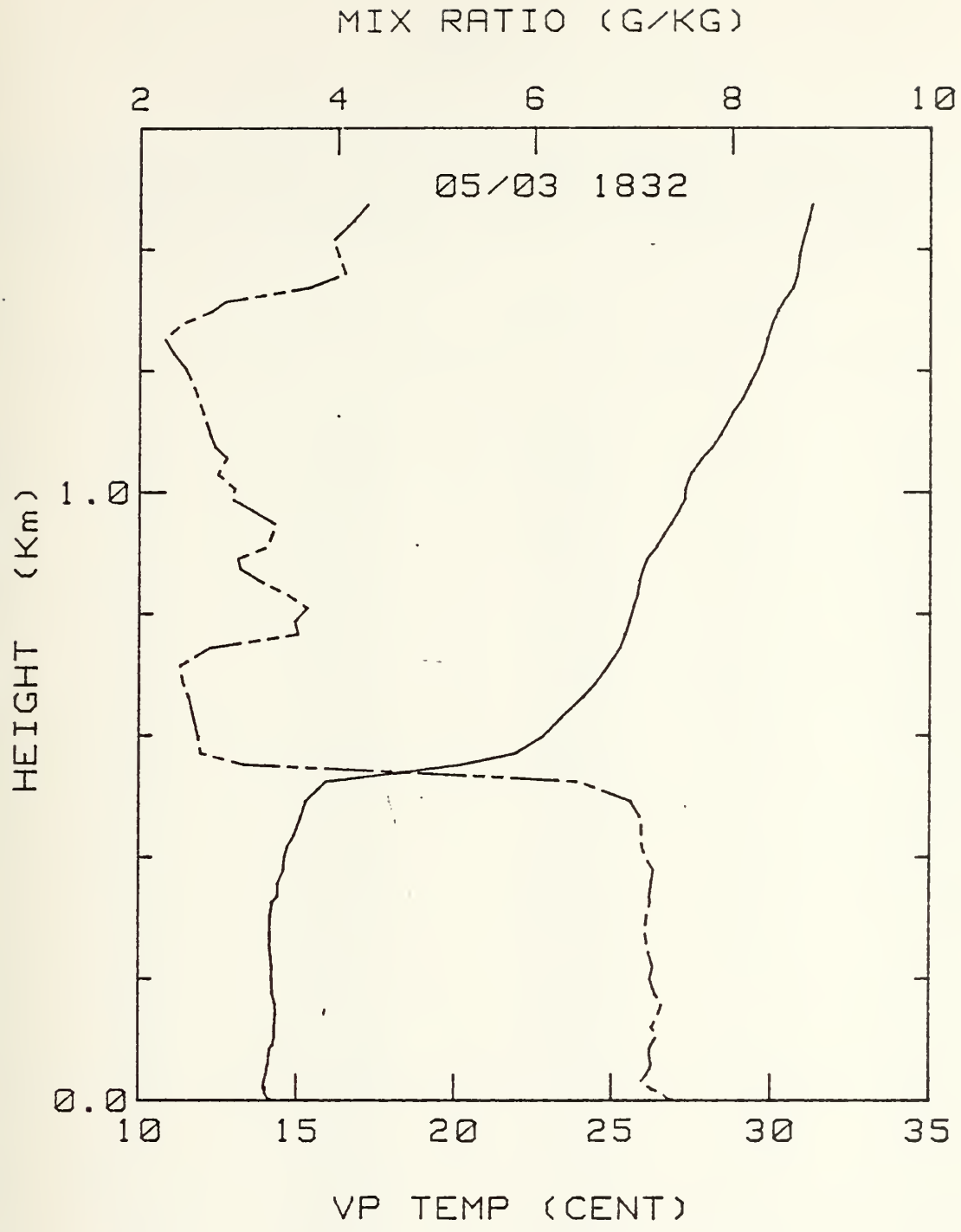

Figure 37. 3 May 1980 at 1832 PDT. Aircraft profile of virtual potential temperature (bottom scale, in degrees Celsius), solid line, and mixing ratio (top scale, in grams per kilogram), broken line, versus height.

TABLE II

Surface Layer Values 3 May 1980

U is wind speed (m/s), T(^{o}c) is temperature in degrees celsius, Ts(^{o}c) sea surface temperature in degrees Celsius, RH(%) is relative humidity in percent, and Z/L is stability index.

Time	U	T(^{o}c)	Ts(^{o}c)	RH(%)	Z/L
00:21	2.9	12.33	13.24	93	-4.90E-01
00:41	3.1	12.40	13.30	93	-4.35E-01
01:12	4.1	12.39	13.39	95	-2.57E-01
04:37	4.2	11.76	13.39	94	-3.90E-01
05:07	5.1	11.92	13.58	91	-2.72E-01
06:37	6.7	12.05	13.24	89	-1.05E-01
07:07	6.9	12.14	13.22	88	-9.32E-02
07:37	6.5	12.17	13.31	87	-1.15E-01
08:07	5.6	12.17	13.35	87	-1.62E-01
08:37	5.8	12.16	13.20	87	-1.33E-01
09:07	5.1	12.27	13.23	87	-1.66E-01
09:37	4.2	12.28	13.11	86	-2.29E-01
10:07	4.0	12.25	13.07	86	-2.54E-01
10:37	3.6	12.38	13.04	86	-2.62E-01
11:07	3.6	12.35	13.08	85	-2.98E-01
11:37	3.4	12.31	13.07	85	-3.59E-01
12:07	4.4	12.33	13.16	85	-2.11E-01
12:37	5.7	12.45	13.64	84	-1.60E-01
13:07	6.2	12.70	14.27	85	-1.76E-01
13:40	7.1	12.87	14.30	85	-1.17E-01
14:10	7.0	12.94	14.30	85	-1.14E-01
14:40	6.9	12.99	14.32	86	-1.15E-01
14:55	6.9	13.01	14.22	85	-1.09E-01
16:14	9.5	13.00	14.05	86	-4.10E-02
16:51	8.3	12.97	14.06	87	-6.09E-02
17:56	6.2	12.86	14.44	88	-1.65E-01
19:00	10.6	12.70	13.44	89	-2.13E-02
19:20	10.3	12.60	13.42	89	-2.56E-02
19:40	9.4	12.61	13.47	88	-3.35E-02
20:13	5.0	12.58	13.08	87	-9.16E-02
20:43	2.9	12.62	12.79	87	-1.21E-01
22:53	6.9	12.74	12.97	89	-1.72E-02
23:32	4.5	12.67	13.47	90	-1.73E-01
23:55	4.1	12.59	13.58	91	-2.65E-01

The airborne (spiral) profiles show a well mixed boundary layer capped by a strong inversion. In the morning (Figures 33 and 34), the mixed layer depth increases from 425 to 500 m along a line extending from 43 to 83 km to the west-northwest of NPS, Figure 11. Hence, the mixed layer is quite uniform in the horizontal. In the afternoon (Figures 35-37), the mixed layer depth increases from 300 to 500 m along a line extending from 13 to 122 km from NPS, Figure 11. All profiles, Figures 38-40, support an assessment of a convective mixed layer but each has an anomolous feature when compared with the others. In the 0800 PDT NPS sounding the level above the mixed layer is much drier than any of the spiral profiles; a mixing ratio of approximately 1 gm/kg compared to approximately 3 gm/kg. The 0845 PDT ACANIA sounding shows a rapid decrease in virtual potential temperature above one km, which is not observed in any of the other profiles. This decrease affected the mixing ratio as well. The location of the ACANIA at 0845 PDT was 39 km to the west-northwest, and at 1555 PDT the location was 64 km to the west-northwest, Figure 7. In the 1555 PDT sounding the virtual potential temperature is approximately six degrees lower than any of the other profiles.

Relative humidity and predicted and observed extinctions for 3 May appear in Figures 41-43. The day has the most representative example of a well mixed boundary layer for relative humidity which increases uniformly with height to the inversion where it drops off sharply. Observed extinctions have rapid increases at the top of the mixed

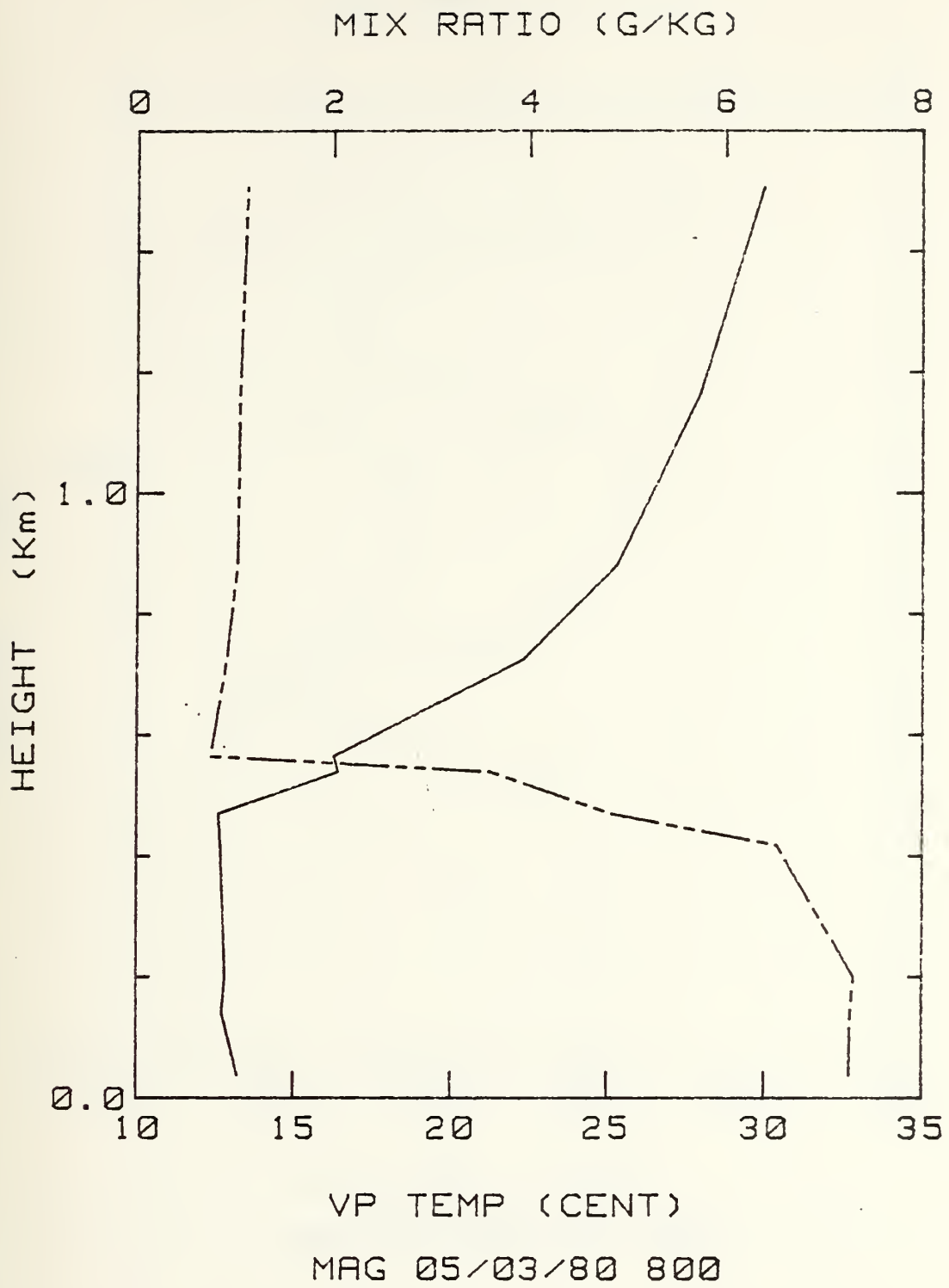

Figure 38. 3 May 1980 at 0800 PDT. NPS profile of virtual potential temperature (bottom scale, in degrees Celsius), solid line, and mixing ratio (top scale, in grams per kilogram), broken line, versus height.

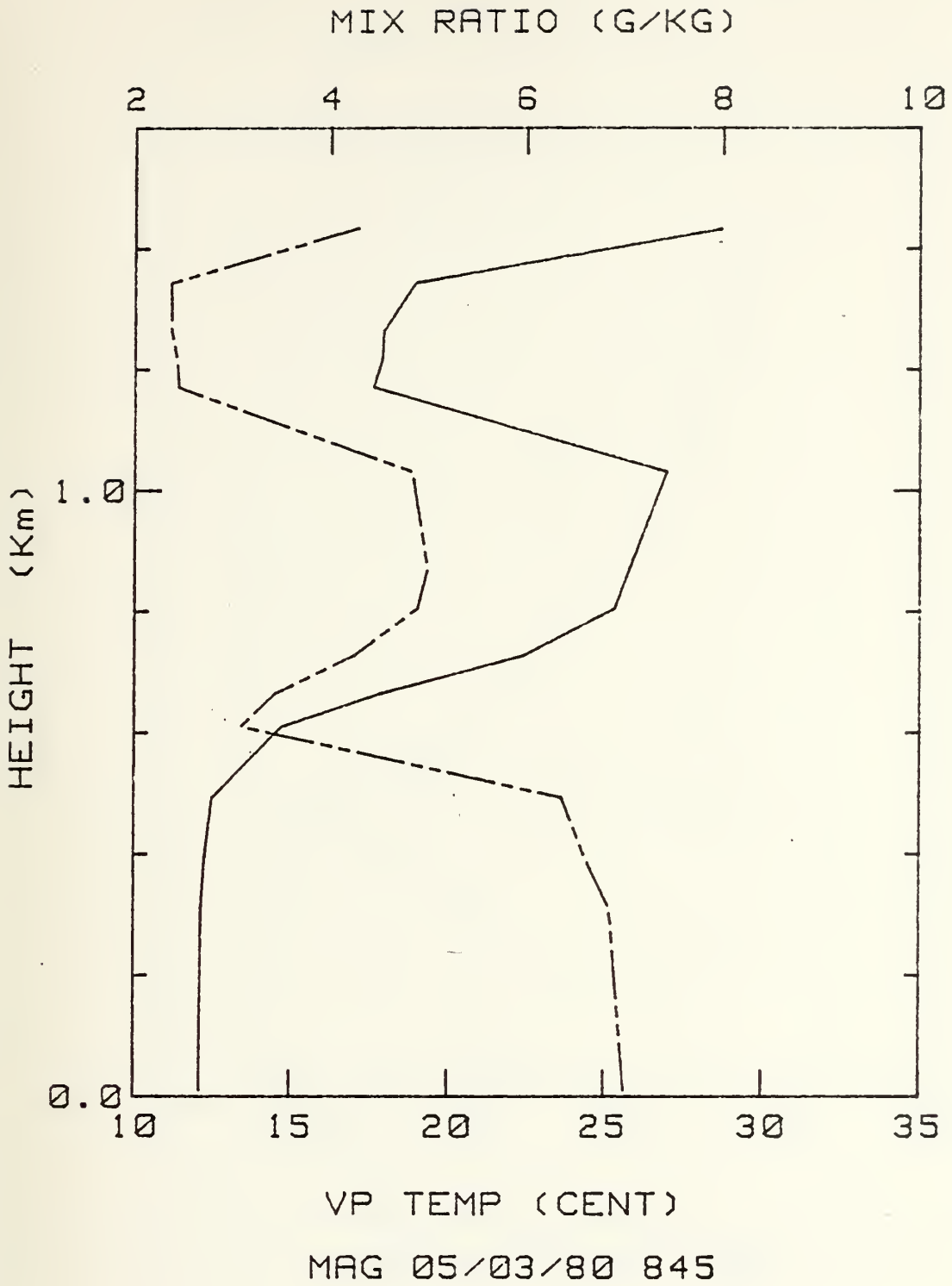

Figure 39. 3 May 1980 at 0845 PDT. ACANIA profile of virtual potential temperature (bottom scale, in degrees Celsius), solid line, and mixing ratio (top scale, in grams per kilogram), broken line, versus height.

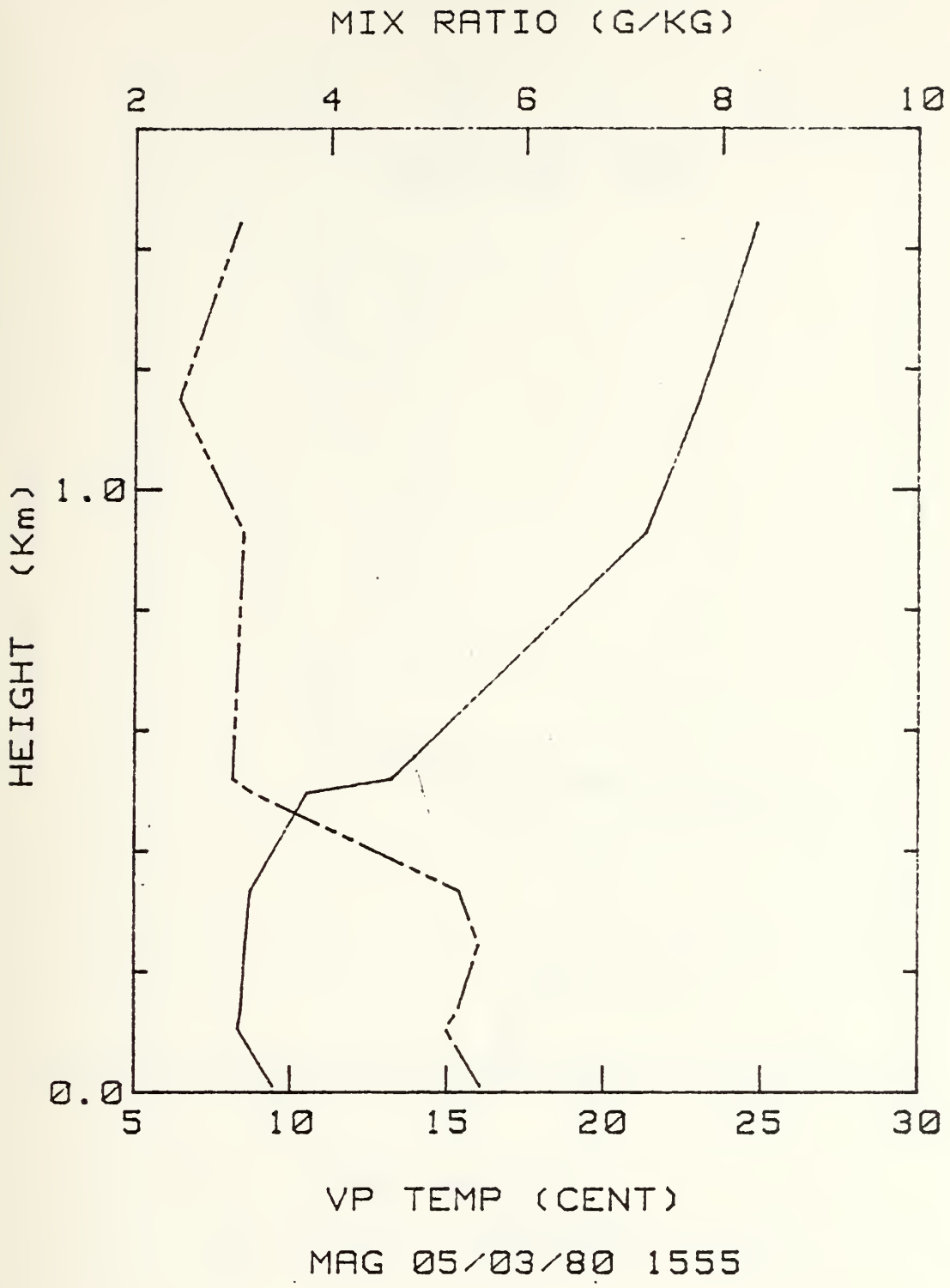

Figure 40. 3 May 1980 at 1555 PDT. ACANIA profile of virtual potential temperature (bottom scale, in degrees Celsius), solid line, and mixing ratio (top scale, in grams per kilogram), broken line, versus height.

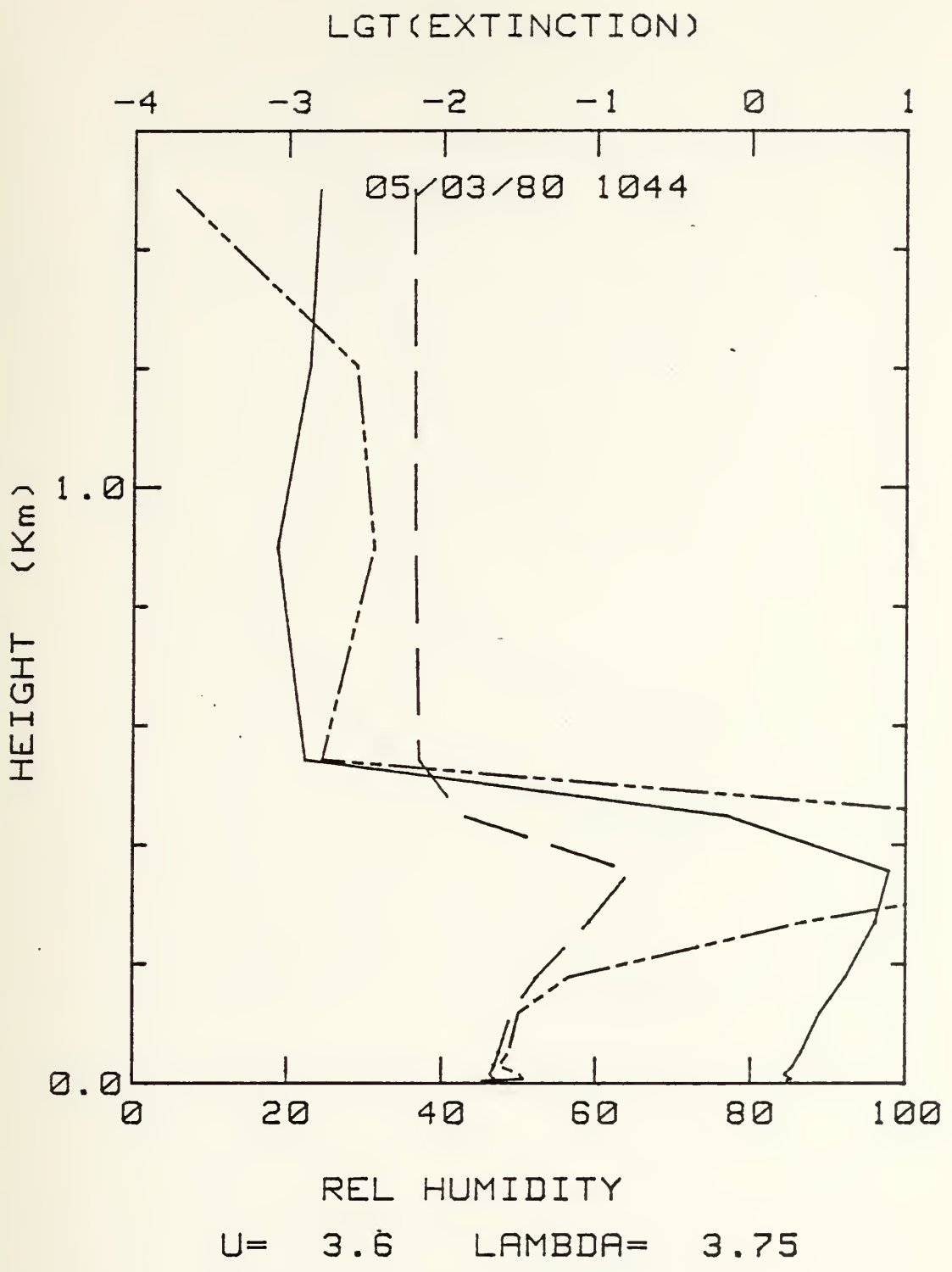

Figure 41. 3 May 1980 at 1044 PDT profile of relative humidity (bottom scale) solid line, observed extinction coefficients (top scale), series of short solid and dashed lines, and predicted extinction coefficients, series of short solid lines versus height. Top scale is logarithmic, where 1 is 10. Wind speed at 3.6 m/s and wavelength (LAMBDA) at 3.75 microns.

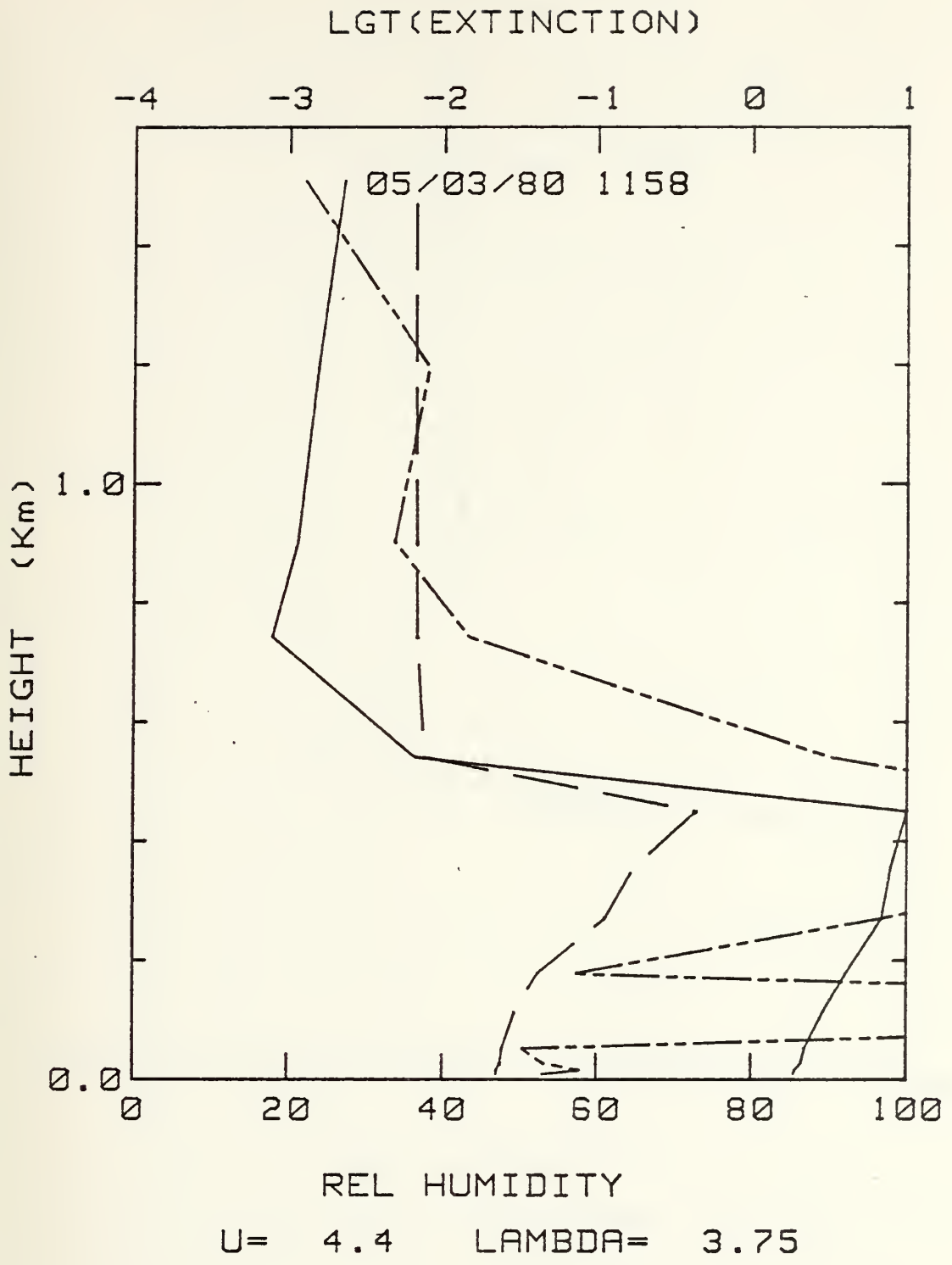

Figure 42. 3 May 1980 at 1158 PDT profile of relative humidity (bottom scale) solid line, observed extinction coefficients (top scale), series of short solid and dashed lines, and predicted extinction coefficients, series of short solid lines versus height. Top scale is logarithmic, where 1 is 10. Wind speed at 4.4 m/s and wavelength (LAMBDA) at 3.75 microns.

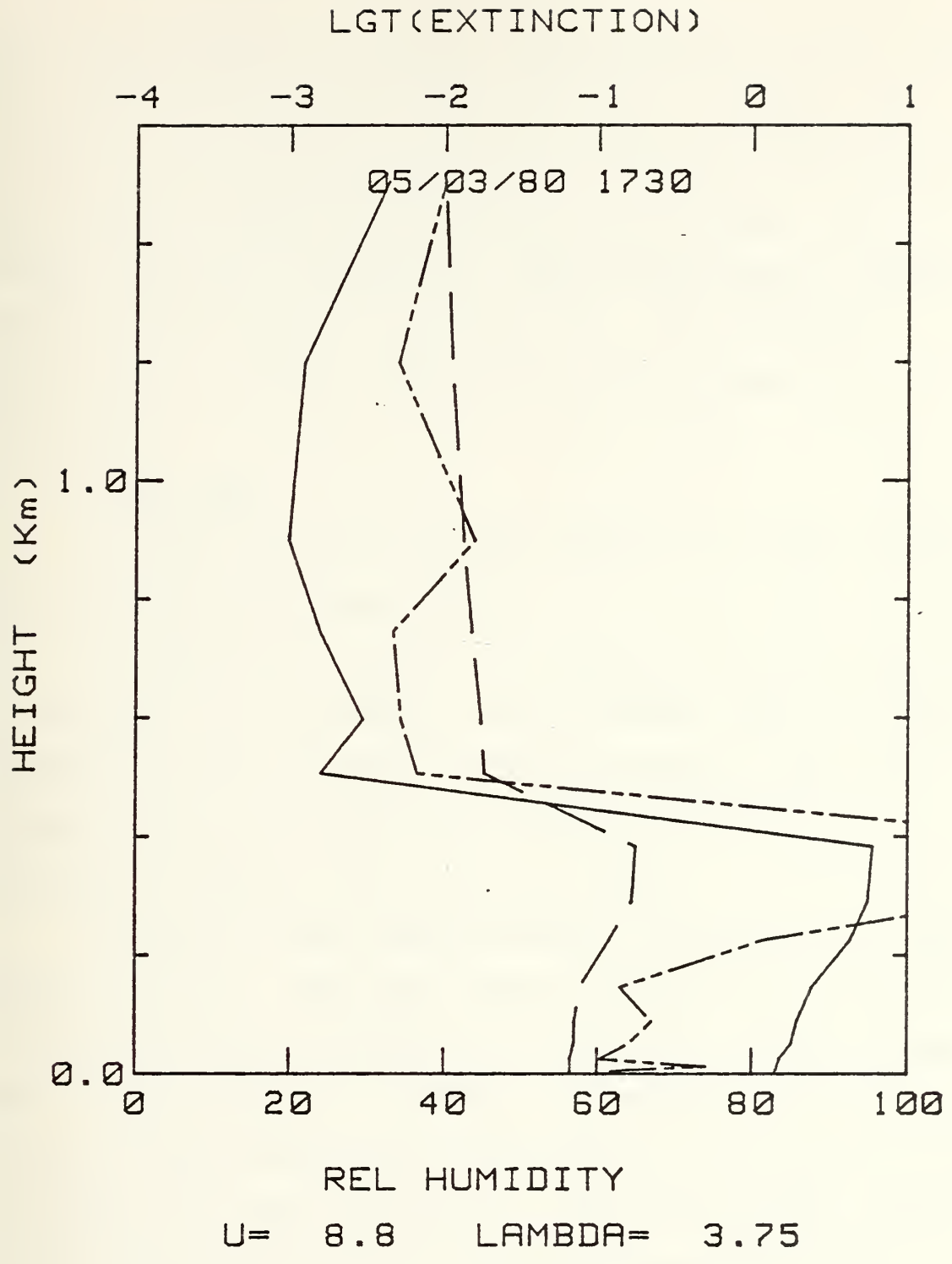

Figure 43. 3 May 1980 at 1730 PDT profile of relative humidity (bottom scale) solid line, observed extinction coefficients (top scale), series of short solid and dashed lines, and predicted extinction coefficients, series of short solid lines versus height. Top scale is logarithmic, where 1 is 10. Wind speed at 8.8 m/s and wavelength (LAMBDA) at 3.75 microns. Wind speed calculated from friction velocity.

layer due to clouds (extinction values greater than 10), and then rapid decreases immediately above the inversion. The predicted extinction also increases at the top of the mixed layer but not as large as the observed extinction. In general, predicted and observed values agree near the surface but not near the top of the mixed layer. The predicted values do not agree with the observed values above the inversion.

3. 5 May 1980

The fifth of May is chosen because of a weak inversion and a relatively deep mixed layer.

The winds are 7 to 10 kt, therefore, active production is occurring in the afternoon and the surface layer is unstable during most of the morning and becomes slightly stable for the rest of the day (Table III). Active production is questionable because of the low wind speeds.

During the hours before sunrise, scattered low clouds dominate the area. From just before sunrise until 0800 PDT, low cloudiness and fog dominate the area with middle and high level clouds moving in. A frontal system passes through the area at approximately 1300 PDT, and the visibility improves to 25 miles and later to 45 miles. After the frontal passage, the sky becomes broken and the winds increase with gusts to 22 kt between 1400 to 1700 PDT. The skies become scattered by 2000 PDT and the high clouds move out of the area.

TABLE III

Surface Layer Values 5 May 1980

U is wind speed (m/s), T(^{o}c) is temperature in degrees celsius, Ts(^{o}c) is sea surface temperature in degrees celsius, RH(%) is relative humidity in percent, and Z/L is stability index.

Time	U	T(^{o}c)	Ts(^{o}c)	RH(%)	Z/L
00:09	7.5	12.49	13.99	93	-1.02E-01
00:16	3.4	12.40	13.70	91	-5.37E-01
00:59	3.0	12.40	13.78	92	-7.42E-01
01:25	2.8	12.37	13.65	92	-7.79E-01
01:37	2.9	12.32	13.40	93	-5.98E-01
02:16	1.9	12.46	13.76	90	-1.68E-00
02:32	2.1	12.60	13.62	90	-1.17E-00
02:38	2.1	12.60	13.65	88	-1.23E-00
02:57	3.4	12.62	13.70	88	-4.49E-01
07:02	7.2	12.76	13.19	89	-3.37E-02
07:32	6.6	12.76	13.11	89	-3.46E-02
08:02	6.5	12.59	13.12	90	-4.98E-02
08:32	6.7	12.65	13.15	89	-4.55E-02
09:02	6.2	12.77	13.12	89	-4.09E-02
09:32	5.5	12.89	13.08	88	-3.19E-02
10:02	5.7	12.96	13.10	88	-2.25E-02
11:11	6.1	13.05	13.10	89	-7.69E-03
11:49	6.2	13.05	12.98	89	7.35E-03
12:19	6.3	13.13	12.91	89	2.28E-02
12:49	7.1	13.25	12.98	89	2.05E-02
13:19	7.1	13.27	12.89	90	3.08E-02
13:49	6.7	13.36	12.89	90	4.53E-02
15:56	9.6	14.16	13.46	87	2.39E-02
18:55	10.3	14.10	13.57	90	1.75E-02
19:25	11.1	13.90	13.47	90	1.17E-02
19:55	11.5	13.97	13.38	88	1.19E-02
20:43	12.1	13.29	13.32	79	-5.77E-03

Before frontal passage, 1300 PDT, the spiral profiles (Figures 44-46) exhibit a weak inversion near 550 to 600 m and slightly stable conditions within the mixed layer. The radiosonde profiles, Figures 50-52, exhibit unstable conditions within the mixed layer but there is no definite height except for the 1150 PDT ACANIA profile which has a well mixed layer with a depth of 400 m. After frontal passage, after 1300 PDT, the spiral profiles (Figure 47-49) exhibit a mixed layer depth increasing from 200 m 9 km from NPS to above 1600 m 95 km from NPS, Figure 14. The NPS radiosonde profile at 1455 PDT (Figure 53) exhibits unstable conditions at the lower levels, while the ACANIA radiosonde profile at 1600 PDT (Figure 54) exhibits a strong stable condition. There is very little agreement in the near surface values of virtual potential temperature between any of the radiosonde profiles.

Extinction results associated with this case are predicted values definitely larger than the observed values except when the aircraft flew into clouds, Figures 55-58.

4. 7 May 1980

The seventh of May is chosen because of the horizontal variation of the mixed layer. The spiral profile exhibits a shallow mixed layer with a strong inversion close to shore and a deep mixed layer with a strong inversion some distance from land. The surface winds are gusting from 18 to 21 kt between 1400 to 2000 PDT and the surface layer is in a slightly

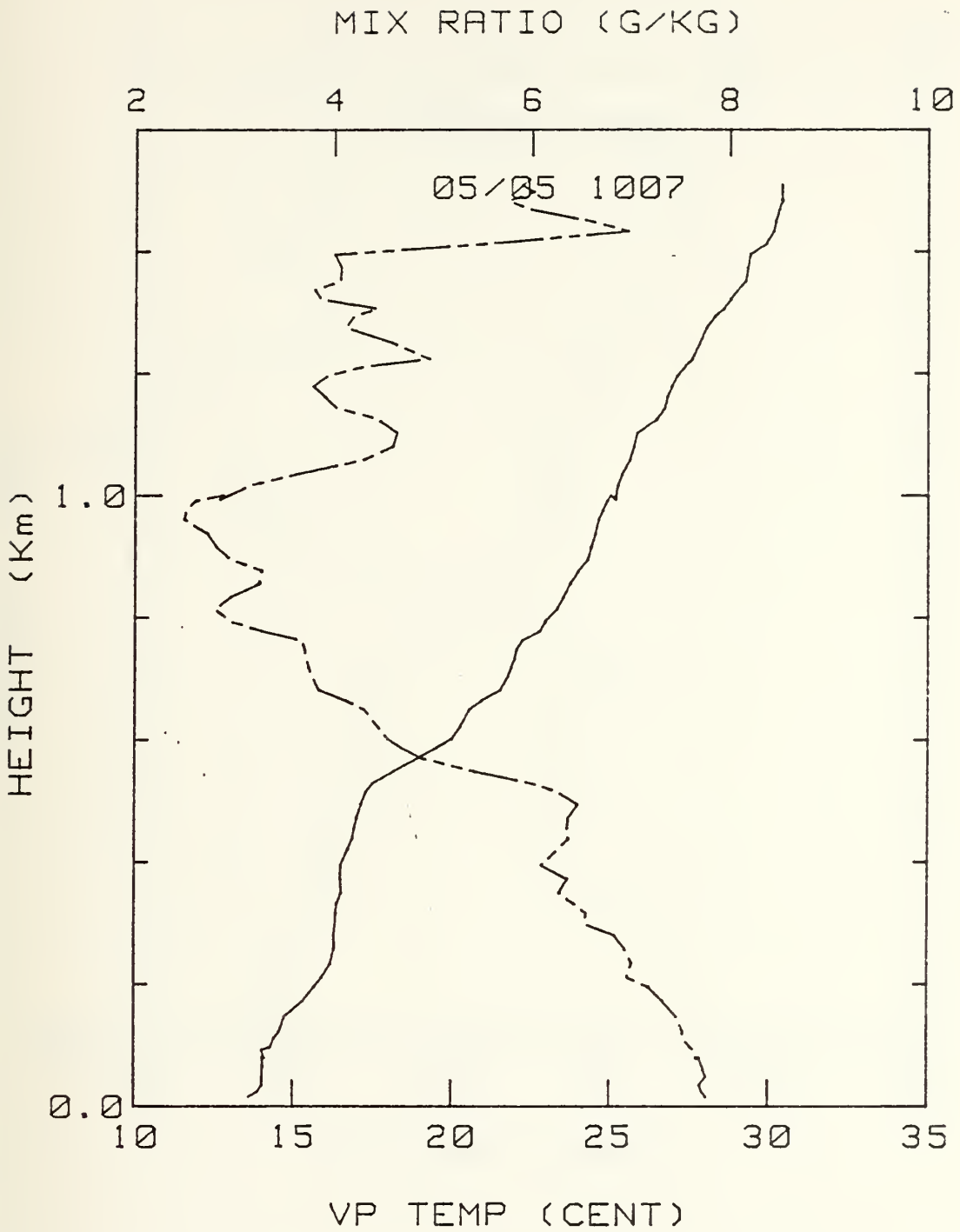

Figure 44. 5 May 1980 at 1007 PDT. Aircraft profile of virtual potential temperature (bottom scale, in degrees Celsius), solid line, and mixing ratio (top scale, in grams per kilogram), broken line, versus height.

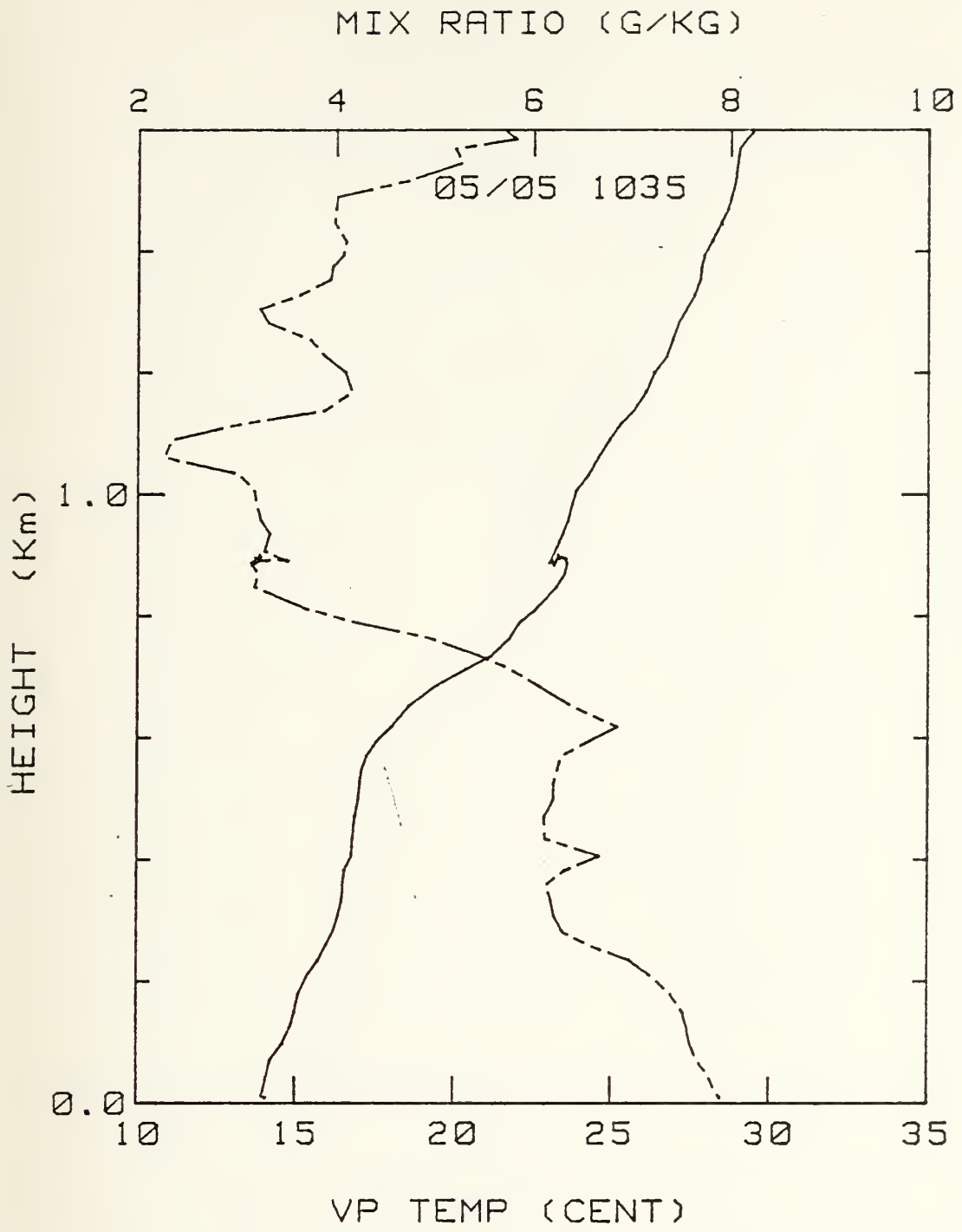

Figure 45. 5 May 1980 at 1035 PDT. Aircraft profile of virtual potential temperature (bottom scale, in degrees Celsius), solid line, and mixing ratio (top scale, in grams per kilogram), broken line, versus height.

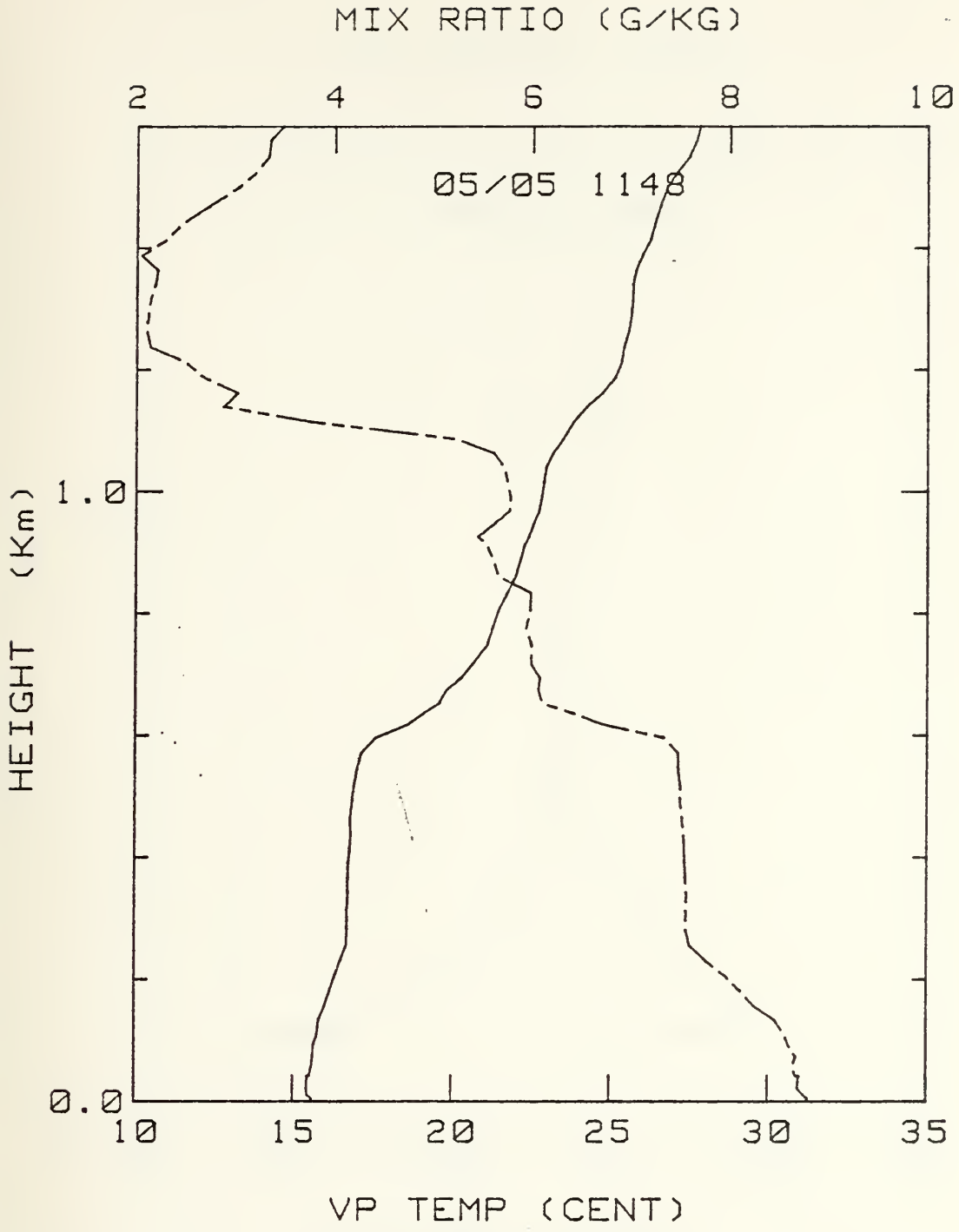

Figure 46. 5 May 1980 at 1148 PDT. Aircraft profile of virtual potential temperature (bottom scale, in degrees Celsius), solid line, and mixing ratio (top scale, in grams per kilogram), broken line, versus height.

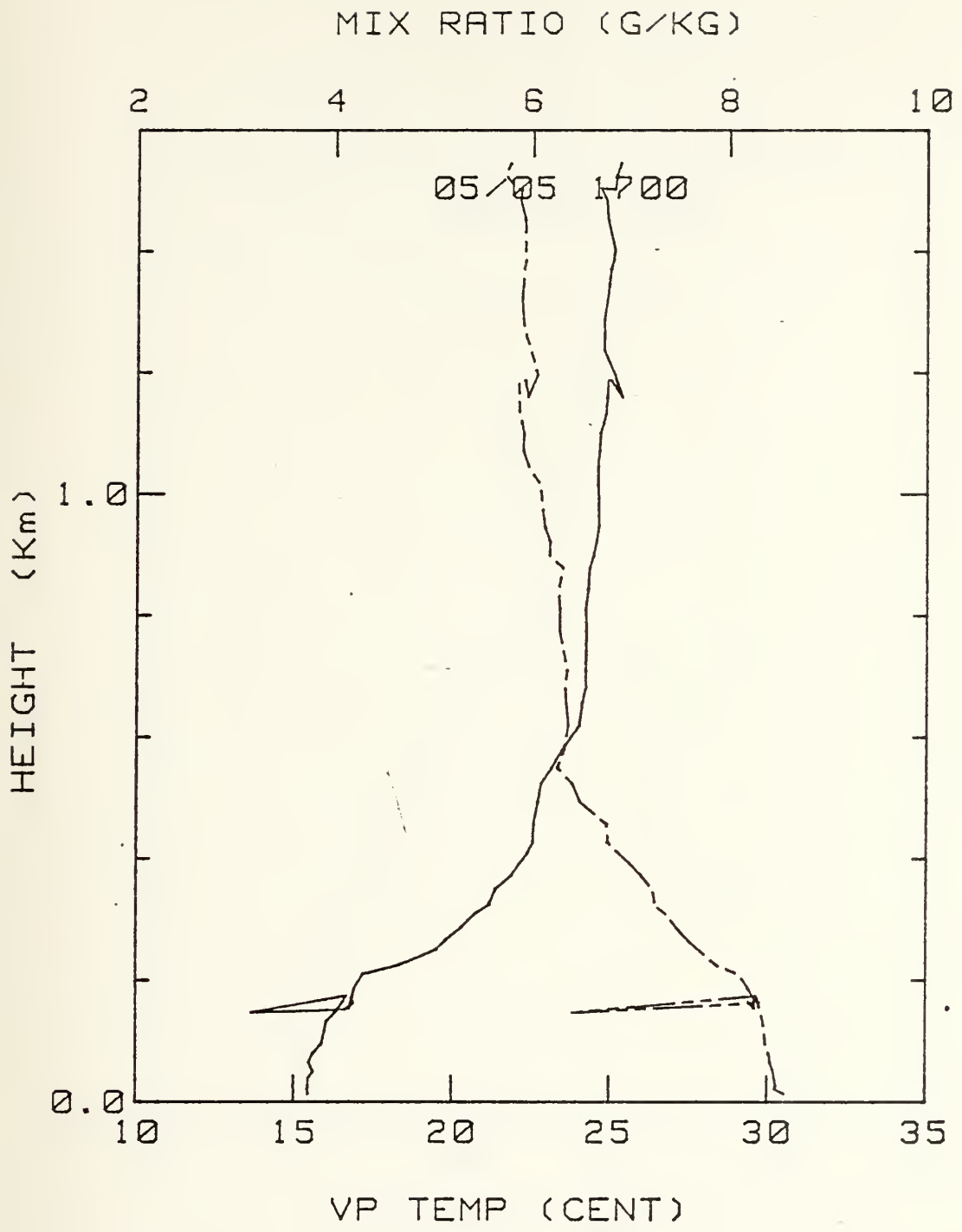

Figure 47. 5 May 1980 at 1700 PDT. Aircraft profile of virtual potential temperature (bottom scale, in degrees Celsius), solid line, and mixing ratio (top scale, in grams per kilogram), broken line, versus height.

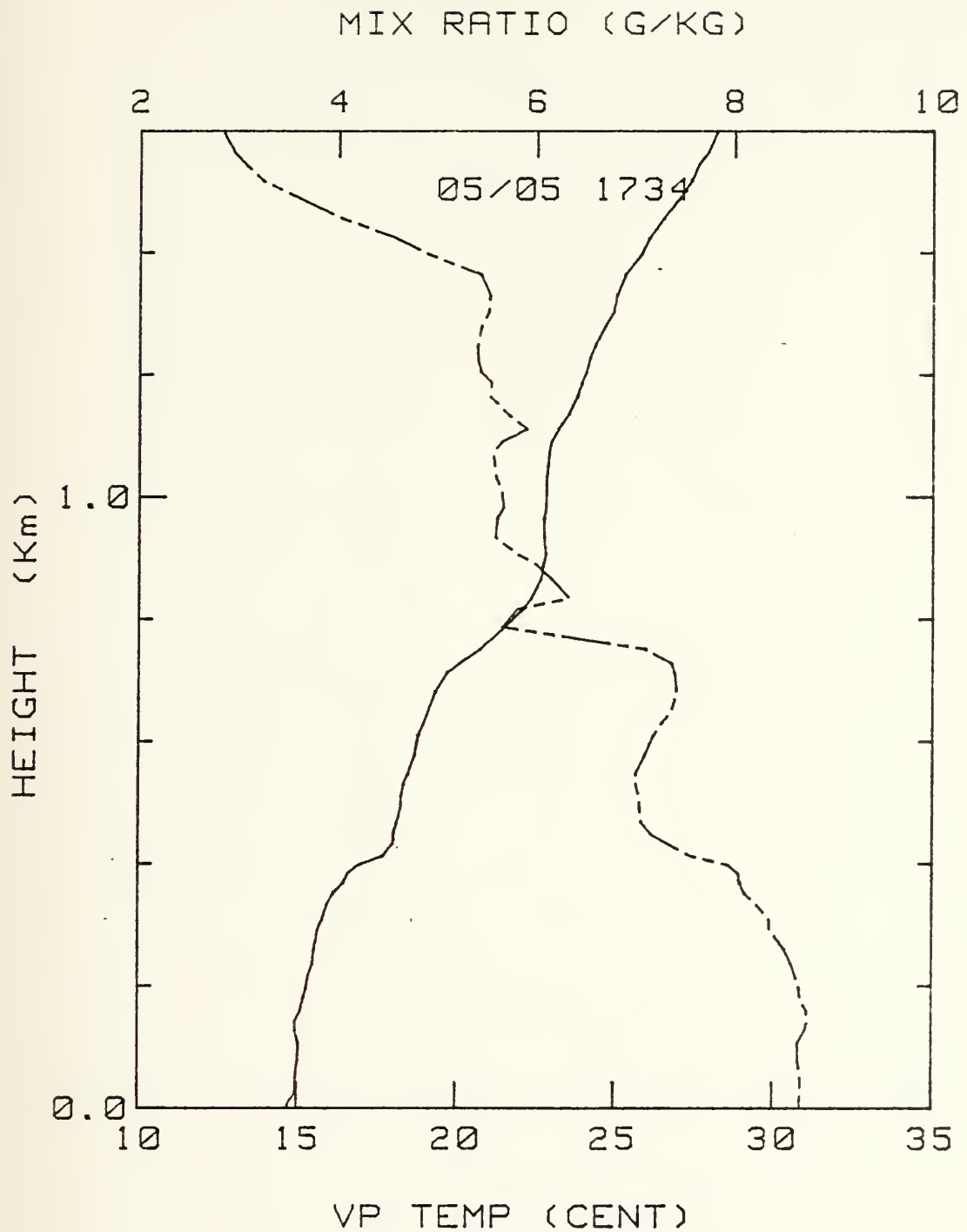

Figure 48. 5 May 1980 at 1734 PDT. Aircraft profile of virtual potential temperature (bottom scale, in degrees Celsius), solid line, and mixing ratio (top scale, in grams per kilogram), broken line, versus height.

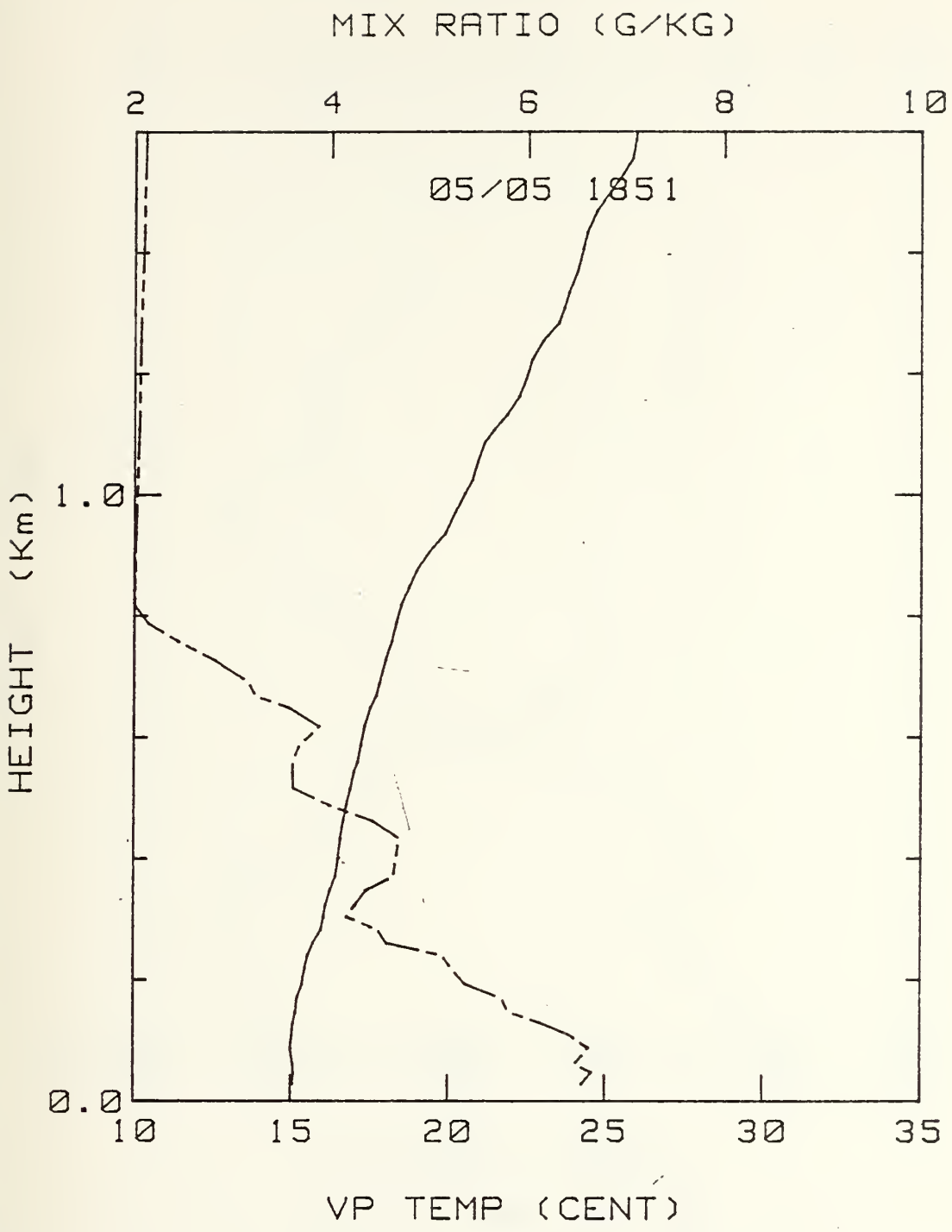

Figure 49. 5 May 1980 at 1851 PDT. Aircraft profile of virtual potential temperature (bottom scale, in degrees Celsius), solid line, and mixing ratio (top scale, in grams per kilogram), broken line, versus height.

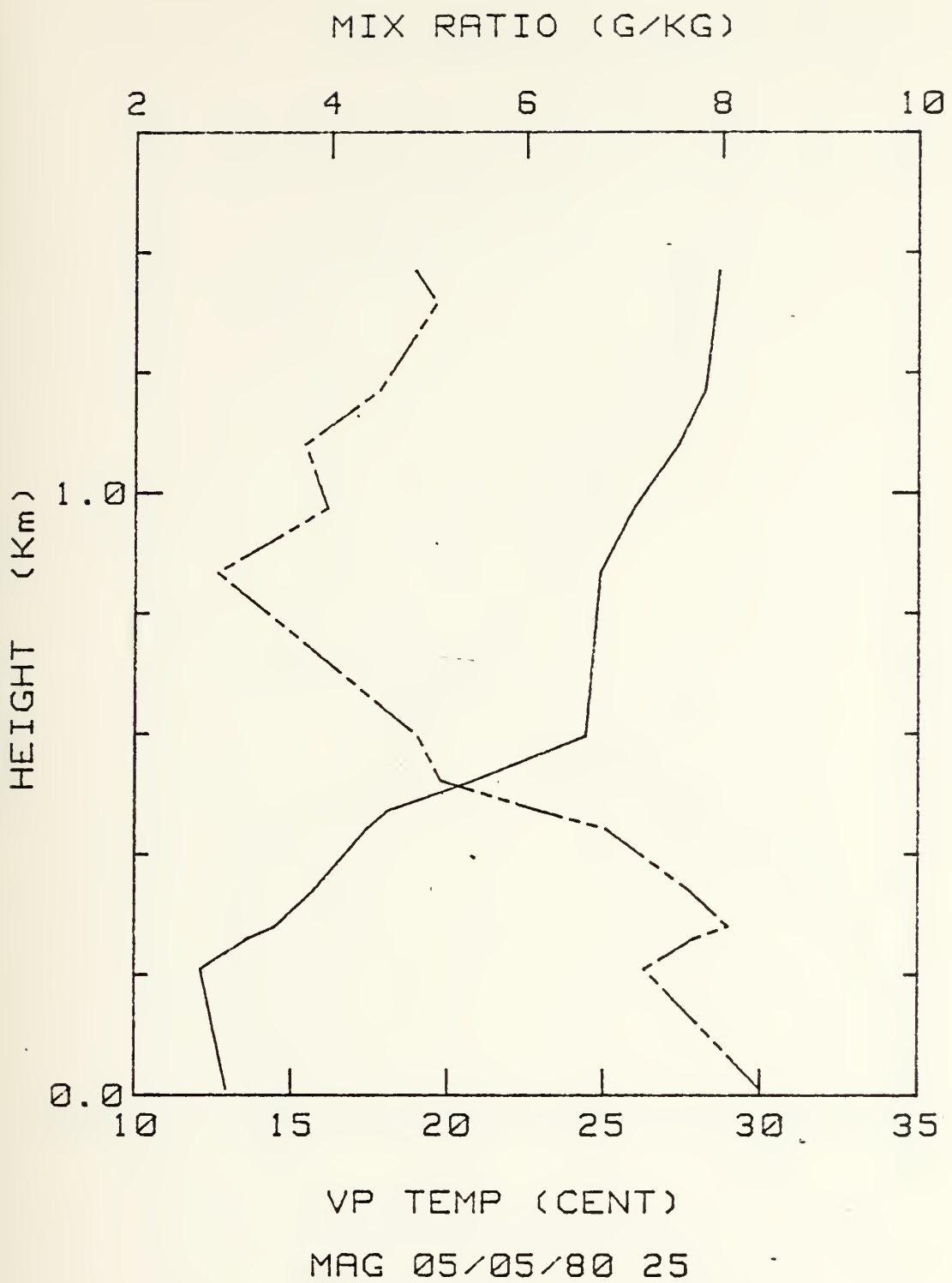

Figure 50. 5 May 1980 at 0025 PDT. ACANIA profile of virtual potential temperature (bottom scale, in degrees Celsius), solid line, and mixing ratio (top scale, in grams per kilogram), broken line, versus height.

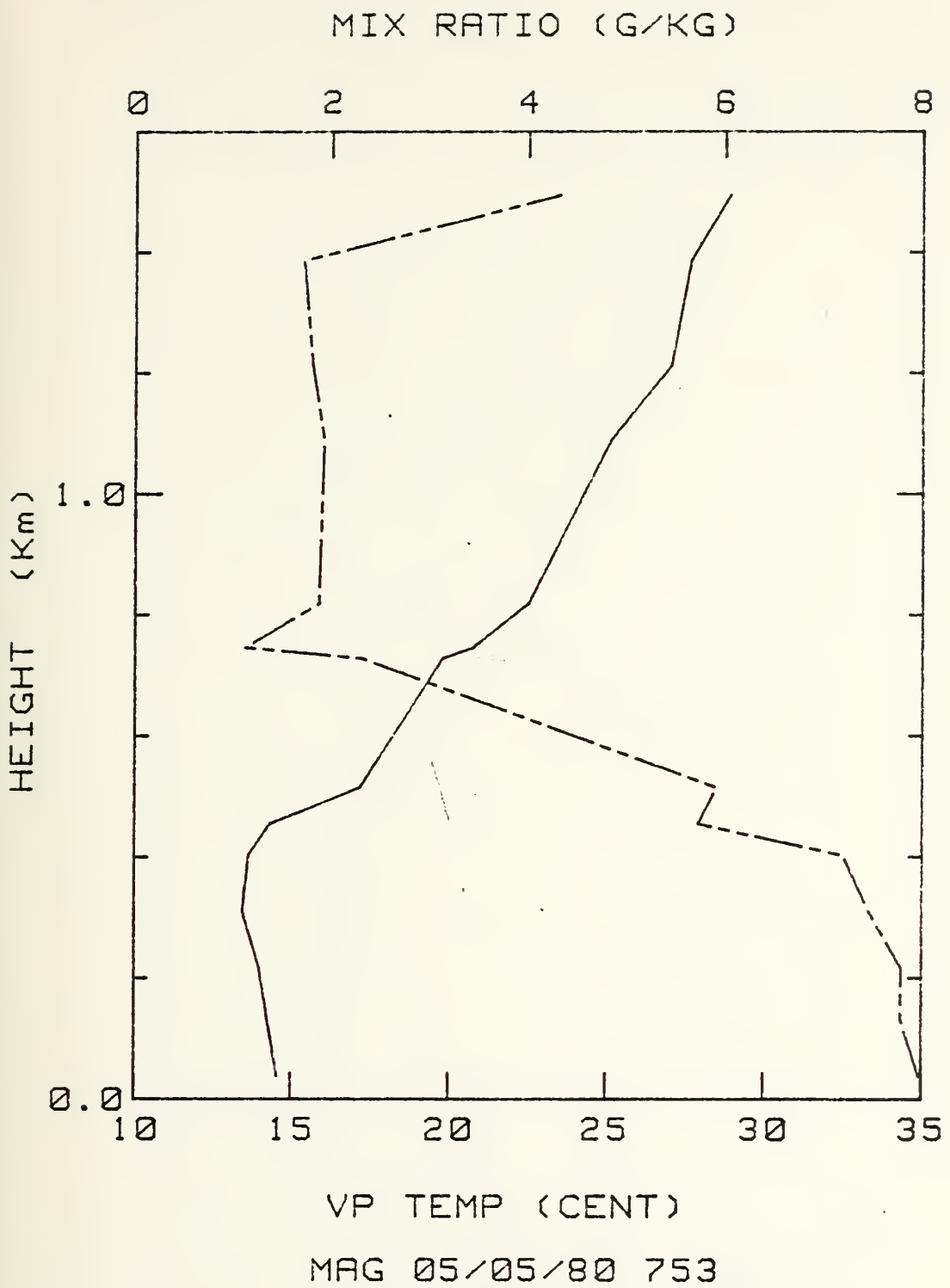

Figure 51. 5 May 1980 at 0753 PDT. NPS profile of virtual potential temperature (bottom scale, in degrees Celsius), solid line, and mixing ratio (top scale, in grams per kilogram), broken line, versus height.

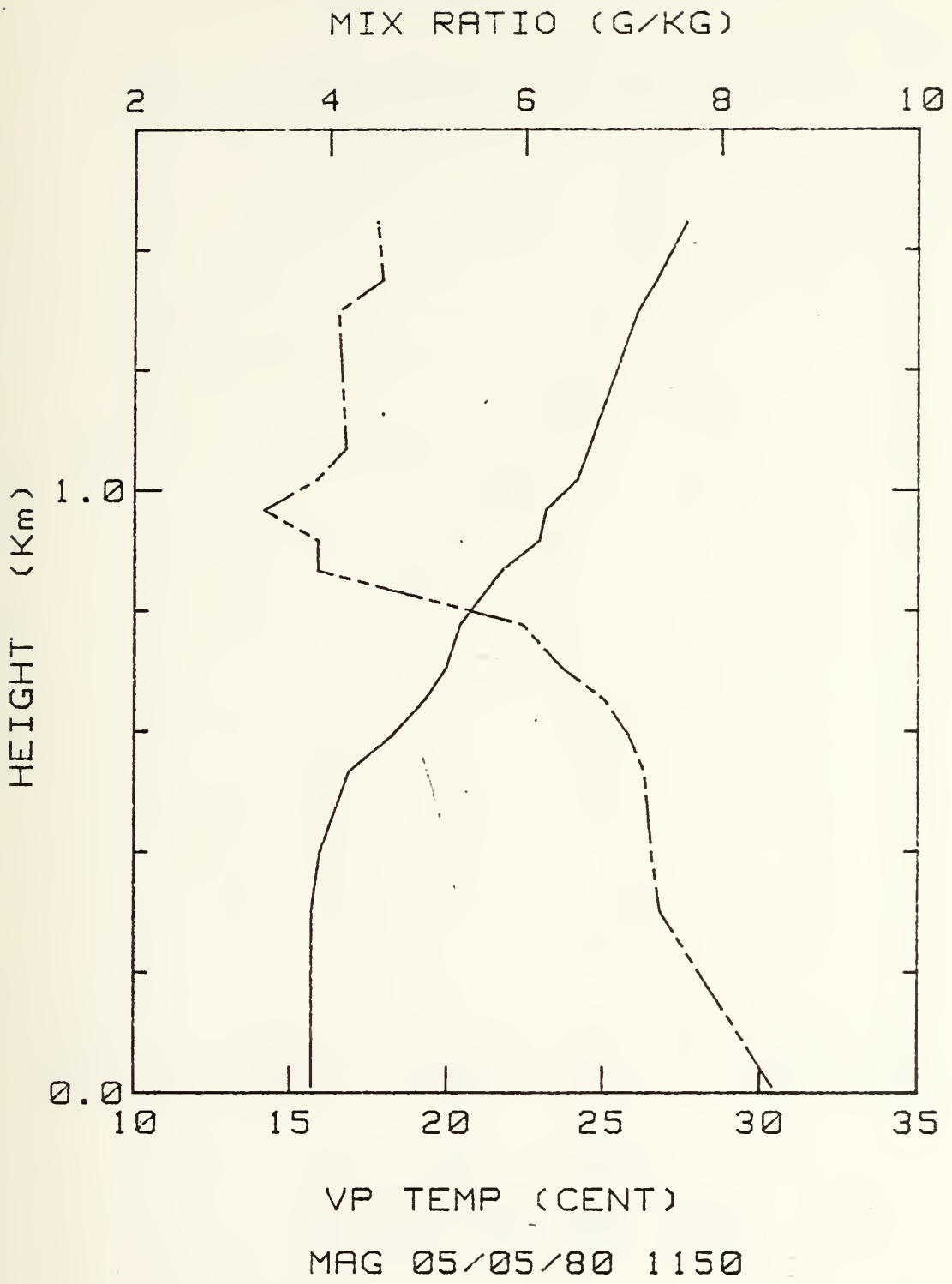

Figure 52. 5 May 1980 1150 PDT. ACANIA profile of virtual potential temperature (bottom scale, in degrees Celsius), solid line, and mixing ratio (top scale, in grams per kilogram), broken line, versus height.

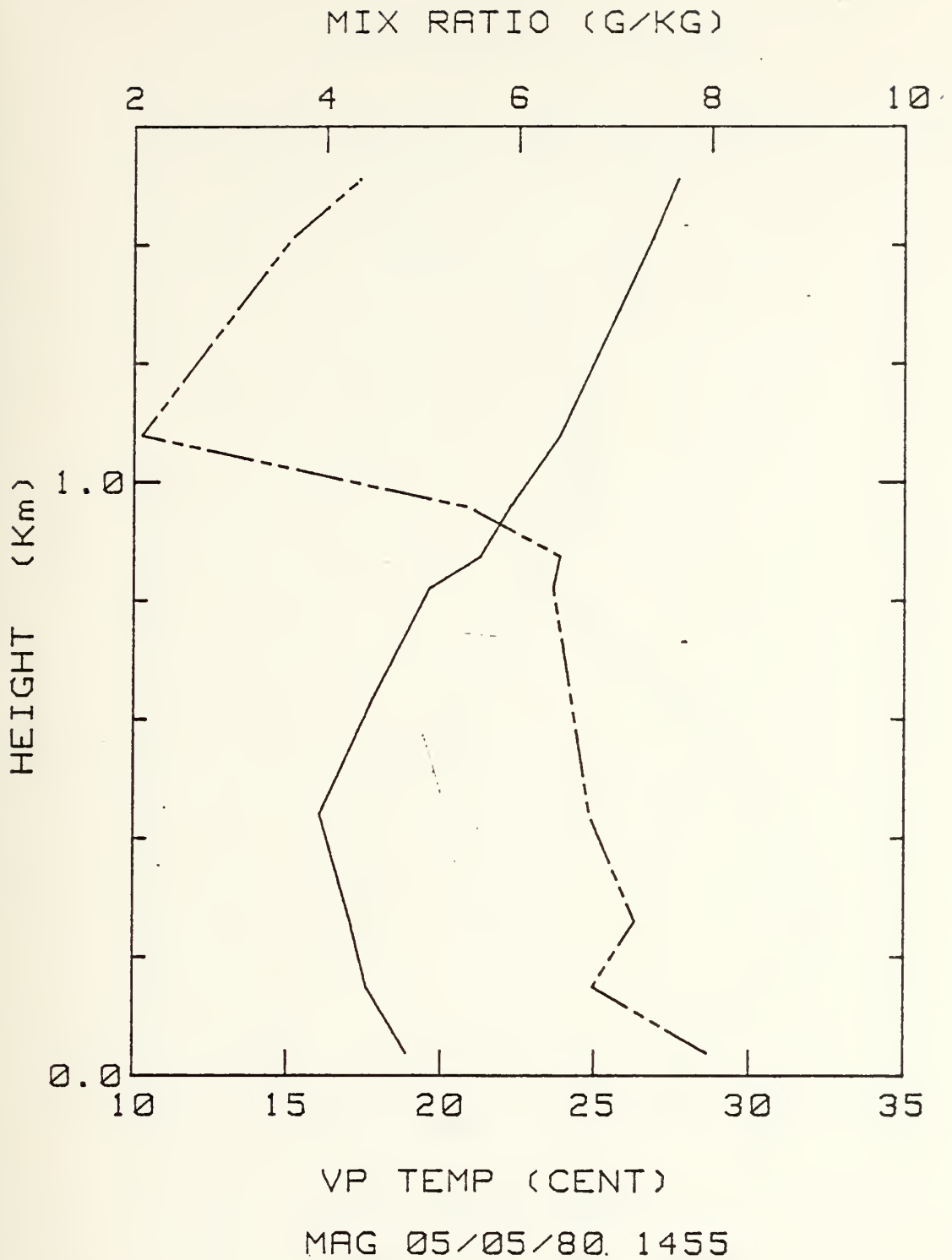

Figure 53. 5 May 1980 at 1455 PDT. NPS profile of virtual potential temperature (bottom scale, in degrees Celsius), solid line, and mixing ratio (top scale, in grams per kilogram), broken line, versus height.

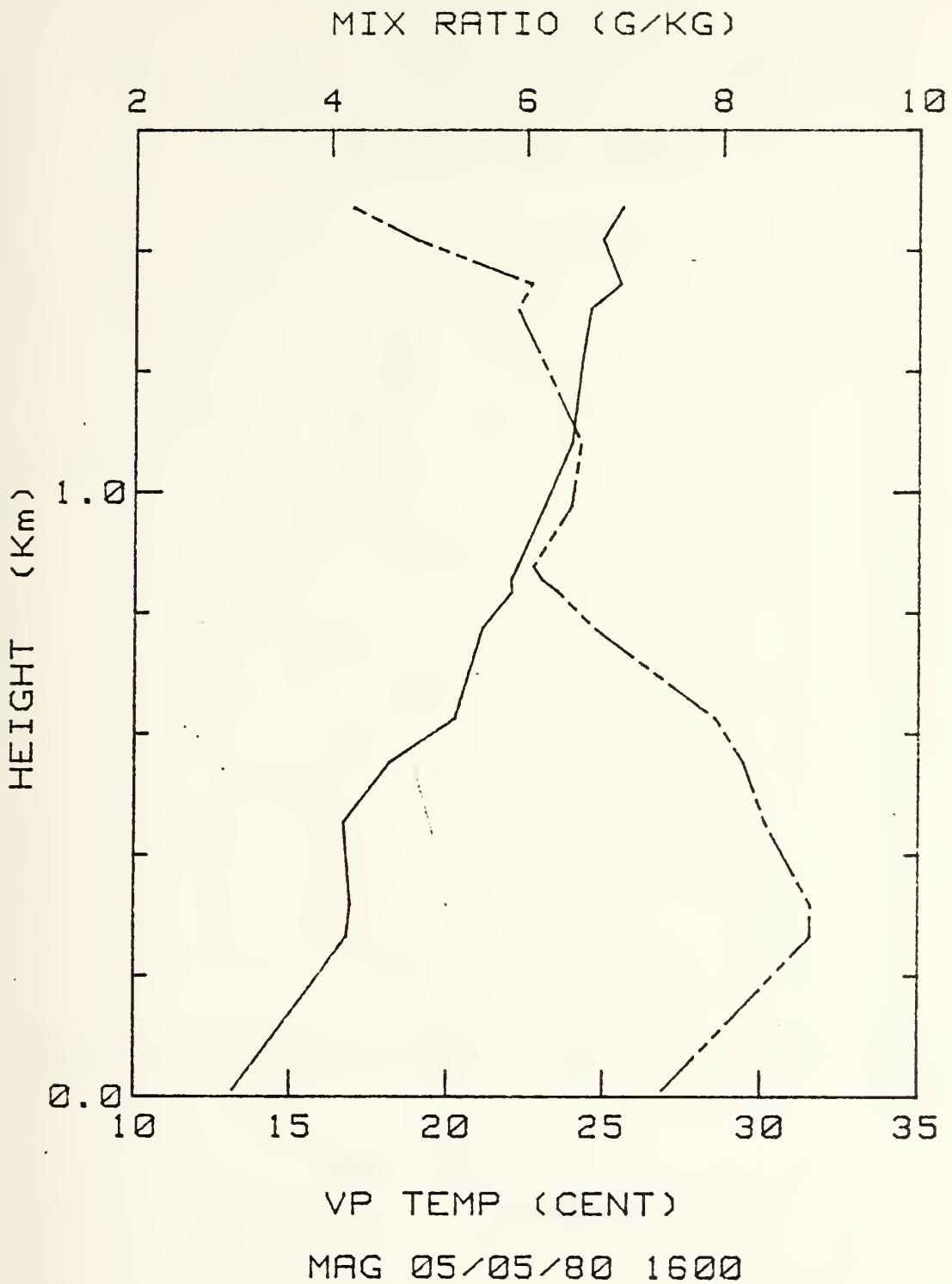

Figure 54. 5 May 1980 at 1600 PDT. ACADIA profile of virtual potential temperature (bottom scale, in degrees Celsius), solid line, and mixing ratio (top scale, in grams per kilogram), broken line, versus height.

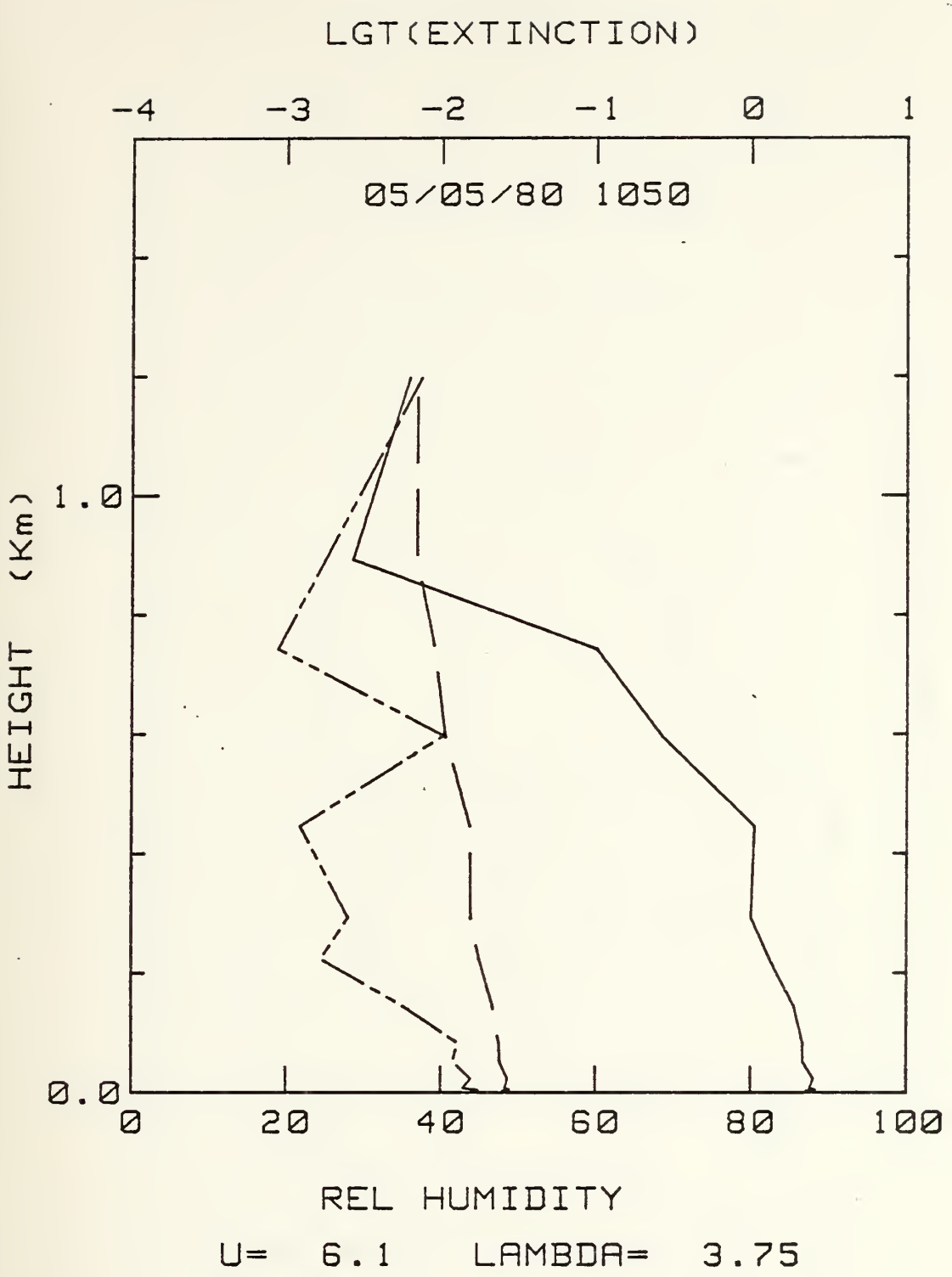

Figure 55. 5 May 1980 at 1050 PDT profile of relative humidity (bottom scale) solid line, observed extinction coefficients (top scale), series of short solid and dashed lines, and predicted extinction coefficients, series of short solid lines versus height. Top scale is logarithmic, where 1 is 10. Wind speed at 6.1 m/s and wavelength (LAMBDA) at 3.75 microns.

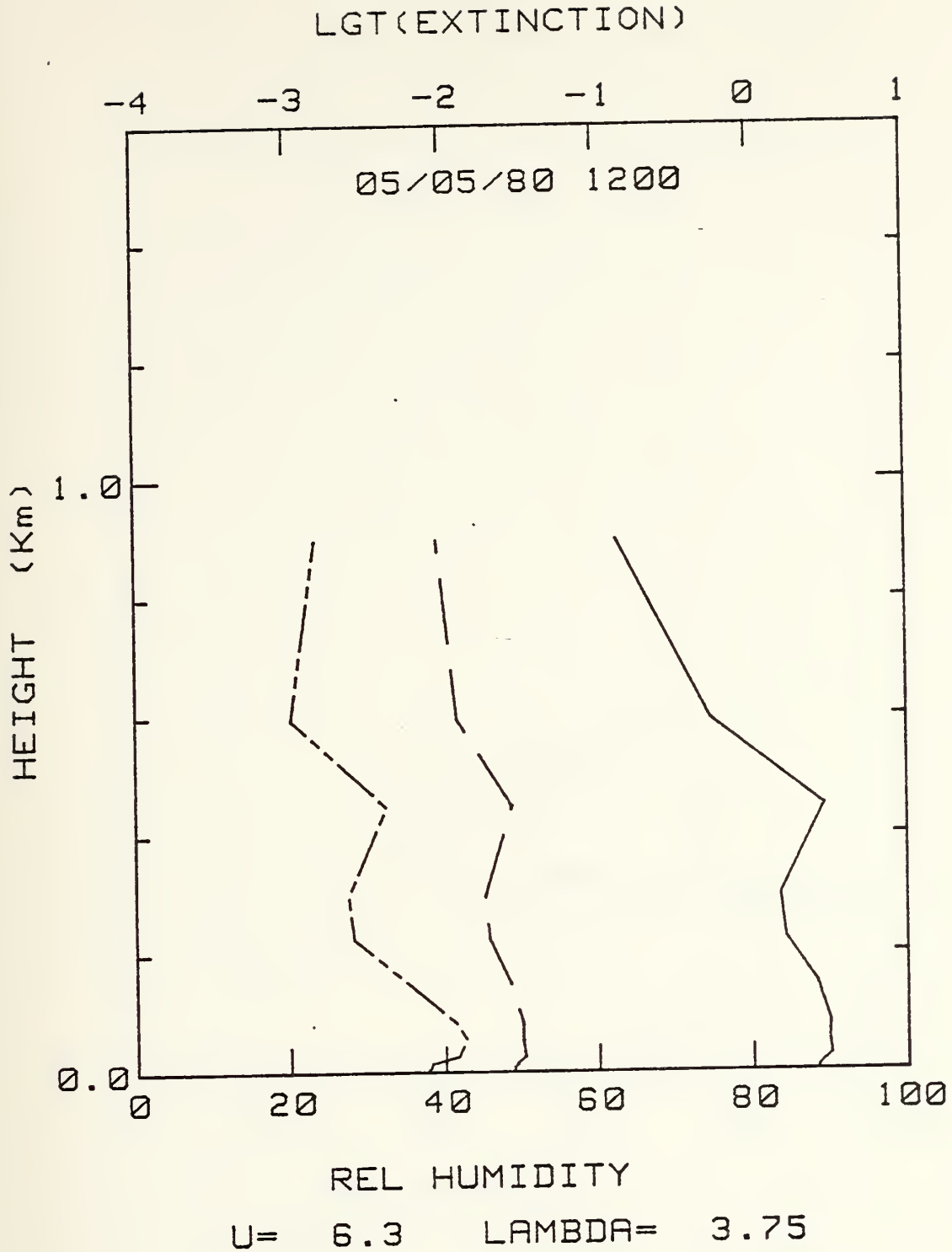

Figure 56. 5 May 1980 at 1200 PDT profile of relative humidity (bottom scale) solid line, observed extinction coefficients (top scale), series of short solid and dashed lines, and predicted extinction coefficients, series of short solid lines versus height. Top scale is logarithmic, where 1 is 10. Wind speed at 6.3 m/s and wavelength (LAMBDA) at 3.75 microns.

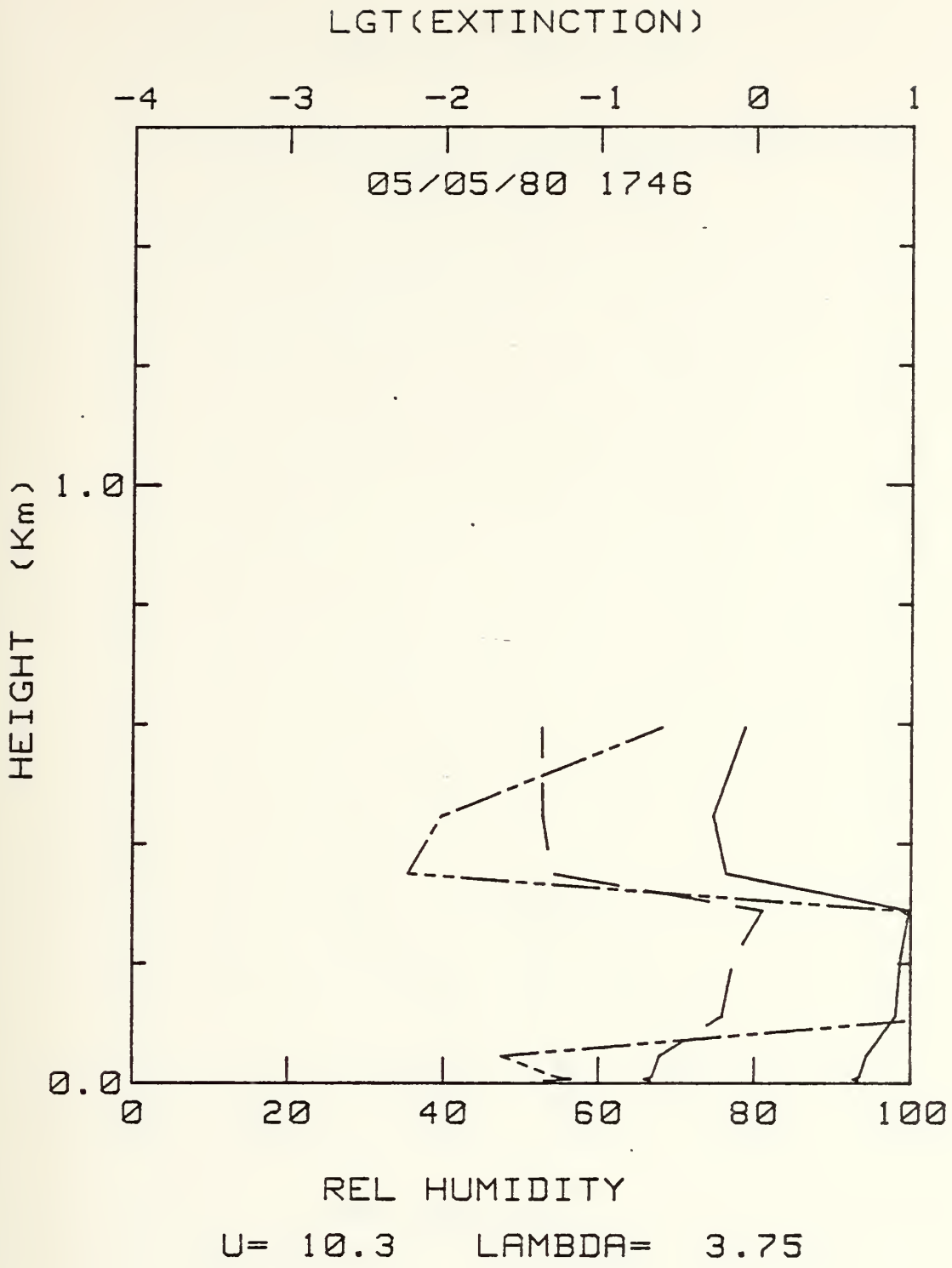

Figure 57. 5 May 1980 at 1746 PDT profile of relative humidity (bottom scale) solid line, observed extinction coefficients (top scale), series of short solid and dashed lines, and predicted extinction coefficients, series of short solid lines versus height. Top scale is logarithmic, where 1 is 10. Wind speed at 10.3 m/s and wavelength (LAMBDA) at 3.75 microns.

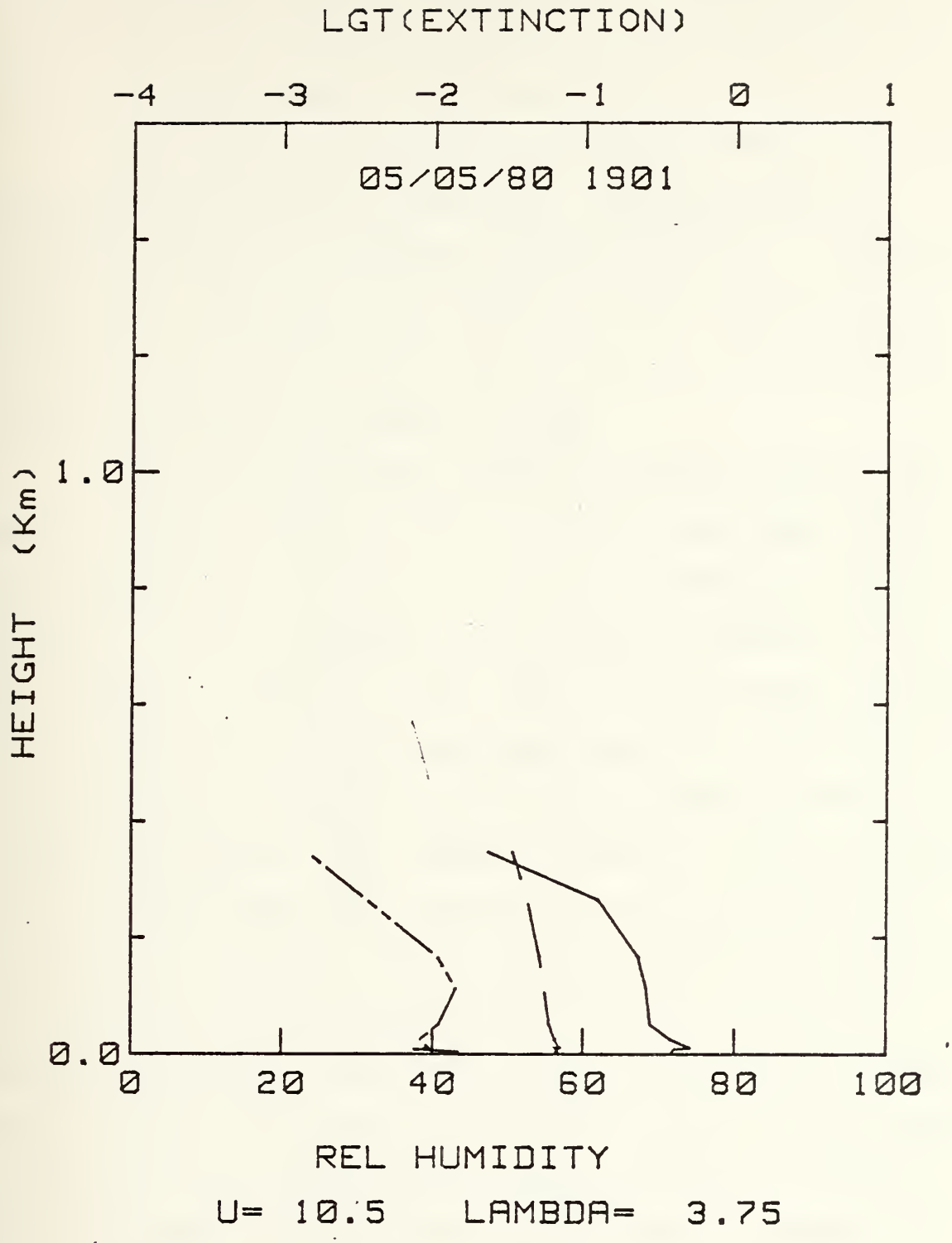

Figure 58. 5 May 1980 at 1901 PDT profile of relative humidity (bottom scale) solid line, observed extinction coefficients (top scale), series of short solid and dashed lines, and predicted extinction coefficients, series of short solid lines versus height. Top scale is logarithmic, where 1 is 10. Wind speed at 10.5 m/s and wavelength (LAMBDA) at 3.75 microns. Wind speed calculated from friction velocity.

unstable condition during the early morning hours and in a neutral condition throughout the rest of the day (Table IV). This is a day with active local generation.

The area is still behind the frontal system which passed through the area on the fifth. Another system is approaching from the northwest, Figures 22 and 24. Scattered clouds, with occasional clear periods, exist over the area until 1553 PDT, when a deck of low clouds moves in. The visibilities remain unrestricted throughout the day.

The morning aircraft (spiral) profiles (Figures 59 and 60) exhibit a shallow (200 m) to moderately deep (425 m) mixed layer at 46 and 89 km to the west-northwest of NPS, Figure 15. In the afternoon, the profiles (Figures 61-63) again exhibit a shallow to deep (200 to 600 m) mixed layer as the aircraft went outward from shore Figure 16. However, the soundings from the ACANIA and NPS do not support a well defined mixed layer. The morning soundings at NPS (0800 PDT) and the ACANIA (0835 PDT), Figures 64 and 65 respectively, could be made to agree with the spiral profiles by neglecting the first two or three levels of the virtual potential temperature profile. This would place the top of the mixed layer at NPS at 200 m and at the ACANIA at 500 m. The ACANIA was 67 km to the west-northwest of NPS, Figure 9. However, above the mixed layer the NPS sounding shows a decrease in the values of virtual potential temperature and an increase in mixing ratio at the middle levels compared to the spiral

TABLE IV

Surface Layer Values 7 May 1980

U is wind speed (m/s), T(°c) is temperature in degrees celsius, T_s(°c) is sea surface temperature in degrees celsius, RH(%) is relative humidity in percent, and Z/L is stability index.

Time	U	T(°c)	T_s(°c)	RH(%)	Z/L
00:03	11.4	12.70	13.05	92	-1.16E-02
00:33	10.2	12.60	13.04	89	-1.66E-02
01:03	10.1	12.53	12.90	94	-1.75E-02
01:33	9.4	12.40	12.56	95	-1.61E-02
02:03	9.0	12.34	12.55	96	-1.63E-02
02:33	9.3	12.34	12.61	96	-1.68E-02
03:03	9.9	12.35	12.50	96	-1.20E-02
03:33	9.8	12.25	12.45	95	-1.92E-02
04:03	8.6	12.23	12.29	95	-1.11E-02
04:33	8.9	12.40	12.51	94	-1.90E-02
05:03	8.4	12.27	12.61	95	-2.64E-02
05:33	7.5	12.09	12.37	95	-2.67E-02
06:03	7.7	12.07	12.19	95	-1.33E-02
06:33	8.8	12.10	11.73	96	1.32E-02
07:03	9.2	12.37	11.90	95	1.49E-02
07:33	9.8	12.58	12.29	94	4.93E-03
08:03	11.3	12.73	12.42	93	4.06E-03
08:33	12.9	12.99	12.50	91	4.39E-03
09:03	13.1	12.95	12.65	92	3.47E-03
09:33	13.0	12.89	12.77	93	5.98E-04
10:03	12.3	12.89	12.98	93	-3.48E-03
10:11	11.8	12.58	13.25	95	-2.03E-02
10:33	12.3	12.91	13.09	93	-4.23E-03
11:03	11.8	13.02	13.01	93	-1.77E-03
11:33	12.4	13.11	13.05	92	-9.48E-04
12:03	12.2	13.19	13.21	92	-2.33E-03
12:33	11.9	13.20	13.33	93	-4.79E-03
13:03	11.3	13.18	13.38	93	-6.95E-03
13:33	11.8	13.14	13.40	93	-7.91E-03
14:03	11.7	13.23	13.41	92	-6.47E-03
14:33	11.7	13.31	13.45	92	-5.99E-03
15:03	12.4	13.35	13.36	91	-2.86E-03
15:33	11.8	13.38	13.34	91	-1.78E-03
16:03	11.3	13.46	13.36	91	-6.21E-04
16:18	11.2	13.52	13.36	91	1.28E-03
16:23	11.4	13.28	13.52	92	-1.11E-02

TABLE IV (CONT'D)

Time	U	T(^{o}c)	Ts(^{o}c)	RH(%)	Z/L
16:33	11.7	13.50	13.37	80	-3.26E-04
17:03	11.7	13.53	13.37	81	3.69E-04
17:33	12.7	13.50	13.39	81	-5.20E-04
18:03	12.6	13.45	13.44	80	-2.42E-03
18:33	12.2	13.39	13.49	80	-4.07E-03
19:07	12.7	13.30	13.37	81	-3.37E-03
19:37	13.1	13.29	13.18	81	-5.67E-05
20.07	13.6	13.21	12.46	79	9.33E-03
20:37	14.3	13.05	12.41	79	6.60E-03
21:07	13.2	12.96	12.55	80	3.77E-03
21:45	12.2	12.94	12.63	79	2.59E-03
22:15	11.7	12.84	12.55	79	3.40E-03
22:45	10.4	12.77	12.47	79	4.95E-03
23:15	9.4	12.77	12.35	79	1.10E-02
23:45	9.9	12.81	12.43	79	7.71E-03

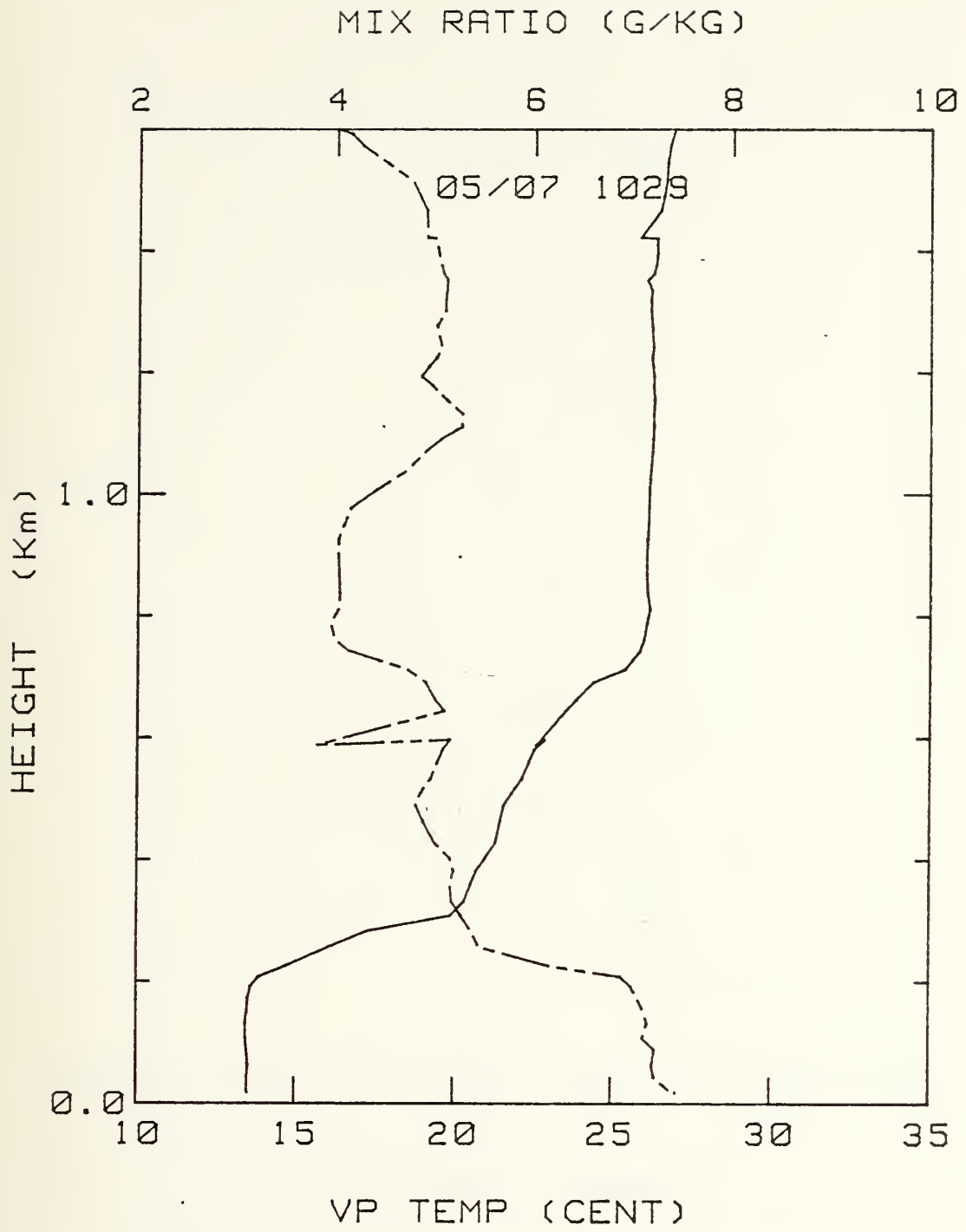

Figure 59. 7 May 1980 at 1029 PDT. Aircraft profile of virtual potential temperature (bottom scale, in degrees Celsius), solid line, and mixing ratio (top scale, in grams per kilogram), broken line, versus height.

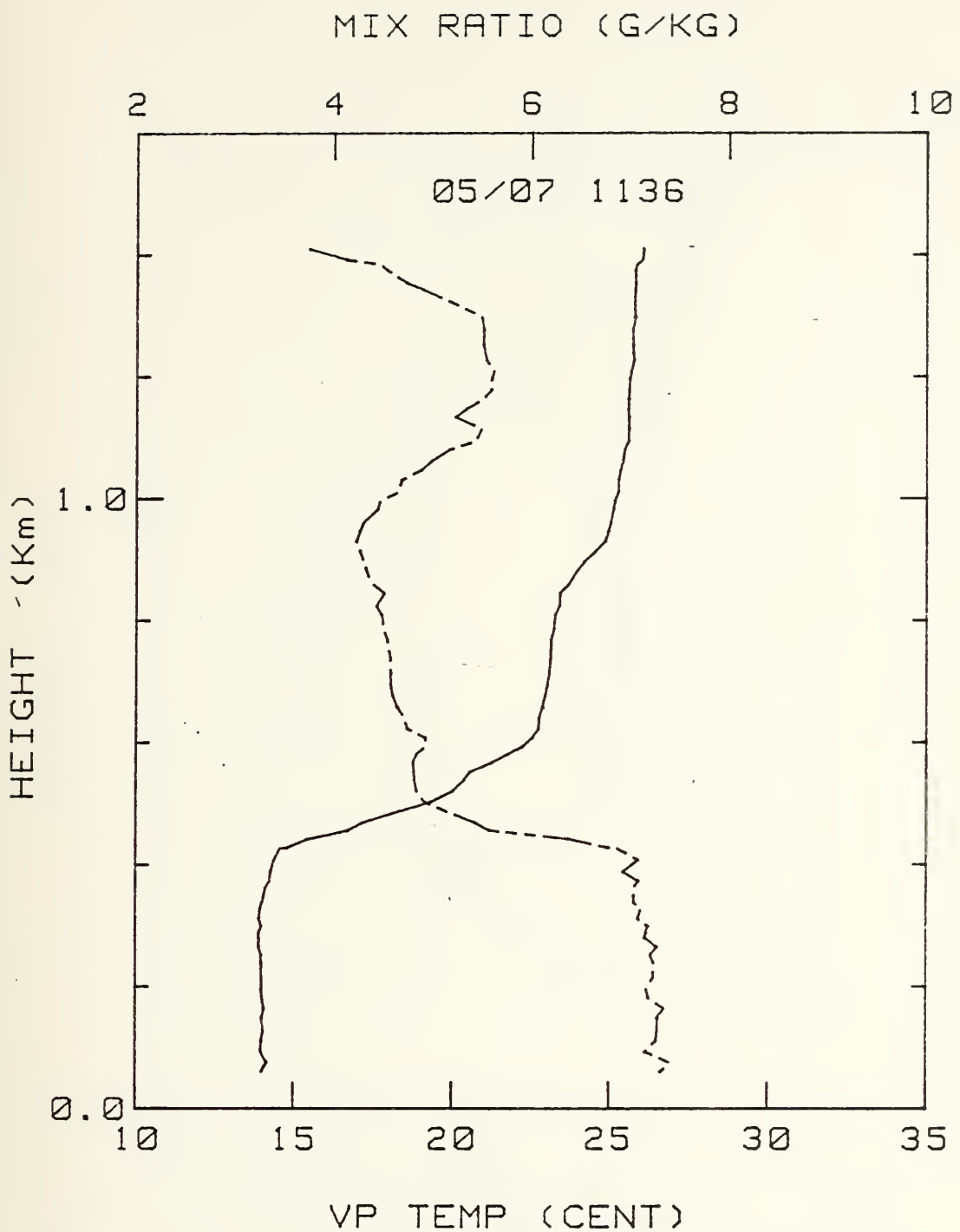

Figure 60. 7 May 1980 at 1136 PDT. Aircraft profile of virtual potential temperature (bottom scale, in degrees Celsius), solid line, and mixing ratio (top scale, in grams per kilogram), broken line, versus height.

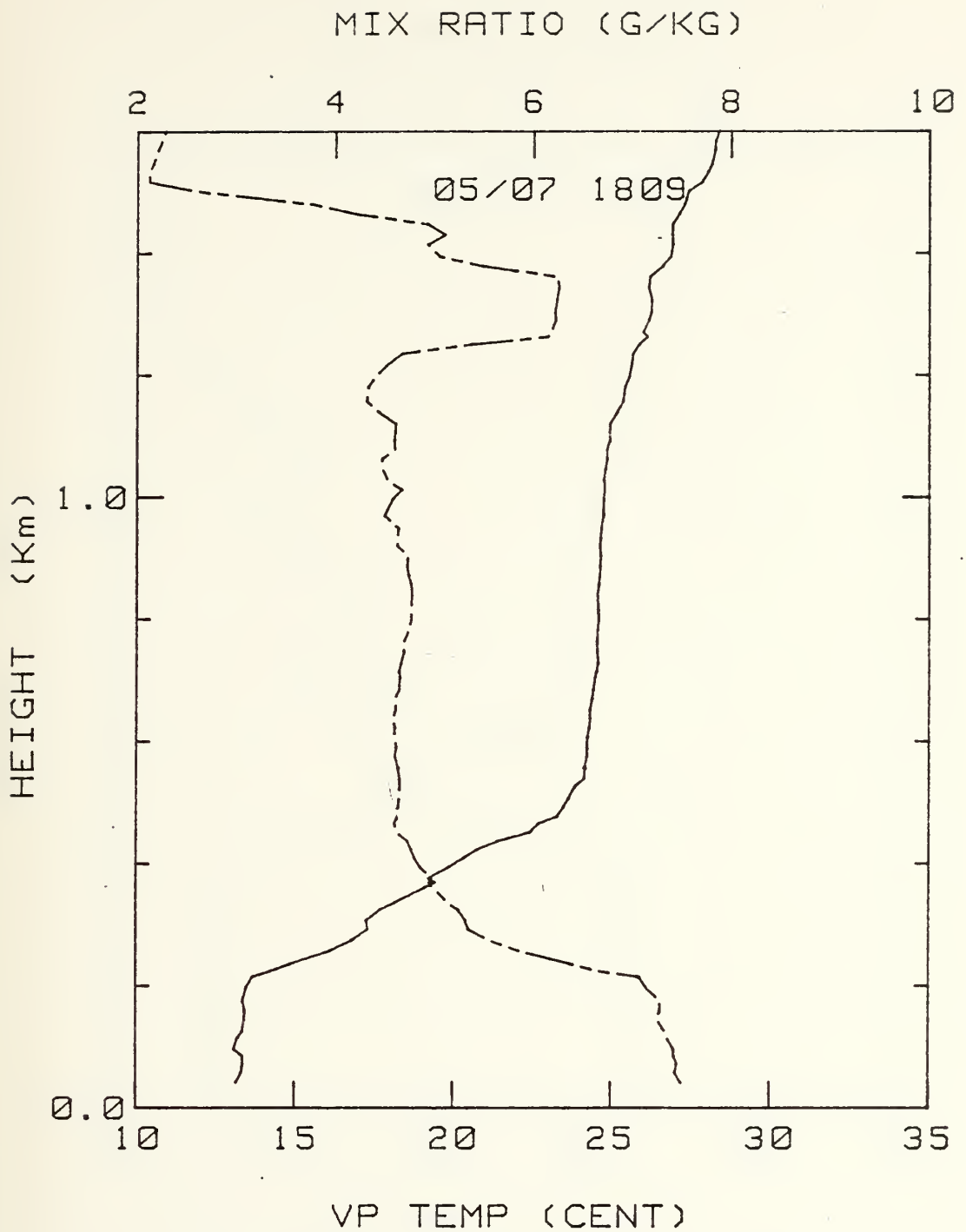

Figure 61. 7 May 1980 at 1809 PDT. Aircraft profile of virtual potential temperature (bottom scale, in degrees Celsius), solid line, and mixing ratio (top scale, in grams per kilogram), broken line, versus height.

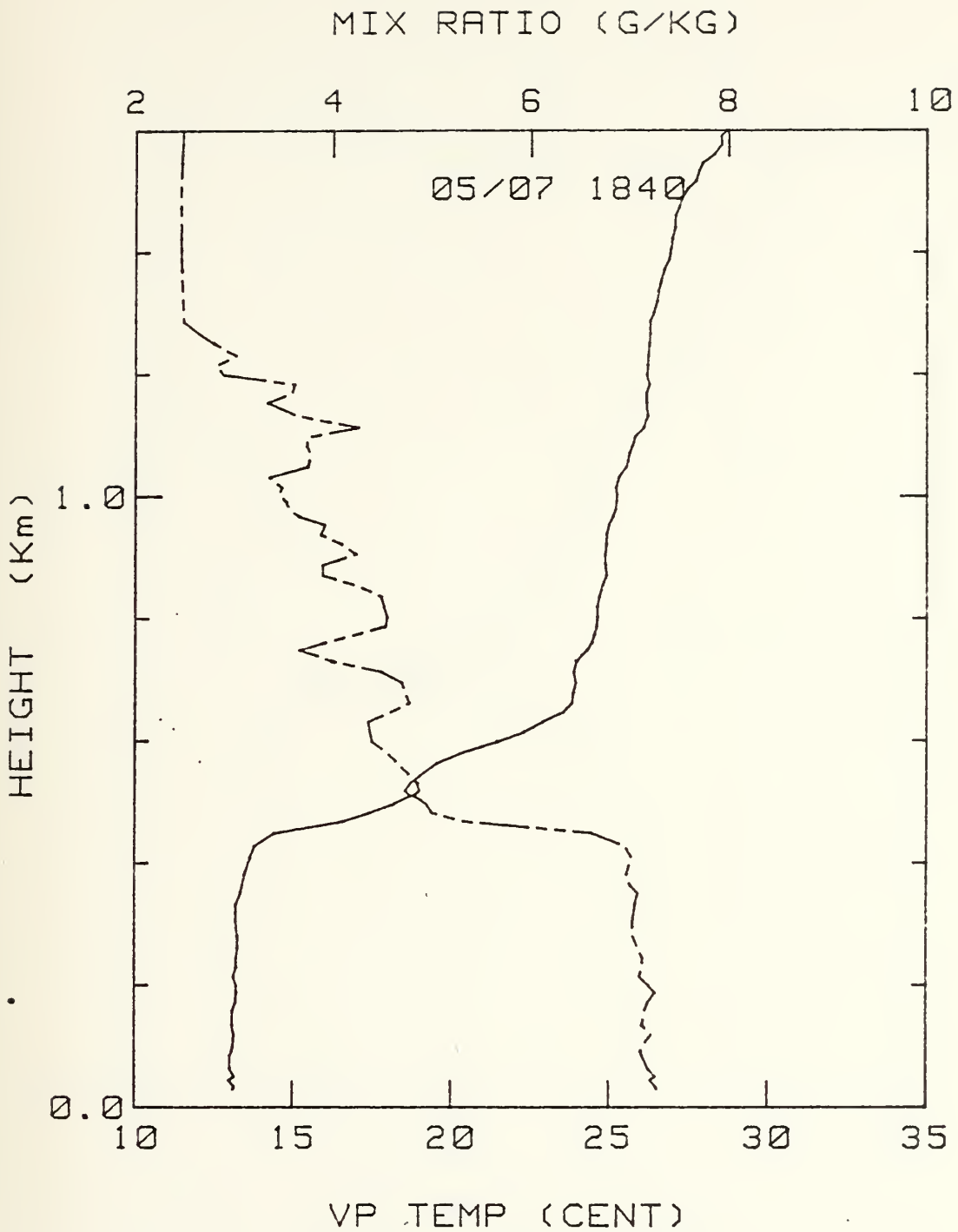

Figure 62. 7 May 1980 at 1840 PDT. Aircraft profile of virtual potential temperature (bottom scale, in degrees Celsius), solid line, and mixing ratio (top scale, in grams per kilogram), broken line, versus height.

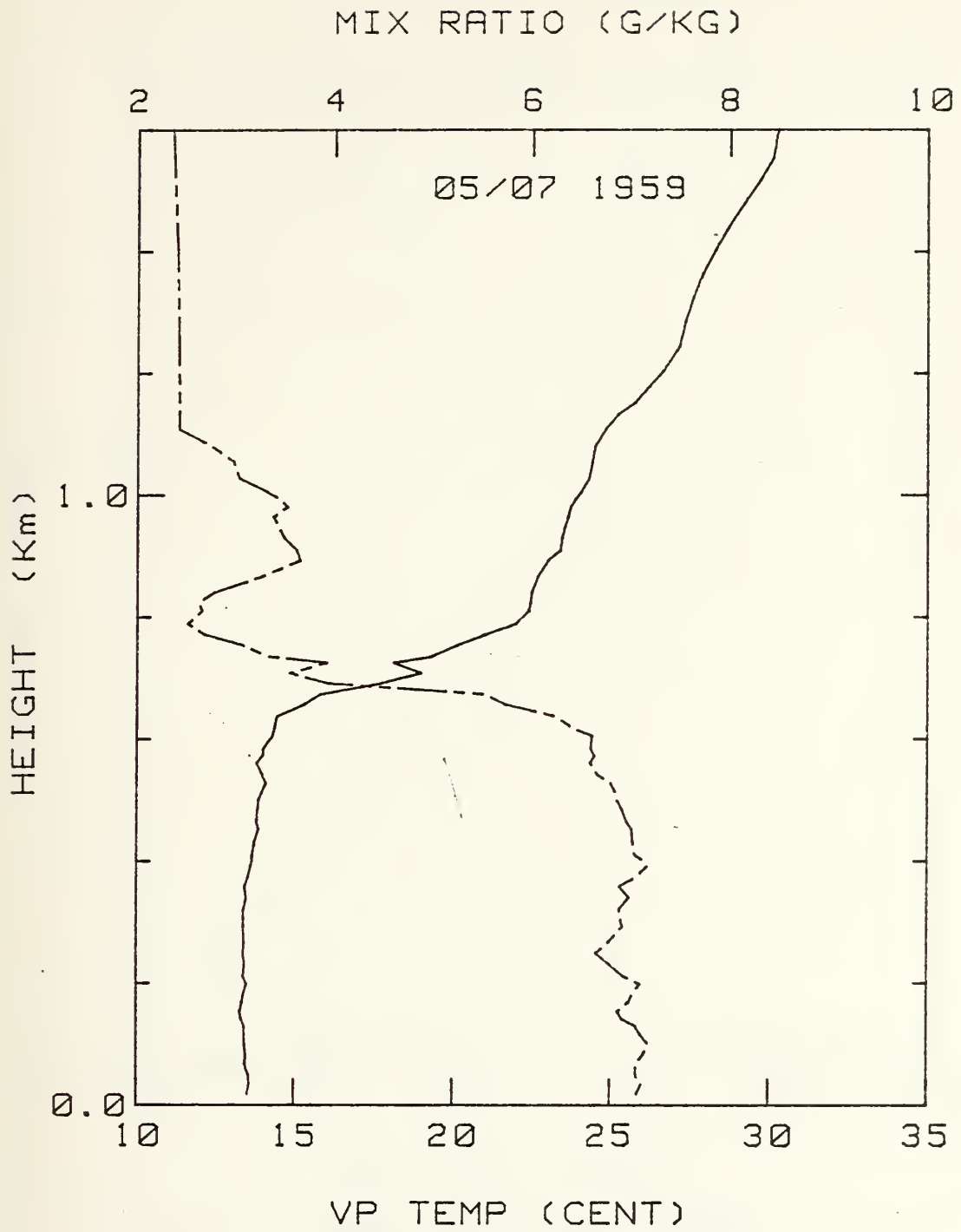

Figure 63. 7 May 1980 at 1959 PDT. Aircraft profile of virtual potential temperature (bottom scale, in degrees Celsius), solid line, and mixing ratio (top scale, in grams per kilogram), broken line, versus height.

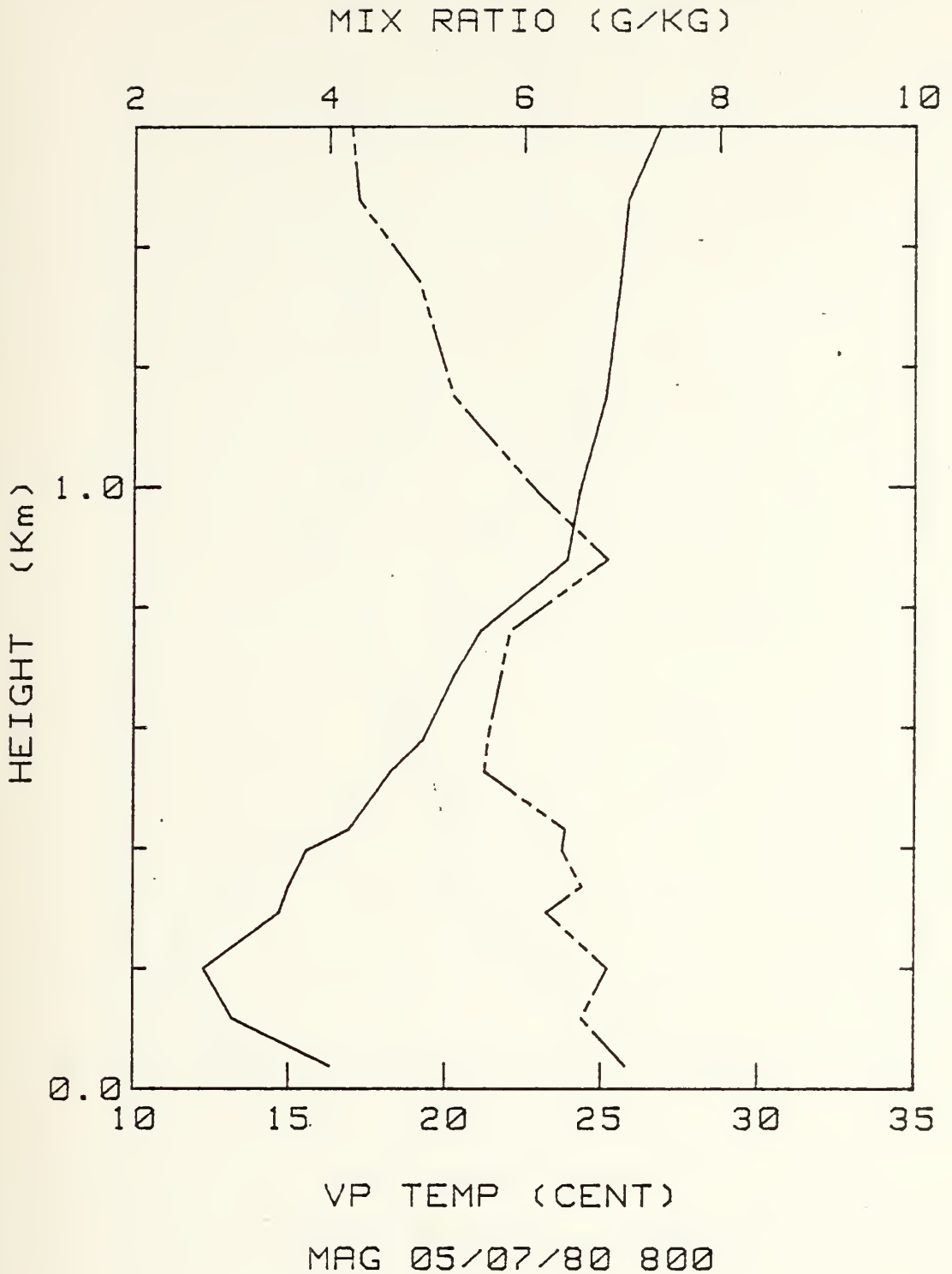

Figure 64. 7 May 1980 at 0800 PDT. NPS profile of virtual potential temperature (bottom scale, in degrees Celsius), solid line, and mixing ratio (top scale, in grams per kilogram), broken line, versus height.

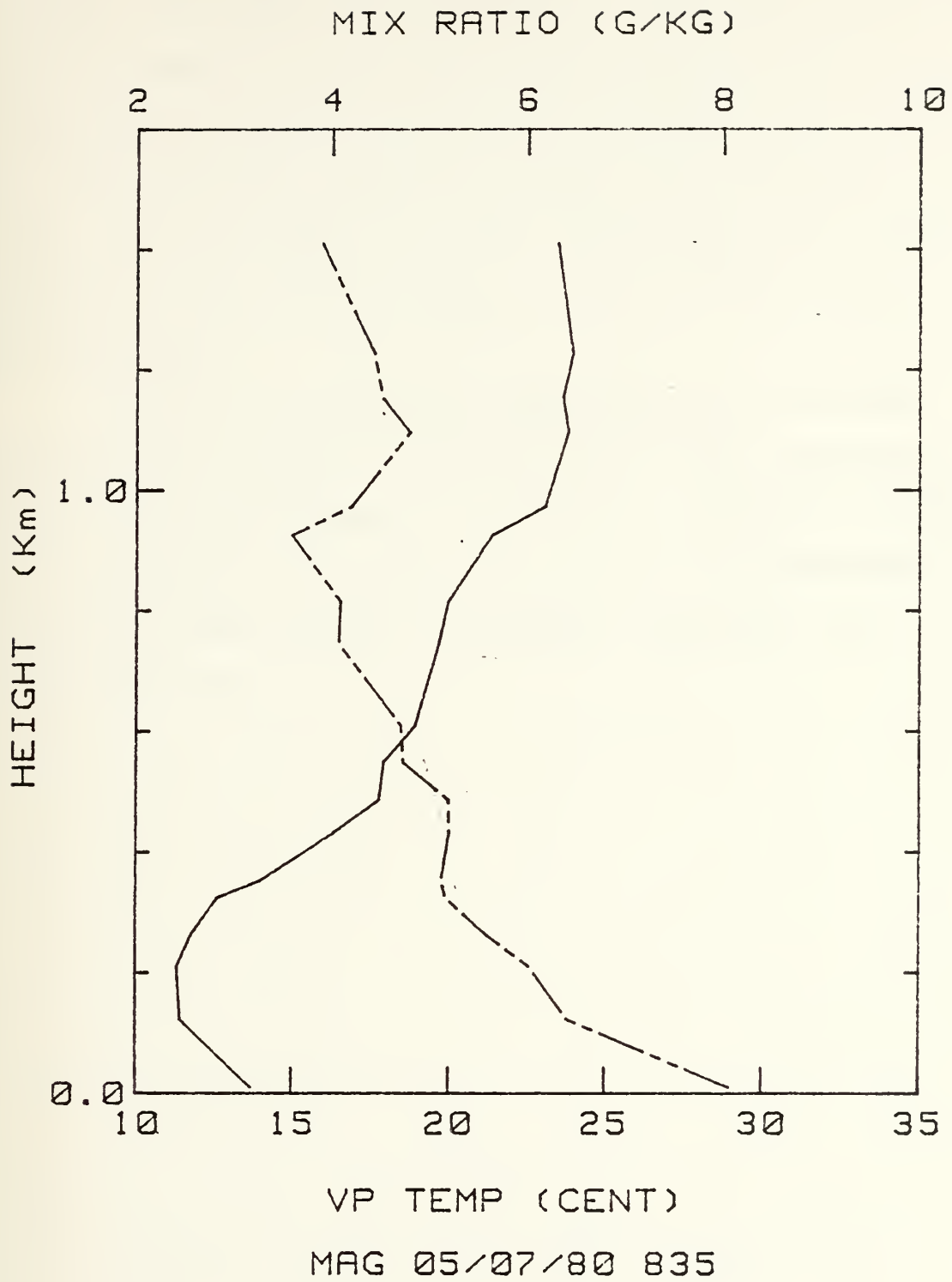

Figure 65. 7 May 1980 at 0835 PDT. ACANIA profile of virtual potential temperature (bottom scale, in degrees Celsius), solid line, and mixing ratio (top scale, in grams per kilogram), broken line, versus height.

profiles. The ACANIA sounding shows a lower value of virtual potential temperature, for all values above the mixed layer, compared to the spiral profiles. The afternoon NPS sounding, 1555 PDT (Figure 66), shows the top of the mixed layer to be at 600 m when it should be at 200 m according to the spiral profiles. It also shows a drier region above the top of the mixed layer.

On this day with active generation and a strong inversion which varies in height with location, predicted extinction values (Figures 67 and 68) are definitely larger than the observed values near the surface. The observed extinction values are not in reasonable agreement with those predicted.

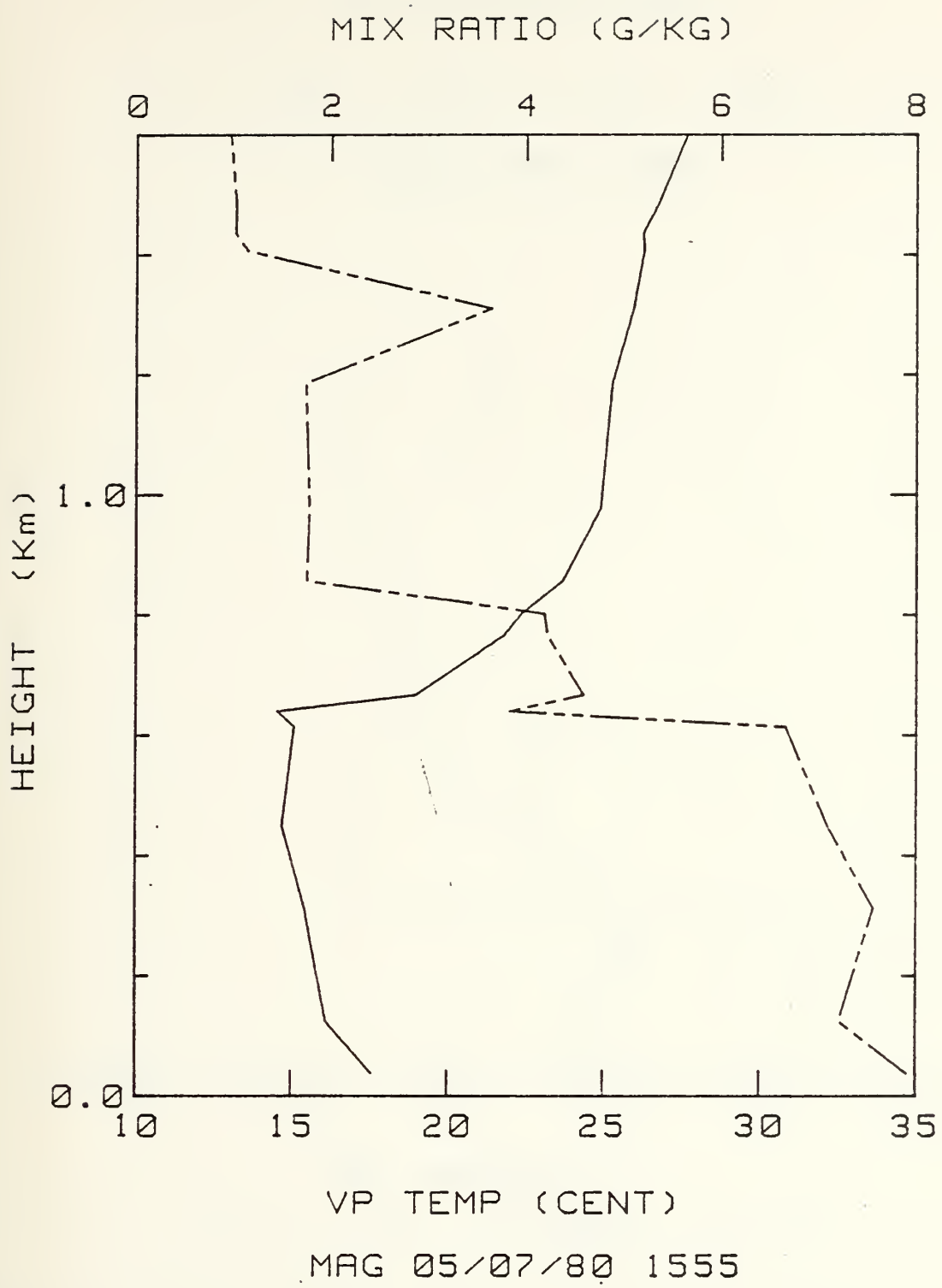

Figure 66. 7 May 1980 at 1555 PDT. NPS profile of virtual potential temperature (bottom scale, in degrees Celsius), solid line, and mixing ratio (top scale, in grams per kilogram), broken line, versus height.

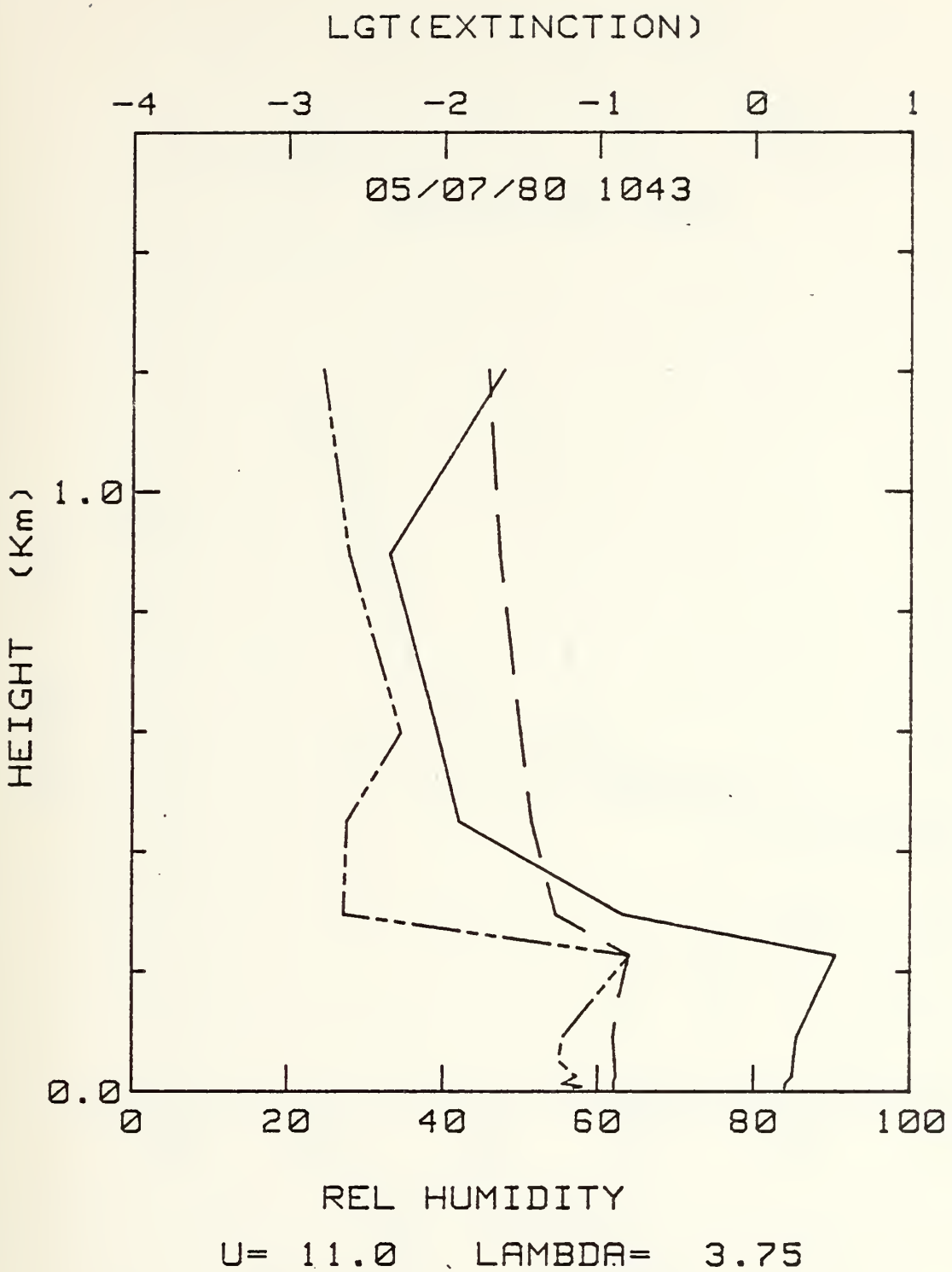

Figure 67. 7 May 1980 at 1043 PDT profile of relative humidity (bottom scale) solid line, observed extinction coefficients (top scale), series of short solid and dashed lines, and predicted extinction coefficients, series of short solid lines versus height. Top scale is logarithmic, where 1 is 10. Wind speed at 11.0 m/s and wavelength (LAMBDA) at 3.75 microns. Wind speed calculated from friction velocity.

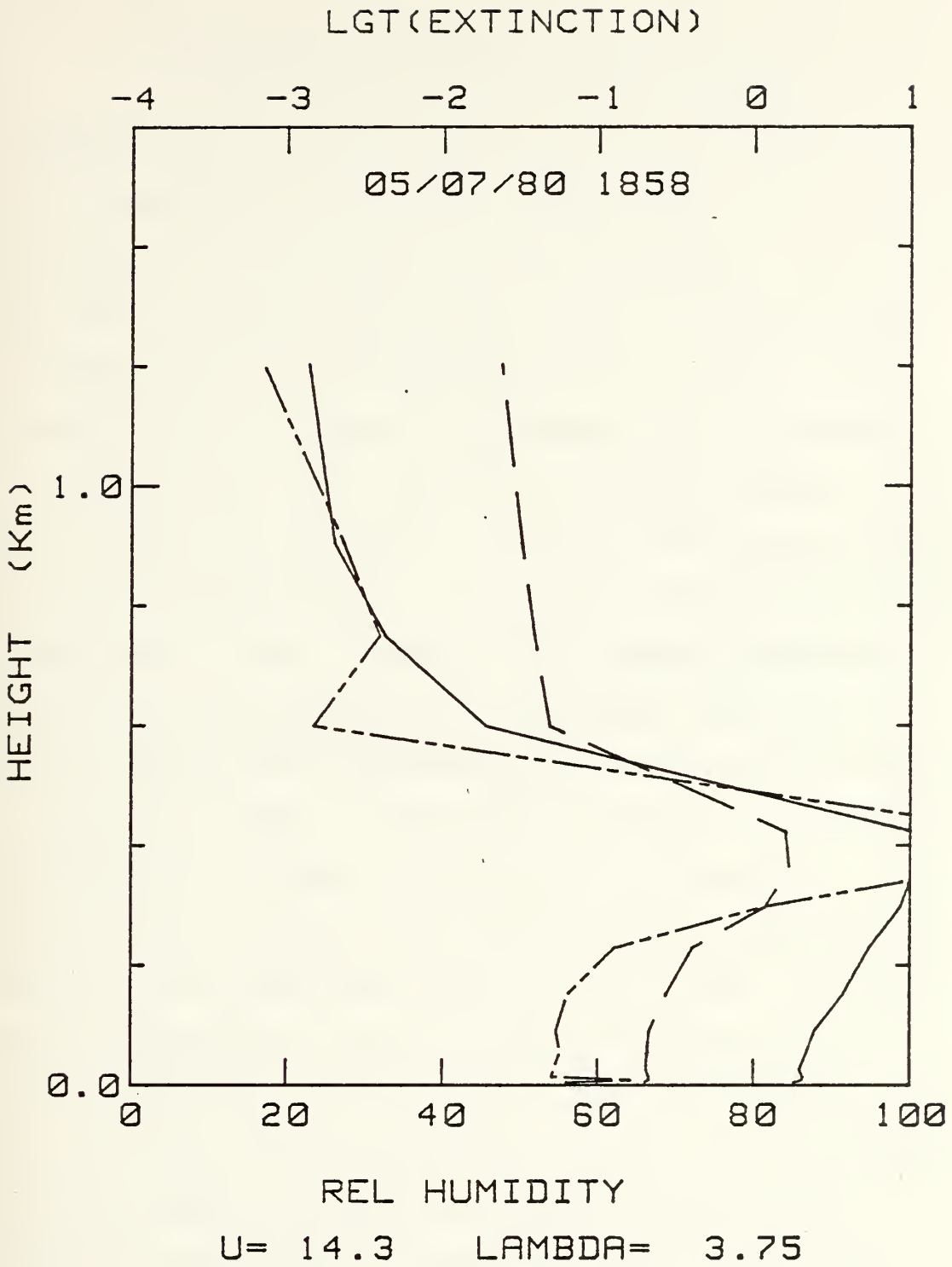

Figure 68. 7 May 1980 at 1858 PDT profile of relative humidity (bottom scale) solid line, observed extinction coefficients (top scale), series of short solid and dashed lines, and predicted extinction coefficients, series of short solid lines versus height. Top scale is logarithmic, where 1 is 10. Wind speed at 14.3 m/s and wavelength (LAMBDA) at 3.75 microns.

V. SUMMARY AND INTERPRETATION OF RESULTS

Results predicted in the previous section clearly show that the predicted values and the actual values of extinction are correlated to some degree in the mixed layer. When they differ, the deviations appear to be due to both wind speed and relative humidity specifications in the model. The wind speeds used in the model are averages over time and are not the local wind at the time of the observed profile. This appears to have had the effect of causing the predicted profile to be biased toward higher or lower values depending on whether the wind speed is over or below 7 m/s. Higher predicted extinctions were associated with wind speeds that are too high and a lower predicted extinction indicates wind speeds too low on the average. Wind speeds recorded from the ship are believed to be within an accuracy of ten percent [Schacher et al, 1980a] and average relative humidity are believed to have accuracies within three percent. In view of these accuracies of the two controlling factors, the results of the predicted extinction values could still not be adjusted to agree with the observed results. Another reason for the differences between the predicted and observed extinction profiles could be round-off and/or truncation errors of the empirically derived coefficients of the prediction model. This is not believed to have been the

reason. Even if all the above measurement and computational errors could have been corrected, the predicted extinction values would not be the same as the actual extinction values in the mixed layer.

A significant aspect of the comparison is that if the predicted value were normalized with the actual value of extinction in the lower mixed layer, there seems to be a higher concentration of aerosols near the top of the mixed layer than predicted by the model. This could be explained on the basis of the relative humidity sensitivity of the growth, as shown by Fitzgerald (1978), Figure 69. It is a reality that at a high value of relative humidity slight errors would drastically affect the predicted values. This has to be considered in view of the three percent uncertainty in the relative humidity measurement.

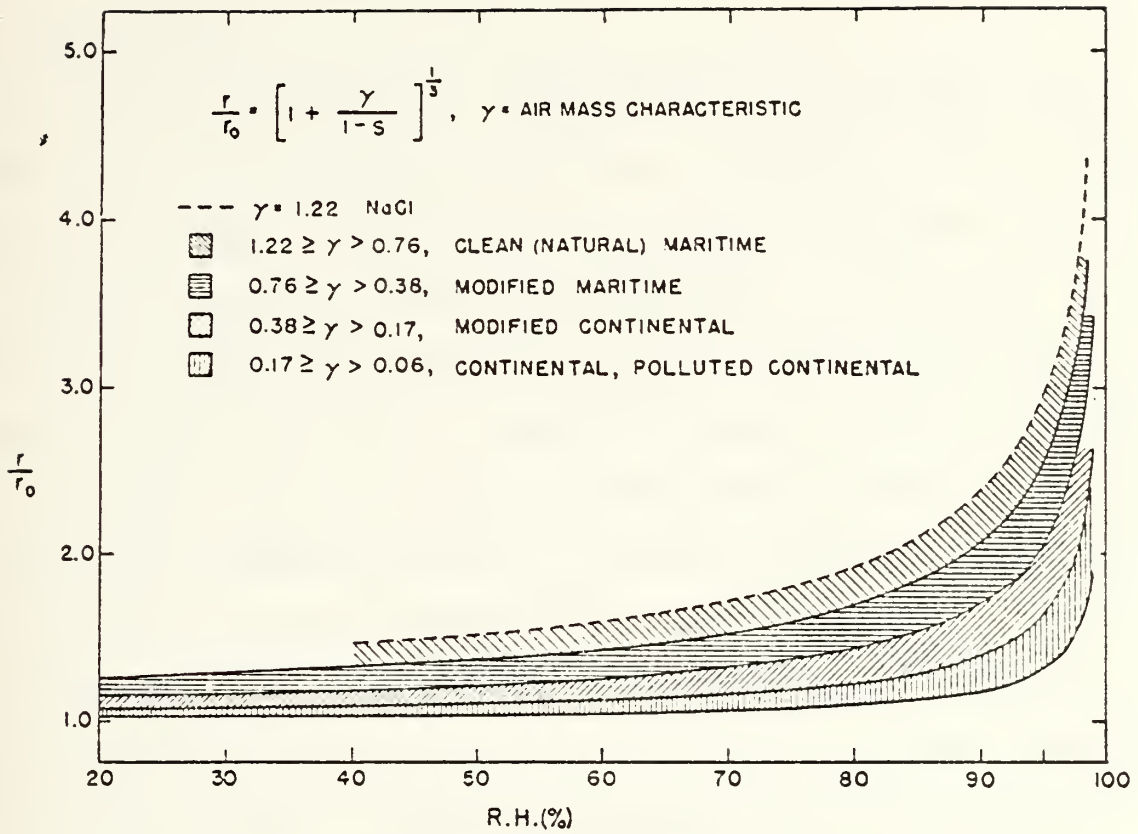

Figure 69. Relative humidity growth cruve for different air-mass characteristics, representing different aerosol types, in terms of ambient (r) versus dry size (r_o) radius. (Fitzgerald, 1978)

VI. CONCLUSIONS AND RECOMMENDATIONS

A. CONCLUSIONS

The model includes both a maritime and continental component above the top of the inversion. However, the maritime aerosols are trapped below the inversion so the region above was composed solely of continental aerosols. This leads to predicted values being larger than those actually measured above the inversion since a maritime source as included which did not exist. Also, the model specifies an exponental decrease with height rate for low relative humidities which was not found in the observed extinction.

Differences between the spiral profiles and the radiosonde profiles suggest that radiosondes can not yield accurate prediction profiles. Extinction profiles from an accurate model based on radiosonde data would be in error due to measurement capabilities.

The LOWTRAN 3B profiles (Figures 1 and 2) are not adequate because they are exponental even within the mixed layer. The model yielded relatively accurate extinction values near the surface, but yielded erroneous values at altitudes. This is because realistic relative humidity distributions are not considered. At sea, as seen, LOWTRAN 3B users risk underestimating the range when a fixed transmittance occurs [Hughes, 1980]. Over long over water slant path ranges, LOWTRAN 3B should not be used for open ocean vertical distributions of aerosol extinction.

B. RECOMMENDATIONS

Based on conclusions in part A the following recommendations are made:

(1) More sensitive radiosonde instruments should be developed along with calibration instruments. The perfect model, without accurate measurements of relative humidity, will not be able to accurately predict extinction.

(2) Experiments should be conducted in the Gulf of Mexico, off the eastern coast of the United States, and in the arid region of the southwest. This is because off the California west coast the relative humidity is usually not high compared to other U.S. continental coastal regions. The Gulf of Mexico would have a higher relative humidity when winds are from the south around the Bermuda High. The northern part of the east coast would have off shore wind flow around the Bermuda High. And the southwest would be lacking a moisture source.

3. One model should not be used to predict vertical aerosol extinction for different type regions. This is because of the continental component. Rather, a basic model should be modified for individual regions. For example: the Wells-Katz model could be modified for the West Coast to have only a continental component above the inversion of a mixed layer. An arid region might have only a continental component. The Gulf region might have only a maritime component during certain seasons and a mixed

component during others. Hence, the model should be verified for the different regions when this is accomplished. Then, the model, or models, would be used for similar regions.

LIST OF REFERENCES

Cottrell, F. G., F. D. Fry, D. D. Hodges, and R. F. Hartmann, 1979: ELECTRO-OPTICAL HANDBOOK, Volume I: Weather Support for Precision Guided Munitions. Air Weather Service Report AWS/TR-79/002, Scott AFB, IL, 97 pp.

Fairall, C. W., 1979: Aircraft Measurements of Micrometeorological Parameters at Panama City, Florida, in 1978. The BDM Corporation Report BDM/W-008-79, Monterey, California, 104 pp.

Fairall, C. W., 1980: Atmospheric Optical Propagation Comparisons During MAGAP-80. The BDM Corporation Report BDM/W-010-80, Monterey, California, 142 pp.

Fairall, C. W., G. E. Schacher, and K. L. Davidson, 1980: Atmospheric Optical Propagation Comparisons During MAGAP-80. Naval Postgraduate School Report NPS-61-81-002, Monterey, California, 33 pp.

Fitzgerald, J. W., 1978: On the Growth of Aerosol Particles with Relative Humidity. Naval Research Laboratory Report NRL Memorandum Report 3847, Washington, D.C., 11 pp.

Goroch, A. K., 1980: Comparison of the Marine Index of Refraction Structure Parameter, C_n^2, Model with Optical Measurement. Naval Environmental Prediction Research Facility Report NAVENVPREDRSCHFAC TR 80-09, Monterey, California, 31 pp.

Hughes, H. G., 1980: Aerosol Extinction Coefficient Variations with Altitude at 3.75 μm in a Coastal Marine Environment. J. Appl. Metecrol., 19, 803-808.

Hughes, H. G. and J. H. Richter, 1980: Extinction Coefficients Calculated from Aerosol Size Distributions Measured in a Marine Environment. J. Optical Engineering, 19, 616-620.

Noonkester, V. R., 1980: Offshore Aerosol Spectra and Humidity Relations Near Southern California. Preprints Second Conference on Coastal Meteorology (paper no. 4.9), American Meteor. Society, Los Angeles, Jan 30 - Feb 1, 1980, 113-119.

Raby, J. W., 1981: Comparison of modeled and Observed Aerosol Extinction and Implications for FLIR Range Assessments in the Northeast Atlantic. M.S. Thesis, Naval Postgraduate School, 66 pp.

Schacher, G. E., K. L. Davidson, D. E. Spiel, and C. W. Fairall, 1980a: Naval Postgraduate School Shipboard and Aircraft Meteorological Equipment. Naval Postgraduate School Report NPS-61-80-017, Monterey, California, 26 pp.

Schacher, G. E., K. L. Davidson, and C. W. Fairall, 1980b: Optical Aerosol Spectrometers Factors Affecting Optical Extinction Predictions. Naval Postgraduate School Report NPS 61-80-013, Monterey, California, 91 pp.

Schultz, M. E., 1981: Meteorological Factors in High Resolution Satellite Imagery (DMSP). M.S. Thesis, Naval Postgraduate School, in preparation.

Wells, W. C., G. Gal, and W. W. Munn, 1977: Aerosol Distributions in Maritime Air and Predicted Scattering Coefficients in the Infrared. J. Appl. Optics, 16, 654-659.

INITIAL DISTRIBUTION LIST

		No. Copies
1.	Defense Technical Information Center Cameron Station Alexandria, Virginia 22314	2
2.	Library, Code 0142 Naval Postgraduate School Monterey, California 93940	2
3.	Commander Naval Oceanography Command NSTL Station, Mississippi 39529	1
4.	Commanding Officer Fleet Numerical Oceanography Center Monterey, California 93940	1
5.	Officer-in-Charge Naval Environmental Prediction Research Facility Monterey, California 93940	1
6.	Prof. R. J. Renard, Code 63Rd Naval Postgraduate School Monterey, California 93940	1
7.	Prof. C. N. K. Mooers, Code 68Mr Naval Postgraduate School Monterey, California 93940	1
8.	Department of Meteorology Library, Code 63 Naval Postgraduate School Monterey, California 93940	1
9.	Captain Brian Van Orman AFIT/CIRF Wright-Patterson AFB, Ohio 45433	2
10.	Air Weather Service Technical Library Scott AFB, Illinois 62225	1
11.	Atmospheric Sciences Lab DELAS-AS-P White Sands Missile Range, New Mexico 88002	1
12.	Captain Edwin S. Arrance 5 WW/DNS Langley AFB, Virginia 23665	1

13.	Captain James N. Heil Det 1 1 MW Box 17 COMNAVMARIANAS FPO San Francisco 96630	5
14.	LCDR T. L. Callahan, Code N341 Naval Oceanography Command NSTL Station, Mississippi 39529	1
15.	LT J. W. Raby NOOF NAS North Island, California 92135	1
16.	Dean of Research, Code 012 Naval Postgraduate School Monterey, California 93940	1
17.	Dr. C. W. Fairall BDM Corporation, 1340 Munras St. Monterey, California 93940	1
18.	Assoc. Prof. K. L. Davidson, Code 63Ds Naval Postgraduate School Monterey, California 93940	10
19.	Prof. G. E. Schacher, Code 61Sq Naval Postgraduate School Monterey, California 93940	1
20.	Dr. A. Goroch Naval Environmental Prediction Research Facility Monterey, California 93940	1
21.	Dr. A. Weinstein Driector of Research Naval Environmental Prediction Research Facility Monterey, California 93940	1
22.	CDR K. Van Dickle Code Air-370 Naval Air Systems Command Washington, D. C. 20360	1
23.	Dr. A. Shlanta Code 3173 Naval Weapons Center China Lake, California 93555	1

24. Dr. Larry Katz 1
Code A42
Naval Surface Weapons Center
White Oak Laboratory
Silver Spring, Maryland 20362

25. Dr. J. H. Richter 1
Code 532
Naval Oceans Systems Center
San Diego, California 92152

26. Dr. Lothar Ruhnke 1
Code 8320
Naval Research Laboratory
Washington, D. C. 20375

27. Officer-in-Charge 1
Naval Oceanography Command Detachment
FPO New York 09571

Thesis 192557
H423325 Heil
c.1
Synoptic scale features associated with vertical distribution of IR aerosol extinction.